T.C.
İSTANBUL UNIVERSITY
INSTITUTE OF GRADUATE STUDIES IN
SCIENCE AND ENGINEERING

Ph.D. THESIS

PREVENTING BIOFILM FORMATION ON LASER-TREATED TITANIUM IMPLANTS

Arzu EROL

Department of Biotechnology

Biotechnology Programme

SUPERVISOR
Assoc. Prof. Dr. İlven MUTLU

November, 2017

İSTANBUL

T.C.
İSTANBUL UNIVERSITY
INSTITUTE OF GRADUATE STUDIES IN
SCIENCE AND ENGINEERING

Ph.D. THESIS

PREVENTING BIOFILM FORMATION ON LASER TREATED TITANIUM IMPLANTS

Arzu EROL

Department of Biotechnology

Biotechnology Programme

SUPERVISOR
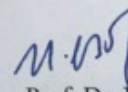**Assoc. Prof. Dr. İlven MUTLU**
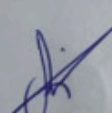
November, 2017

İSTANBUL

This study was accepted on 5/12/2017 as a Ph. D. thesis in Department of Biotechnology, Biotechnology Programme by the following Committee.

Examining Committee Members

Assoc. Prof. Dr. İlven MUTLU(Supervisor)
İstanbul University
Faculty of Engineering

Assoc. Prof. Dr. Tuba GÜNEL
İstanbul University
Faculty of Science

Assoc. Prof. Dr. Nagehan ERSOY TUNALI
Medeniyet University
Faculty of Engineering and Natural Sciences

Assoc. Prof. Dr. Sevim KARAKAŞ
ÇELİK
Bülent Ecevit University
Faculty of Science and Arts

Assist. Prof. Dr. Murat PEKMEZ
İstanbul University
Faculty of Science

As required by the 9/2 and 22/2 articles of the Graduate Education Regulation which was published in the Official Gazette on 20.04.2016, this graduate thesis is reported as in accordance with criteria determined by the Institute of Graduate Sttudies in Science and Engineering by using the plagiarism software to which İstanbul University is a subscriber.

FOREWORD

This work was completed at Saarland University in the Clinic of Operative Dentistry. I am grateful that Prof. Dr. Matthias HANNIG accepted me in his laboratory and supported my work.

I express my thanks and gratefulness to my family for their understanding, inspiration and persistence. I am also very grateful for all my associates, Natalia UMANSKAYA, Simone GRASS, Nobert PUTZ, Kevin and Chen, who made my stay at Saarland University a noteworthy and significant experience.

November 2017   Arzu EROL

TABLE OF CONTENTS

Page

LIST OF FIGURES

LIST OF TABLES

LIST OF SYMBOLS AND ABBREVIATIONS

Symbol	Explanation
ASTM	: American Society For Testing And Materials
BSI	: British Standard
CFDA	:Carboxyfluorescein Diacetate
CFU	:Colony Forming Unit
CLSM	:Controlled low strength material
cp	: Commercially Pure
CW laser	:Continuous-wave Laser
DLVO	:Boris Derjaguin and Lev Landau, Evert Verwey and Theodoor Overbeek
EDX-EDS	:Energy-Dispersive X-Ray Spectroscopy
EPMA	:Electron Probe Microanalyzer
FDA	:Fluorescein Diacetate
FEPA	**:**European Producers of Abrasives
LDS	:Live-Dead Staning
NTs	: Nanotextured- Nanotubes
NWs	: Nanowire
SEM	:Scanning Electron Microscopy
SYTO®9	:The Live/Dead Kit Stains
TEM	:Tranmission Electron Microscopy
VLS	:Vapour Liquid Solid
WDX/WDS	:Wavelength Dispersive X-Ray Spectroscopy

Abbreviation	Explanation
nm	: Nanometer
μm	: Micrometer
V	: Volt
h	: Hours
eV	: Electrovolt
KVa	: Kilovolt Ampere
M	: Mean

ÖZET

DOKTORA TEZİ

LAZER İLE İŞLEME TABİ TUTULMUŞ TİTANYUM İMPLANTLARIN YÜZEYLERINDE BIYOFILM OLUŞUMUNUN ENGELLENMESİ

Arzu EROL

İstanbul Üniversitesi

Fen Bilimleri Enstitüsü

Biyoteknoloji Anabilim Dalı

Danışman : Doç. Dr. İlven MUTLU

Titanyum alaşımları diş implantları için en çok tercih edilen malzemedir. Birçok implant uygulamalarında, titanyum alaşımlarının biyouyumluluğu ispat edilmiştir. Dental implantların osseointegrasyonunu artırmak için, çeşitli desenlendirme yaklaşımları vardır. Pürüzlendirme, lazerle iyileştirme, kumlama, ince film kaplama tercih edilen metodlardır. Kaplama için gerekli malzemeler geniş yelpaze sağlarken, yüzey topografisi bu yaklaşımlarla sınırlıdır.

24- 71 yaş arası sağlıklı erkek ve kadınlardan oluşan, 9 kişilik gönüllü grubu için, cilalanmış, asit ile pürüzlendirilmiş, ince film kaplandıktan sonra lazerle yüzeyi iyileştirilmiş 4 çeşit Ti numunesi çalışmamızda kullanıldı. Çalışmaya katılan tüm gönüllülerin sigara ve alkol öyküsü olmaksızın, aşırı miktarda polifenolik içecek ve gıdaları tüketmeden, günlük düzenli beslenme yöntemlerine devam etmişlerdir. Yüzey, taramalı elektron mikroskobu, x-ışını spektrokopi ve flouresence mikroskobu ile değerlendirildi. Kimyasal modifikasyon da, bakteri tutunmasını ve biyofilm oluşumu, cilanlanma sonrası nano-tel (NW) ile kaplanmış yüzeye göre daha fazladır. Diğer yandan, yüzey pürüzlülüğü nano-tekstil'in (NT) yüzeye tutunmasına neden olur ama cilalanmış yüzeye, NT'in tutunma kabiliyeti düşüktür ve kolayca yüzeyden ayrılır.

Yüzeye bakteri tutunmasındaki anahtar faktör, yüzey üzerindeki nano-yapının geometrisi ve mekanik özellikleridir. Ayrıca, *in vitro* modellerin sözü edilen dezavantajları göz önünde bulundurulduğunda, *in situ* tasarlanan çalışmalar, ağız boşluğunda olan olayları daha elverişli olarak yansıtmaktadır. Dolayısıyla, mevcut incelemelerde gerçekçi sonuçlar in situ modellemeye bağlandı.

Kasım 2017, 111. sayfa.

Anahtar kelimeler: Biyofilm, Ti, Dental İmplant, Yüzey Modifikasyonu

SUMMARY

Ph.D. THESIS

PREVENTING BIOFILM FORMATION ON LASER-TREATED TITANIUM IMPLANTS

Arzu EROL

İstanbul University

Institute of Graduate Studies in Science and Engineering

Department of Biotechnology

Supervisor : Assoc. Prof. Dr. İlven MUTLU

Titanium alloys are the most preferred materials for dental implants. The biocompatibility of titanium alloys has been demonstrated in several implant applications. There are several approaches to increase the osseointegration of such dental implants by patterning the surface; etching, laser treatment, sand blasting and coating with a functional thin film are some of the preferred methods. While coating provides a broad spectrum of materials, the surface topography is limited by this approach.

We evaluated the bacteria adhered to polished, acid-etched and coated titanium surfaces after 24 h of in situ biofilm formation. In our study, a total of 4 different types of titanium specimens were polished, acid etched, or thin-film coated after being surface treated and were then placed in nine healthy female and male patients aged between 24 and 71 years. The surfaces were evaluated by scanning electron microscopy, dispersive X-ray spectroscopy and fluorescence microscopy. Chemical modification increased bacterial adherence and biofilm formation more than polishing and polishing after coating with nanowires (NWs). Conversely, the surface roughness caused by nanotextiles (NTs) was very stable and reduced biofilm formation; however, if the NTs were applied to a polished surface, they were easily removed from the surface and were thus ineffective.

The key factors that affect bacterial adhesion are the geometry and mechanical properties of the surface nanostructures. Hence, the in situ appearance was included in the present examinations.

November 2017, 111 pages.

1. INTRODUCTION

Titanium-based alloys are the best examples of biological cell and tissue bio-compatibility. Grade 1 titanium (cp-Ti) is the softest and most ductile titanium grade, and it exhibits the greatest formability. There are many applications of titanium alloys including oral, neuron and other human body part implants.

The most essential characteristic of an implant is surface control, which is synthetic and morphological at the small-scale level. The tissue reaction to an implant is basically controlled at the nanometer level. There are a few approaches that can be used to improve the osseointegration of dental implants by modifying their surface [1]; drawing, laser treatment, sand impacting and covering with a utilitarian thin film are some of the favored techniques [2]. While covering can be performed with a wide range of materials, surface geology is constrained by this approach. For enhanced osseointegration, scratching is acknowledged as a superior strategy; however, scratching roughens the surface and increases porosity, triggering microbial adhesion [3]. The goal of surface treatment is to incorporate nano-level geography and coatings for optimal osseointegration with inserts made to last for the duration of a patient's life. Investigations assessing these diverse approaches are often contradictory [4-17].

Nanostructures do not lead to increased bacterial adherence and growth or biofilm formation, which is important for various applications in the medical field as well as for implants. Such surfaces will be prepared at my host institute (Prof. Hannig, Saarland University) in collaboration the Leibniz Institute for New Materials. Current research is focusing on various ways to address, anticipate and treat biofilms. Biofilm research can be separated into two objectives. Primary investigative efforts are concentrating on ways to shape biofilm formation by examining the microbial metabolites and by-products that are produced and can be used to restrain or disturb biofilm development. Another biofilm advancement focus is to change the biomaterials utilized as part of restorative implants to make them impervious to biofilm development given our understanding of atomic biofilm arrangement on nanowire surface-covered Ti.

1.1. BIOMATERIALS

The most recent dental implant advancements have incorporated fluoride, antibody poisons, advancement factors and laminin. The exterior of a dental implant is the primary part that is in contact with the bio-environment, and the uniqueness of the surface determines the response and impacts the mechanical nature of the insert/tissue interface. There are four pure Ti formulations as well as one titanium combination that is uncommonly used for dental implant applications.

The alterations that comprise the surface topology and roughness of oral implants have been changed from a small scale to a nanometer scale. At the microscale, surface properties such as harshness and other changes are critical for cell responses, tissue mending and implant durability [18]. Other adjustments include machining, air-scraping spots, corrosive drawing, electrochemical oxidation and laser treatment, which are techniques that are applied to adjust the surface topology of titanium implants at different thicknesses.

1.2. SURFACE MODIFICATION ON TITANIUM

The fundamental approaches for adjusting titanium and titanium alloys are mechanical, manufactured and physical methods that induce morphological alterations and other changes to achieve unmistakable coverings on the objective surface. These coverings fuse into hydroxyapatite, biomolecule-functionalized coatings, and calcium phosphate coatings. The strategies can be categorized into mechanical or physical approaches or covering techniques per the instrument used to develop the adjusted layer on the material surface (Table 1.1).

Table 1.1: Overview of surface modification methods [19].
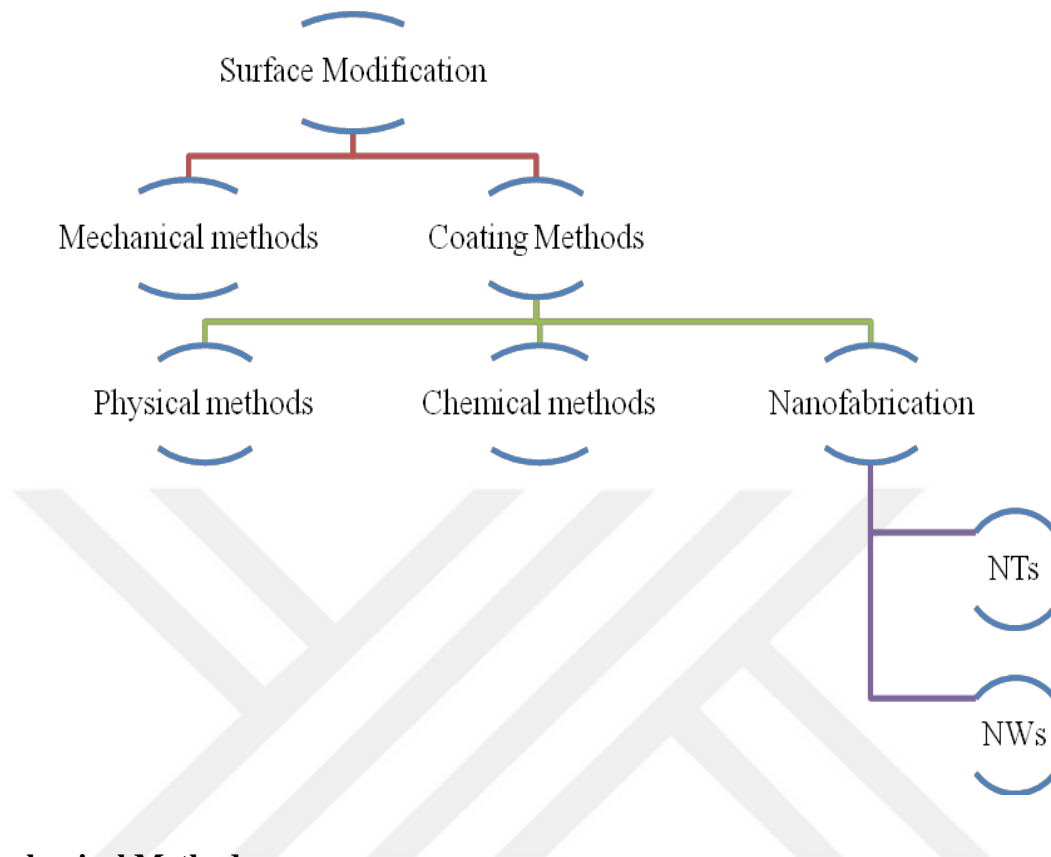
Mechanical Methods

Mechanical strategies include outer activities that use strength to alter surface qualities. Normal physical surface change strategies include machining, cleaning, coarseness impacting and physical-based treatment by forming or expulsion.

Coating Methods

The application of coatings is one of the potential approaches available to modify the surface of materials. The main reason for the coating and modification of metallic biomaterials is to modify the biological response of the host tissue in the peri-implant region. Bioactive coatings can have a surface profile that allows bone to grow or a layer of additional material onto which bone could attach.

Different procedures have been used to accomplish biomechanical similarity, for example, permeable surface advancement, nano-artistic particle covering [19], HAP covering, oxide covering and surface warmth treatment to lessen the grain.

Physical methods

Physical surface change strategies incorporate procedures such as warm splashing, physical vapor testimony, particle implantation and sparkle release plasma treatment in which compound responses do not happen.

Chemical methods

By and large, the most used creation systems are destructive and solvent scratching, electrochemical iodization, substance declaration and biochemical surface covering methodologies [19-23], all of which will be further discussed. The chemical strategies considered herein incorporate chemical formulations that absorb NaOH after warmth treatment, HCl after scratching [24], or other ensuing NaOH processes [25-27], hydrogen peroxide treatment [28], substance vapor testimony [29, 30], and bio-chemical adjustment [31, 32].

Nanofabrication

The establishment of nanoscience has dramatically altered numerous exploratory fields. Nanostructures are characterized as structures with no less than one measurement under 100 nm. Quantities of iotas are countable, making the properties of nanostructures dissimilar from those of their mass partners or single molecules, even though they are similarly synthesized [33] (Figure 1.1).
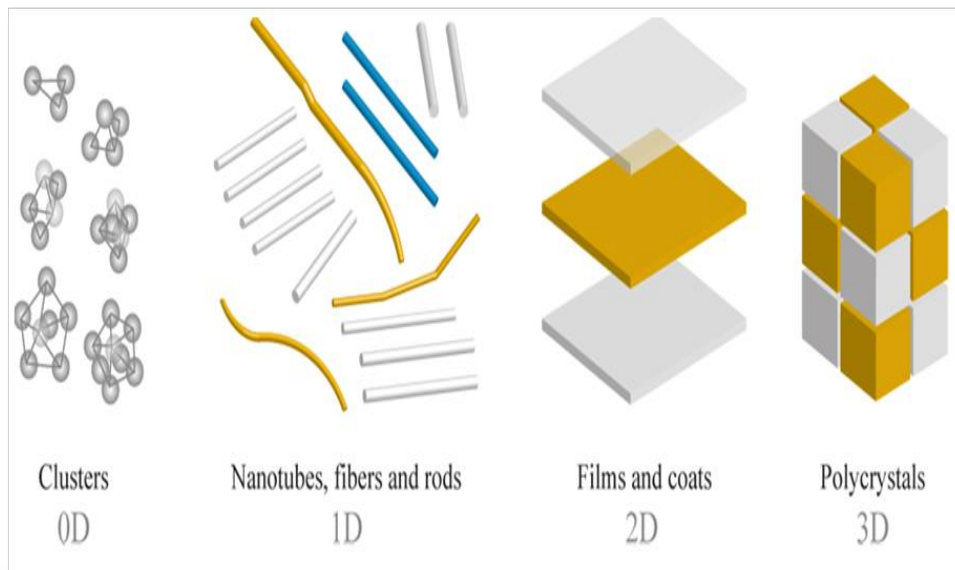
Figure 1.1: Types of nanocrystalline materials by the size of their basic components [33].

0-D (zero-dimensional) groups; 1-D (one-dimensional) nanotubes, strands and bars; 2-D (two-dimensional) films and coats; and 3-D (three-dimensional) polycrystals [33]. One-dimensional nanomaterials can be used as both wiring and gadget components in future structures for useful nanoframeworks. Two material classes, carbon nanotubes (NTs) and nanowires (NWs), have displayed particular promise.

Nano-tubes (NTs) can be either electrically conductive or semi-conductive, contingent upon their attractive helicity.

Nano-wires (NWs) are amazingly thin wires with a measurement on the order of a couple nanometers (nm) or less. NWs have a nanostructure with the width of a nanometer, which is very small. There is no restriction on their width, yet they cannot be more than a couple of nanometers in height.

1.3 RECENT APPROACHES FOR DESIGNING BETTER IMPLANTS

Numerous small micro/nano-creation advancements have been imagined and produced over the past few decades. Some of them now broadly connect to cell sciences, for example, delicate lithography, electrospinning, nano-organized designing advances (including the counting plunge pen, e-shaft composing, nano-engrave lithography, nano-shaving, etc.), and three-dimensional creations.

CVD strategies have been utilized to create strands, fibers, and nanowires composed of different materials in the last few years. CVD has various focal points that serve as strategies for saving flimsy films [34]. One of the essential points of interest is that CVD films are for the most part very conformal, which is essential for covering complex-formed items, as shown in Figure 1.2 [35-39].
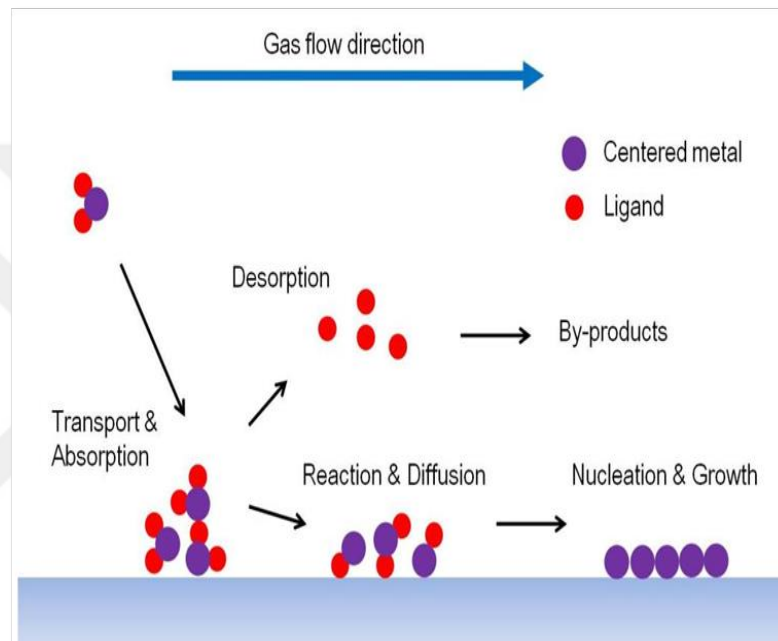
Figure 1.2: Schematic diagram of the CVD mechanism [39].

Prior to treatment, the material to be treated with the laser is heated. Lee and Zumgahr could execute breaking and make a smooth and pore-free surface by pre-warming high flawlessness alumina earthenware in a high-temperature electric warmer both before and in the midst of CO_2 laser treatment [40-50]. In their work, the material was warmed to 1200 °C. Such a temperature is necessary for the substrate material. The treated surfaces were not fragmented, yet such an approach is more sensible for thicker layers or for mass alumina ceramics. Notwithstanding that the method fruitfully joined a thick alumina layer, the crystallinity of the layer was low [50-58].

1.4. BIOCOMPATIBILITY OF TITANIUM ALLOYS

The artificial inserts, once embedded in vivo, initiate a course of responses in the natural

microenvironment through cooperation of the biomaterial with body liquids, proteins and different cells.

Cell Adhesion Process and Cell-Biomaterial Interactions

Cells and their microenvironment are connected through dynamic and bidirectional communication that directs the entire tissue and organ physiology [59, 60]. Two strategies are utilized to assess biomaterial associations: bacterial cell connections and cell adhesion.

Fundamentals of Bacterial cell attachment

The DLVO hypothesis depends on the correlation of bacterial cells with smooth colloid particles that connect with a surface and is therefore an electrostatic attraction [61]. Nonetheless, a few reviews have demonstrated that this hypothesis is of constrained application for bacterial adhesion because bacterial cells are not smooth-surfaced particles. Bacterial surfaces are somewhat secured by hydrophobic exopolysaccharides and infrequently by an exceptionally organized protein shell. There are distinctive systems of adherence that occur due to the usage of flagella or pili, which create windrows of cells [62]. Pathogens demonstrate reversible and irreversible adherence [62-64], implying that bacterial cells can adhere to a surface and also segregate from a material and leave the region again before connecting irreversibly and initiating biofilm development. When harsh conditions occur, the development of a thick protein layer on implant surfaces can stifle the adhesion of microscopic organisms. The attachment procedure can be distinctive for different materials with various surface structures due to short, extended van der Waals cooperation and surface vitality (Figure 1.3.) [65].
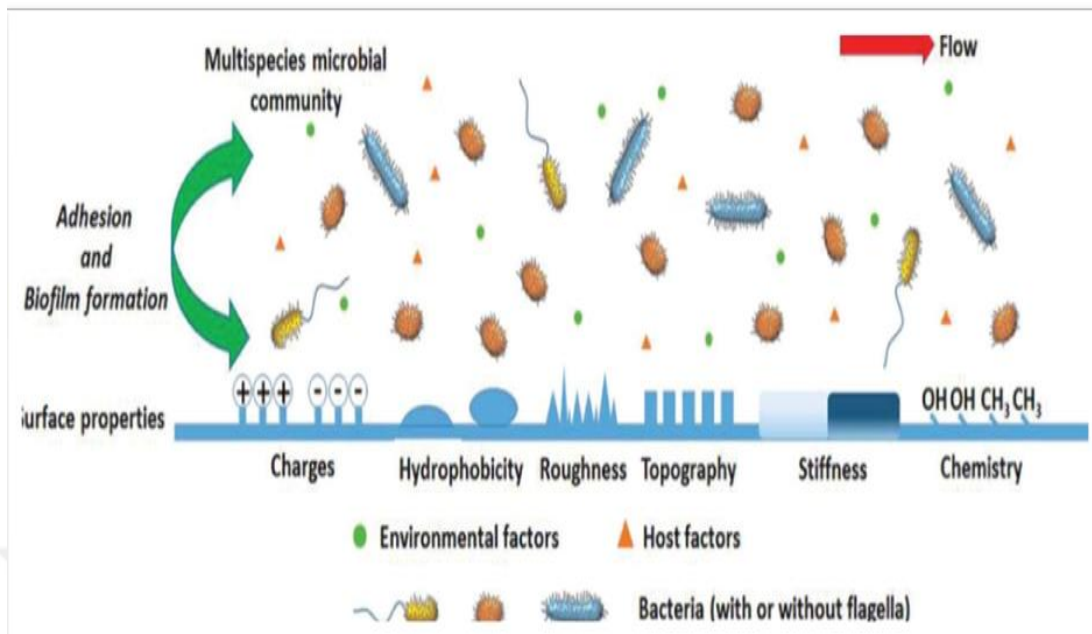
Figure 1.3: The relationship between surface roughness/chemistry and bacterial adhesion [65].

1.5. BIOFILM FORMATION

Essential structures connected with microorganisms composed of an assortment of bioparticles, biofilms are characterized as polymeric lattices that involve a gathering of microorganisms [66].

The polymeric substances in biofilms differ in their physical and chemical properties; for the most part, they are composed of polysaccharides. However, biofilms contain more than microbial cells and polymeric grids: they comprise an assortment of bioparticles including proteins, compounds and particles (Figure 1.4.).

Figure 1.4: Composition of biofilms [66].

Dental Plaques as a Biofilms

Biofilm formation requires specific steps and is typically described as a five-step process, which is shown in Figure 1.5.
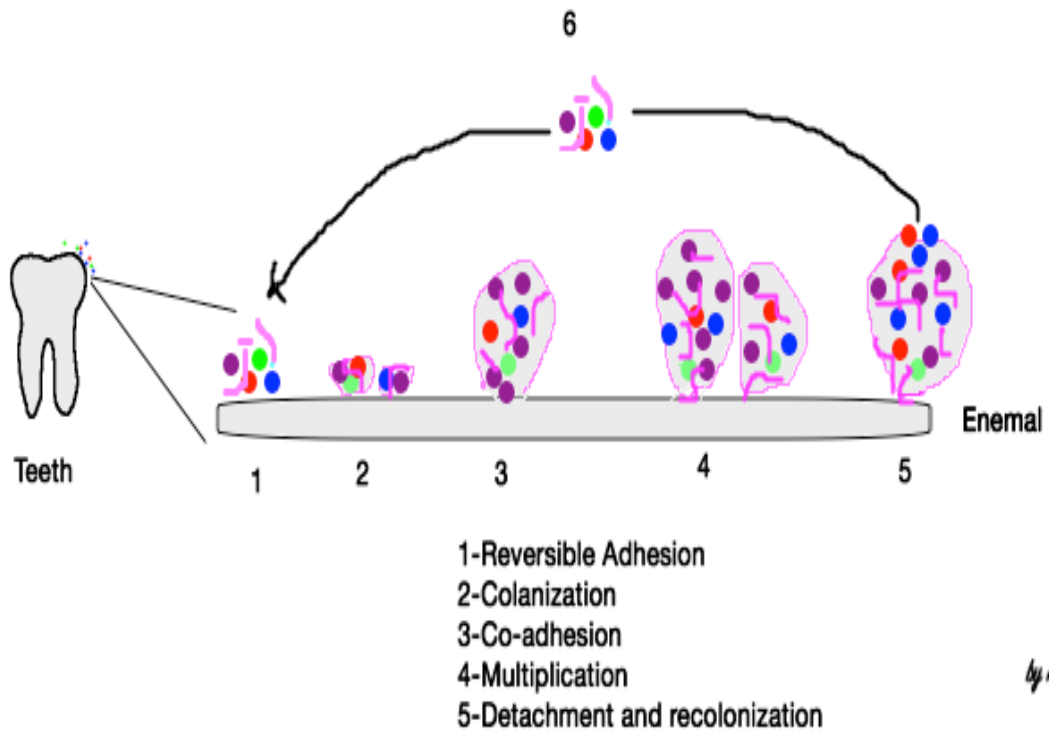
Figure 1.5: Dental biofilm formation [67].

Biofilm arrangement around common teeth occurs in minutes, and some species begin colonizing within 2-6 h [67-69]. A pellicle begins to take shape on the implant surface as soon as 30 min after the implant is uncovered in an oral pit.

1.6. LITRATURE REVIEW

Various studies have been performed on titanium implant surfaces.

Jayaraman et al. [5] investigated osteoblastic-based cells and found that they are better for the study of model implants when implanted in vivo.

Tobias et al. [6] investigated the behavior of osteoblasts and fibroblasts by means of roughness gradients.

Craig A. Simmons et al. [7] investigated the healing dynamics of IZ tissues in post-implantation periods.

Beutner R. et. al. [10] investigated ECM proteins for the generation of Ti bioactive behavior to enhance osseointegration.

Schliephake et al. [11, 12] investigated how the use of dental implant organic coatings that provide binding sites for integrin receptors can enhance peri-implant bone formation.

Kerstin Lange et al. [14] investigated EGF coatings for the enhancement of tissue integration in the transmucosal areas of dental implants.

An extensive variety of bacterial-resistant surfaces has been proposed to restrain biofilm formation. Normal techniques depend either on the use of biocidal mixes or on the prevention of adhesion. Diverse inorganic and natural compounds inhibit bacterial movement. The natural compounds include carboxylic acids, alcohols and aldehydes, which cause protein precipitation or disturb microbial biofilms. Such natural solutions are used to prevent bacterial colonization due to their mechanisms of action.

2. MATERIALS AND METHODS

2.1 SUBJECTS

Specimens

The specimens used in this study were cp-Ti circles that were 5 mm wide and 1 mm thick (Figure 2.1).

Figure 2.1: The different sizes of the Ti discs.

Group 1 included acid-etched implants, and those in Group 2 were polished. The samples were machined from grade 4 bars. The acid-etched samples were dipped in a solution of HNO_3, HCl and H_2SO_4. Group 3 consisted of implants that were acid etched after being covered with NWs, and the last group of implants were polished after being covered with NWs and NTs (Table 2.1).

Table 2.1: Treatment parameters, analyzing methods and aims

Type of Ti surface	Surface modification	Analyzing methods	Aim
Polished	Machined	SEM, LDS, EDX	Studying the surface topology, Measurement of biofilm thickness, Identify the bacterial species.
Etched	Chemical	SEM, LDS, EDX	Studying the surface topology, Measurement of biofilm thickness, Identify the bacterial species.
Polished+NWs	Machined, Coated with NWs, Laser treated	SEM, LDS, EDX	Studying the surface topology, Measurement of biofilm thickness, Identify the bacterial species.
Etched+NWs	Chemical, Coated with NWs, Laser treated	SEM, LDS, EDX	Studying the surface topology, Measurement of biofilm thickness, Identify the bacterial species.
Polished+NTs	Machined, Coated with NTs, Laser treated	SEM, LDS, EDX	Studying the surface topology, Measurement of biofilm thickness, Identify the bacterial species.
Etched+NTs	Chemical, Coated with NTs , Laser treated	SEM, LDS, EDX	Studying the surface topology, Measurement of biofilm thickness, Identify the bacterial species.

Laser treatment was performed under a nitrogen atmosphere, which leads to nitriding and surface patterning simultaneously. Such surfaces were prepared in collaboration with the Leibniz Institute for New Materials (Saarbrucken).
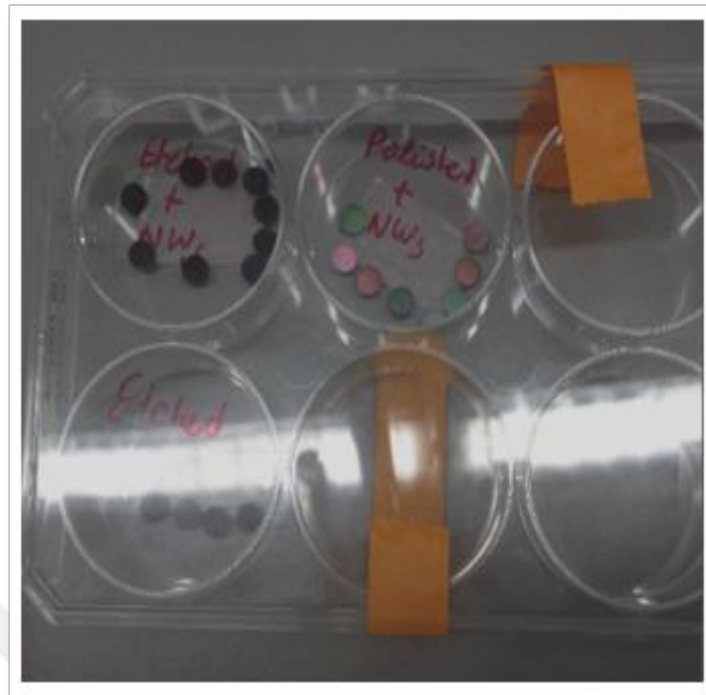
Figure 2.2: The Ti specimens coated with NWs after surface modification.

Different surfaces, including those etched after being coated with NWs, polished after being coated with NWs and simply etched, are shown.

Production of polished specimens

Ti specimens were ground under permanent water-cooling using a polishing machine with silicon carbide grinding paper. Then, the surface was ground and polished. The thickness of specimens was 1 mm. A light microscope was used.

Disinfection of the treatment specimens

According to the method of Hannig et al. [70], the specimens were pretreated with NaOCl and disinfected with ethanol. All specimens were first cleaned using a 3% NaOCl solution for 10 s and were then washed five times in distilled water, followed by disinfection in ethanol for 10 min and another five washes in double distilled water.

Production of splints

Individual intraoral fixtures for mounting dentinal specimens were manufactured for all subjects in the form of acrylic appliances in the first and second quadrants of the upper jaw.
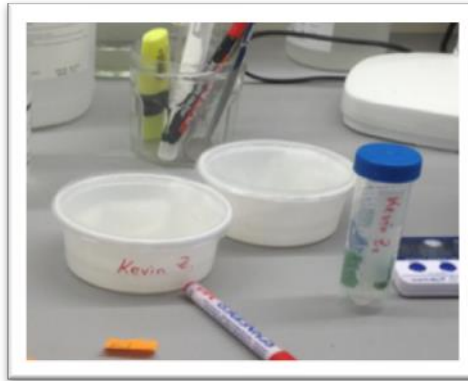
Figure 2.3: Individual splints were stored in individual boxes to prevent contamination.

The right image shows the splints. Impressions of the maxilla were taken with alginate impression material to produce an elastic mold. A plaster model was produced, and the appliances ('minisplints') were constructed. The minisplints were composed of Duran with thicknesses between 0.5 mm and 0.7 mm, and they covered the molar and premolar teeth on the left and right upper jaw, extending 3 mm beyond the buccal/palatal marginal sulcus.

Fixing/mounting of dentinal specimens

Specimens were fixed on the maxillary minisplints at a defined position by means of a thin layer of polyvinyl-siloxane impression material (President light-body). The samples were placed on the buccal sites of the left and right upper 1st molar (16, 26) and upper 2nd molar (17, 27) (Figure 2.4, 2.5).
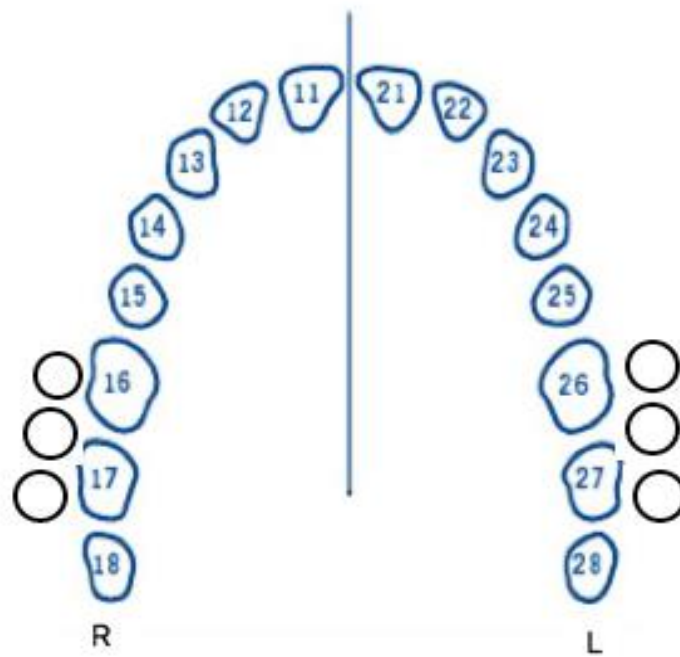
Figure 2.4: Locations of the specimens

Figure 2.5: Splint with mounted specimens

2.2. IN SITU BIOFILM FORMATION

Seventy Ti discs were partitioned among 9 healthy volunteers (aged 20-65 years; 5 females and 4 males). The volunteers were designated MHe, BK, SS, NL, KZ, SR, NG, KL and JK (Table 2.2).

Table 2.2: Ti discs in nine healthy volunteers

Surface /volunteers	1	2	3	4	5	6	7	8	9
Polished	x	x	x	x	x	x	x	x	x
Etched	x	x	x	x	x	x	x	x	x
Polished+NWs	x	x	x	x	x	x	x		
Etched+NWs	x	x	x	x	x	x	x		
Polished+NTs								x	x
Etched+NTs								x	x

Three or 4 of the Ti discs were situated at the buccal site of the molar and premolar teeth with silicon impression material on the uniquely crafted maxillary braces (Figure 2.6).

Figure 2.6: Removable maxillary splints

Seventy specimens were assigned among the 9 volunteers, who were divided into the control group (only polished and acid-etched) and the surface treatment group, which served as a positive control. Each subject wore 4 specimens for 1 day. The splints with mounted dentinal specimens were exposed to the oral environment for 1 day and were only removed and stored

in a 100% humidity environment during meals and daily tooth brushing. After 1 day, the implants were removed and washed to remove bacteria.

Fixation of the in situ biofilm

Biofilm-coated specimens were washed and fixed in 1.5% glutaraldehyde in PBS (pH 7.4). Specimens were washed 5 times in PBS (pH 7.4) for 10 min each and stored in buffer solution at 4 °C.

2.3 SCANNING ELECTRON MICROSCOPY

The dentinal specimens were examined using an XL 30E SEM-FEG scanning electron microscope (FEI, Netherlands).

2.4. LIVE/DEAD STAINING

Stain was prepared by combining 5 μl of SYTO®9 and 5 μl of propidium iodide in 5 ml of water. The stain was added to the samples, which were then mixed and incubated for 15 min. Each of the examples was added to a glass slide, secured with mounting oil and then placed in darkness at 4 °C. The samples were assessed under an epifluorescent microscope fitted with a camera using AxioVision software. Five pictures were taken in focus from each of the 4 quadrants. Live/dead pictures of the surfaces were isolated using red and green shading channels, and the middle regions of the red and green fluorescence were ascertained. The green fluorescence values are communicated as a percentage of the red fluorescence.

2.5. ENERGY-DISPERSIVE X-RAY SPECTROSCOPY

An electron microscope can be used for applications beyond imaging: combining an electron microscope (SEM or TEM) with an Electron Probe Microanalyzer (EPMA) provides a powerful tool for chemical analysis. EPMA analyzes the characteristic X-ray photons emitted from the elements in a sample, i.e., the "fingerprints" of the elements.

There are two types of EPMA: wavelength-dispersive x-beam spectroscopy (WDX/WDS) and energy-dispersive x-beam spectroscopy (EDX/EDS). The latter is significantly faster, but WDX has a superior resolution and accuracy. EDX is preferred because it provides subjective assurance of the components in a specimen quickly; additionally, acquiring data on the

dispersion of components over the analyzed territory by mapping is possible. Quantitative examination requires reference spectra from a specimen with a known synthesis. While subjective and semi-quantitative estimations can be performed quickly with EDX, much of the time, exact quantitative investigation is very troublesome and must be performed with care and mastery (which is not generally the case in the literature). Obtaining bond or concoction shifts is not possible with EDX, and furthermore, light components such as C are hard to measure.

2.6. IMAGE ANALYSIS

All analyses (live/dead staining, microbiology and scanning electron microscopy) were assessed using ImageJ software, which is of great help in reducing manual labor and increasing accuracy, objectivity, and reproducibility.

For image processing, ImageJ was used to produce an altered form of the SEM and fluorescence captured images. Picture examination was performed to extract the components of interest from each picture to analyze the microscopic outcome. Computational representation can be considered the reverse of picture examination: it delivers a picture from given inputs, which could be numbers, parameterized shapes, or numerical capacities, to give data about Ti implant surfaces.

Computational representation creates an abnormal state of understanding of what is contained in a picture as a record of microscopic organisms at first glance. This is called picture understanding. The point of perception is to change higher-dimensional picture information into a more primitive representation to encourage investigation of the information.

ImageJ software was used to study the data as follows:

1. Counting cells;
2. Image thresholding;
3. Area measurements of cells; and
4. Subtract background "noise".

3. RESULTS

3.1. BACLIGHT VIABILITY ASSAYS

Bacteria in the in situ biofilms

BacLight[TM] examination permitted the live and dead microscopic organisms in the biofilms to be visualized and identified at the same time (Figure 3.1).
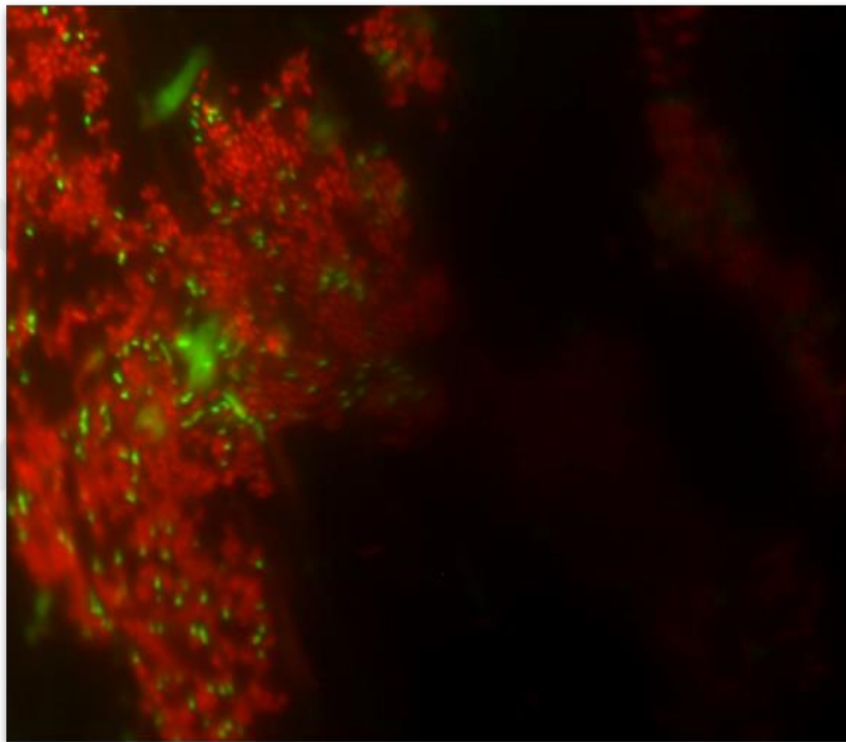
Figure 3.1: Differentiation of live and dead bacteria in the biofilms.

Green: live bacteria; red: dead bacterial. Original magnification: 1.000-fold. The bacteria were coccoid in shape.
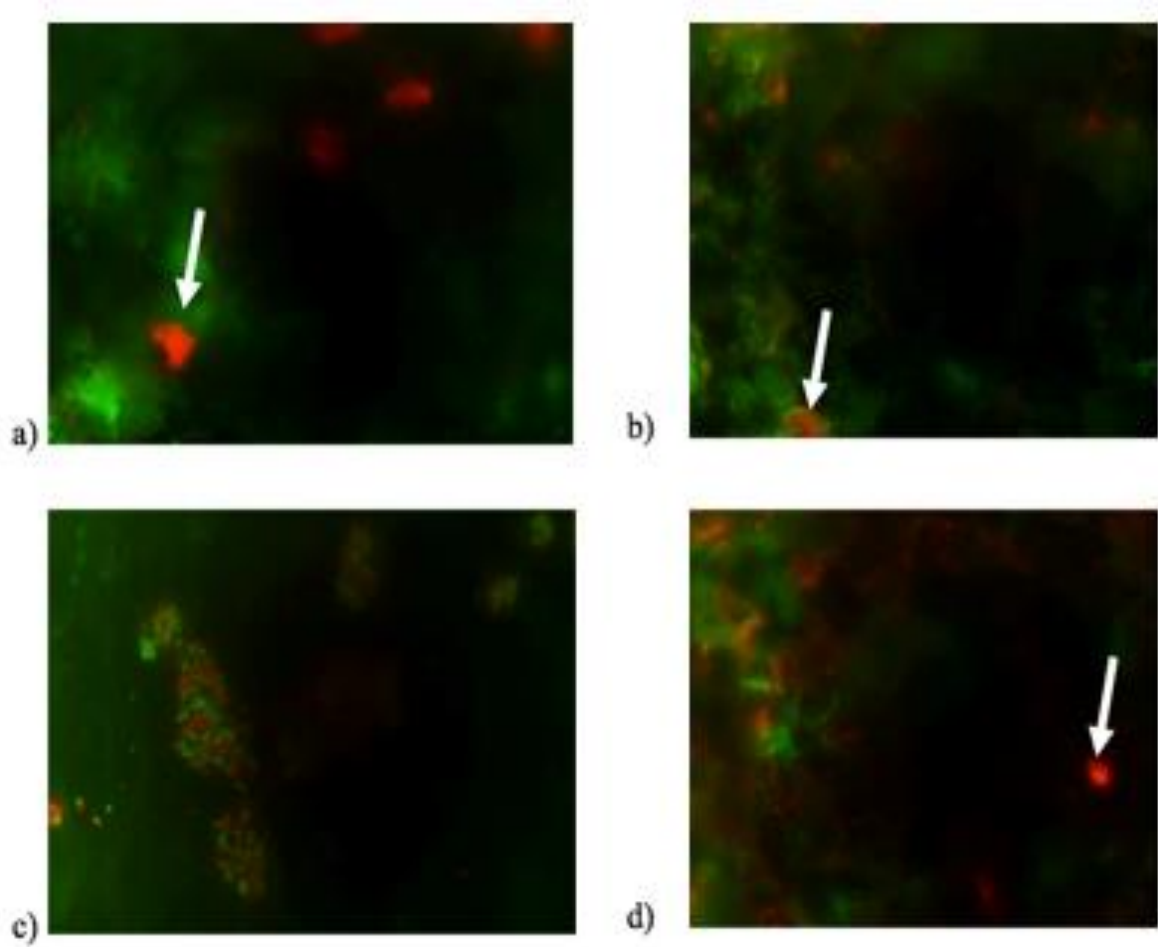
Figure 3.2: Images of epithelial cells on the surface of the 24-h biofilms.

Arrows show the nuclei of epithelial cells in images a, b and d. (a) Control (Ti with a polished surface); (b) control (Ti with an etched surface); (c) Ti with a polished surface, coated with NWs; (d) Ti with an etched surface, coated with NWs. Original magnification: 1.000-fold.
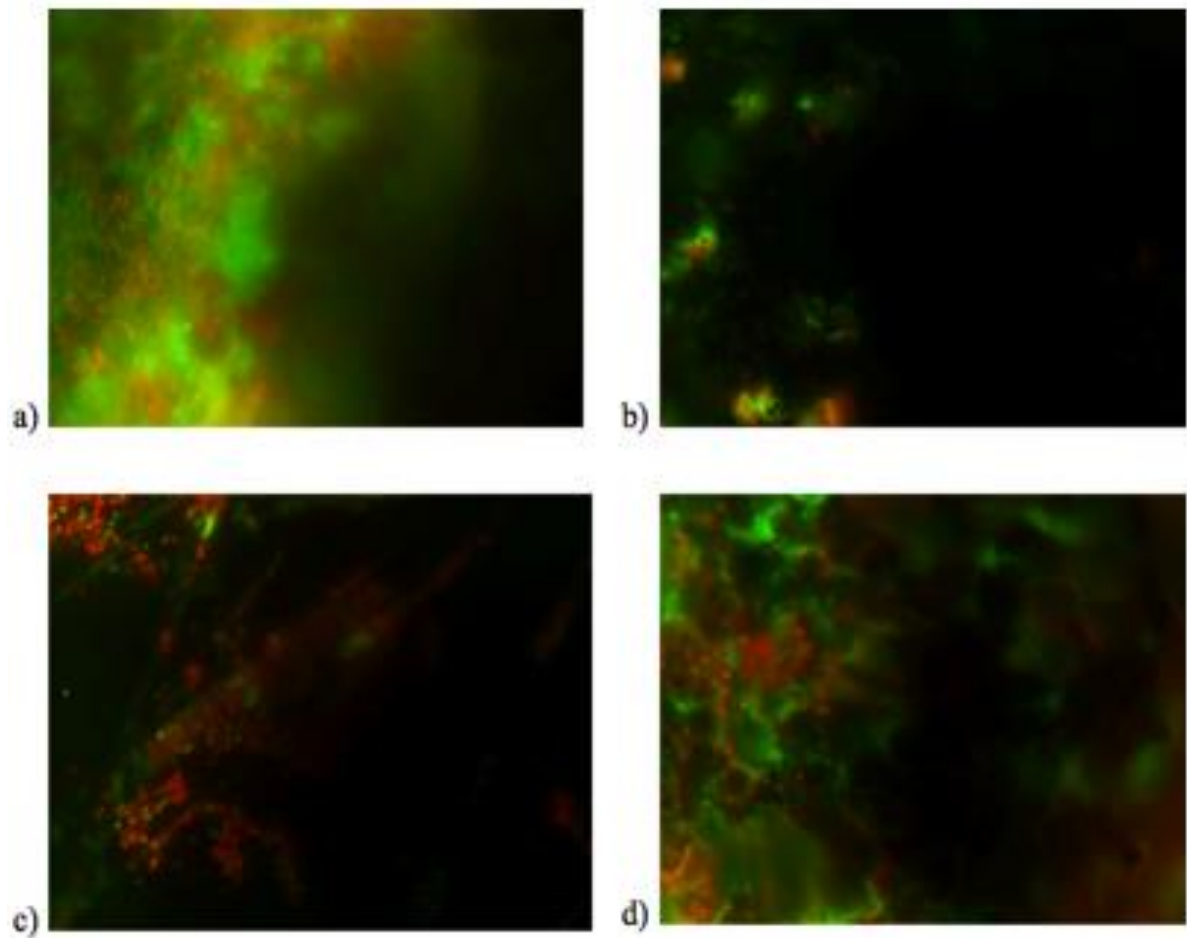
Figure 3.3: Visualization of bacteria in the 24-h biofilms.

Single-layer chains or colonies were observed. (a) Control (Ti with a polished surface); (b) control (Ti with an etched surface); (c) Ti with a polished surface, coated with NWs; (d) Ti with an etched surface, coated with NWs. Original magnification: 1.000-fold.
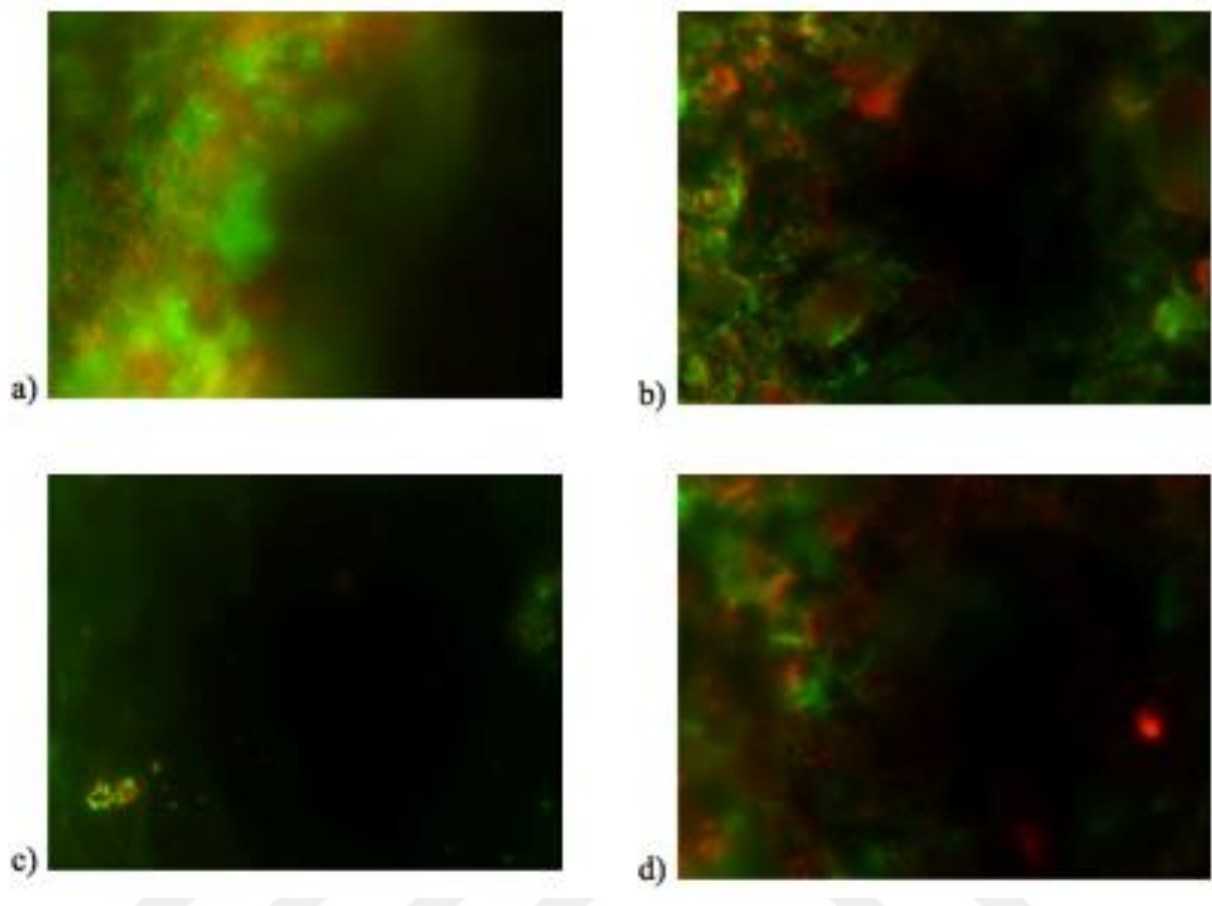
Figure 3.4: Bacteria in the 24-h biofilms on treated and untreated surfaces.

Volunteer KZ (the abbreviation is the experimental name of the volunteer). (a) Control (Ti with a polished surface); (b) control (Ti with an etched surface); (c) Ti with a polished surface, coated with NWs; (d) Ti with an etched surface, coated with NWs. Original magnification: 1.000-fold.
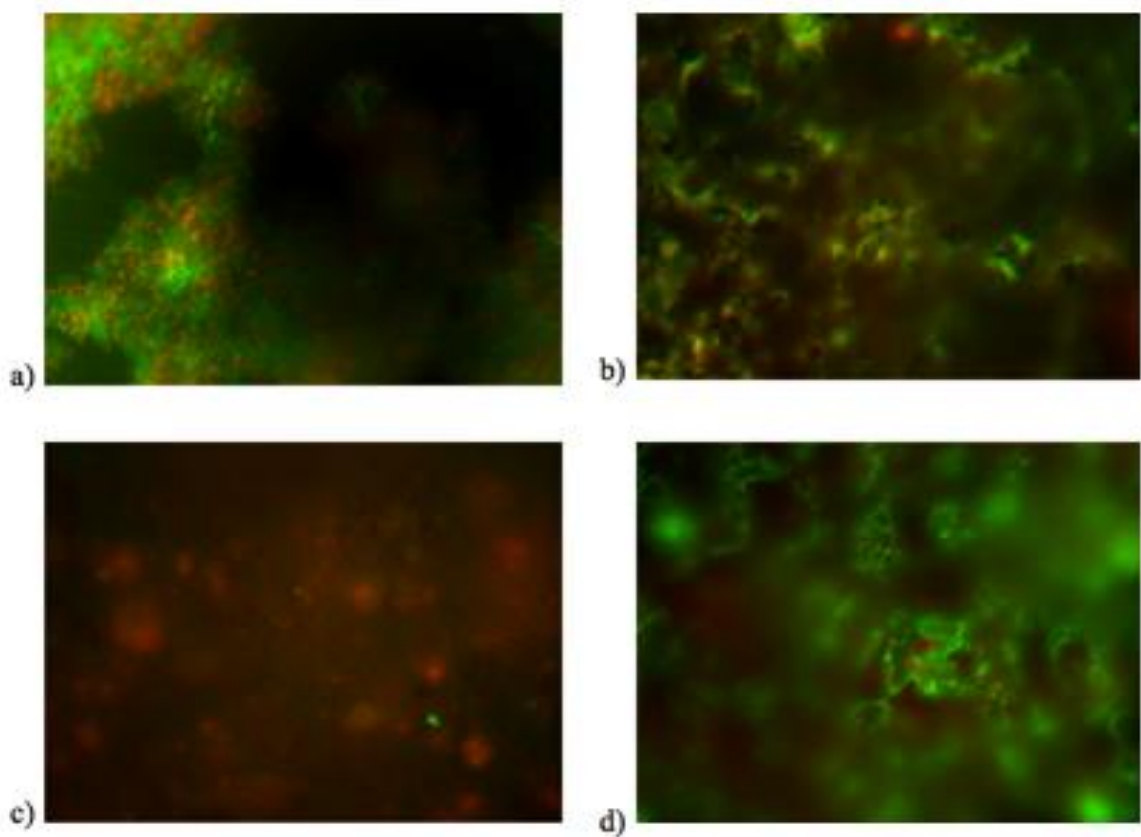
Figure 3.5: Visualization of bacteria in the 24-h biofilms on treated and untreated surfaces.

Single-layer chains or colonies were observed for SS. (a) Control (Ti with a polished surface); (b) control (Ti with an etched surface); (c) Ti with a polished surface, coated with NWs; (d) Ti with an etched surface, coated with NWs. Original magnification: 1.000-fold.

a) Left a)Right
b)Left b)Right
c)Left c)Right
d)Left d)Right
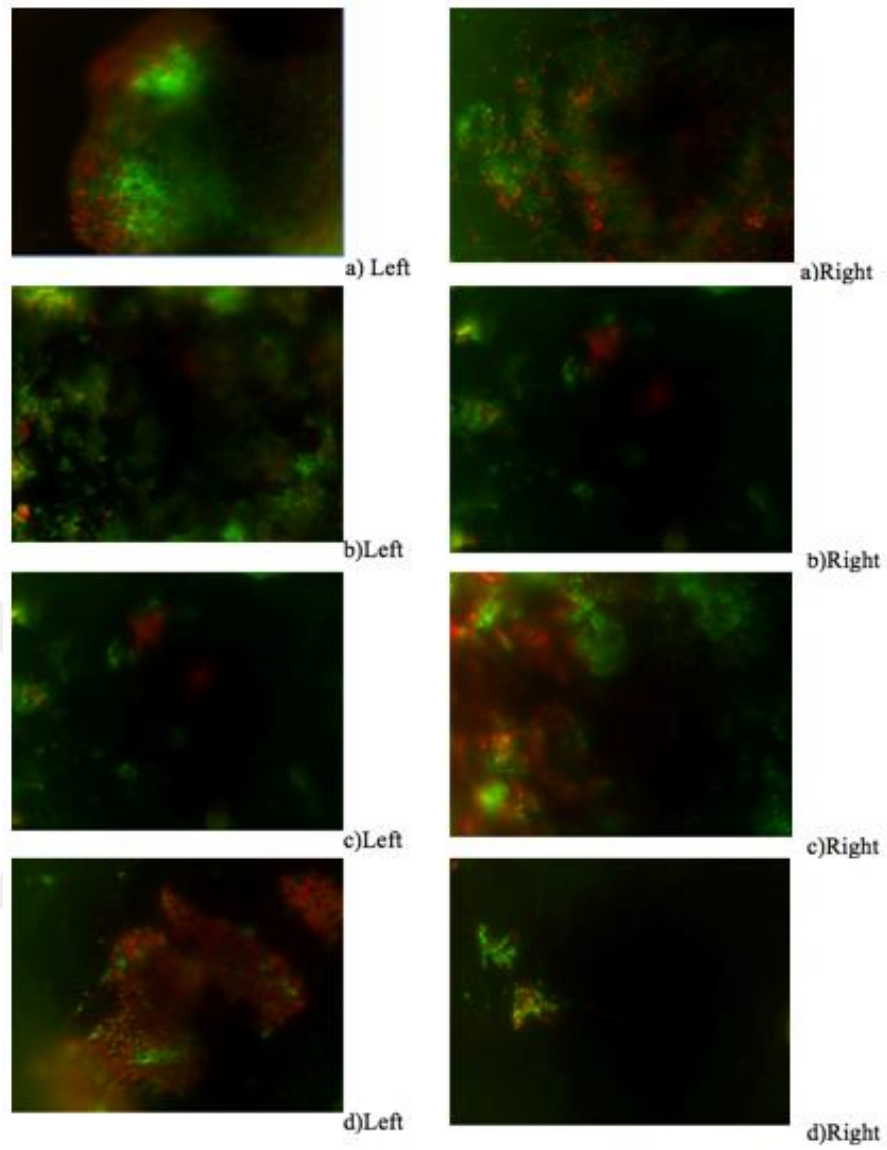
Figure 3.6: Visualization of bacteria in the 24-h biofilms on treated and untreated surfaces.

The surfaces observed from volunteer KZ. Bacterial adherence was detected using BacLight assays for each side of each volunteer, shown as left and right. (a) Control (Ti with a polished surface); (b) control (Ti with an etched surface); (c) Ti with a polished surface, coated with NWs; (d) Ti with an etched surface, coated with NWs. Original magnification: 1.000-fold
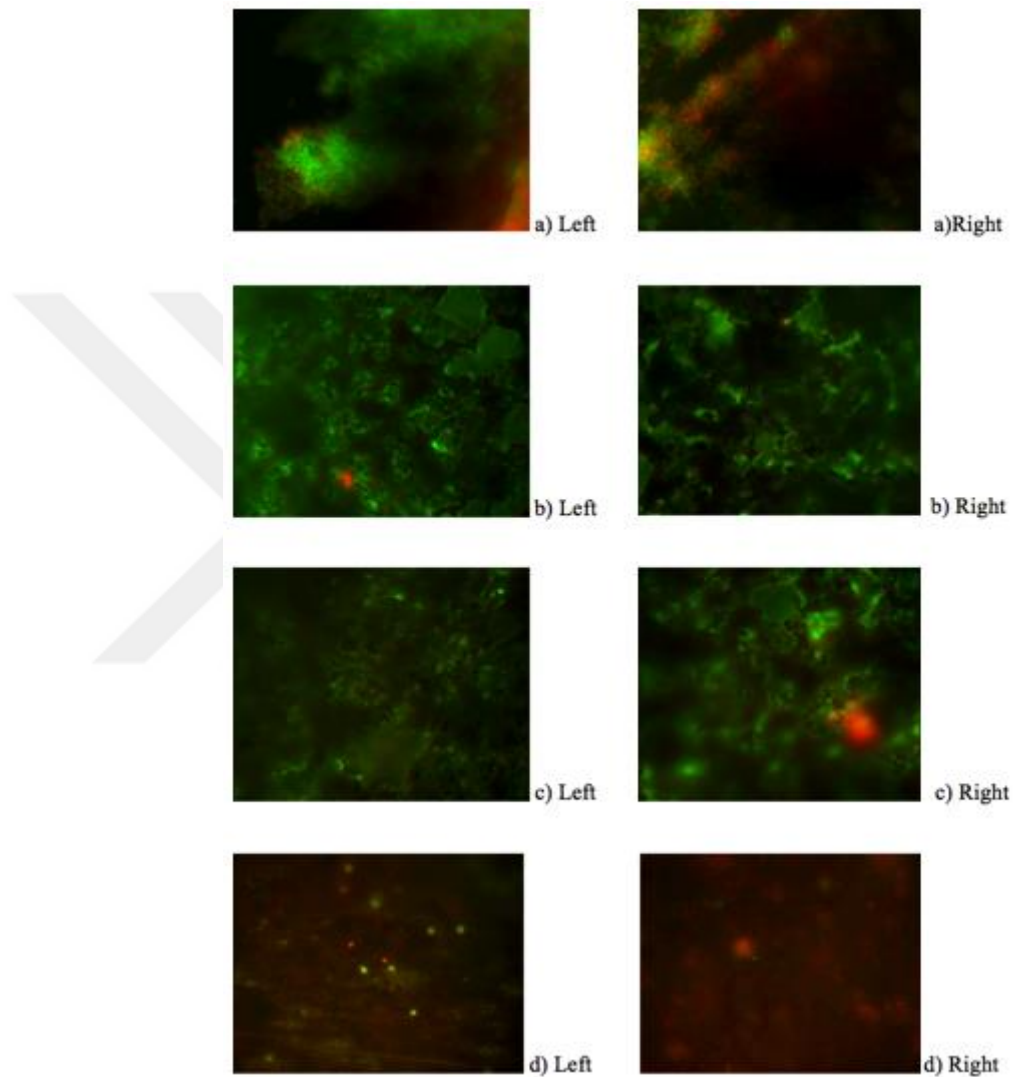
Figure 3.7: Visualization of bacteria in the 24-h biofilms on treated and untreated titanium surfaces.

Surfaces observed for SS. Bacterial adherence was detected using BacLight assays for each side of each volunteer, shown as left and right. (a) Control (polished surface); (b) control (etched surface); (c) polished surface, coated with NWs; (d) etched surface, coated with NWs.

3.2 SEM ANALYSIS

All surfaces were observed via electron microscopy, including the polished, acid-etched and laser-treated surfaces (Figure 3.8).
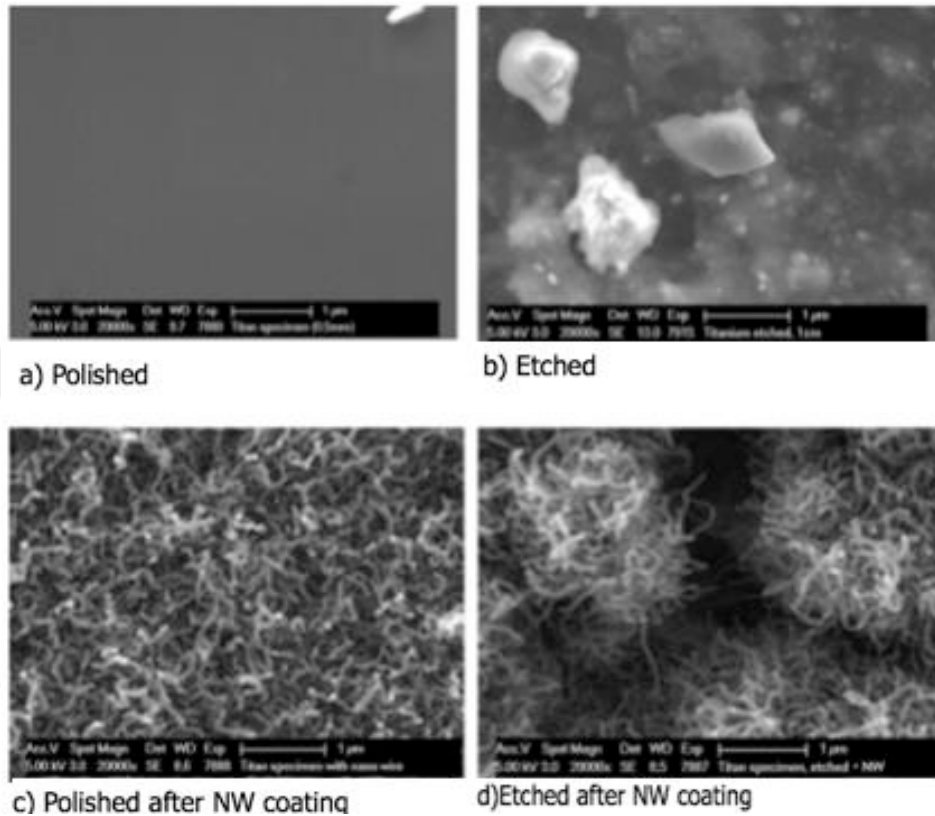
Figure 3.8: Scanning electron microscopy images of various surface nanostructures.

(a) Control (Ti with a polished surface); (b) control (Ti with an etched surface); (c) Ti with a polished surface, coated with NWs; (d) Ti with an etched surface, coated with NWs. Original magnification: 20.000X.
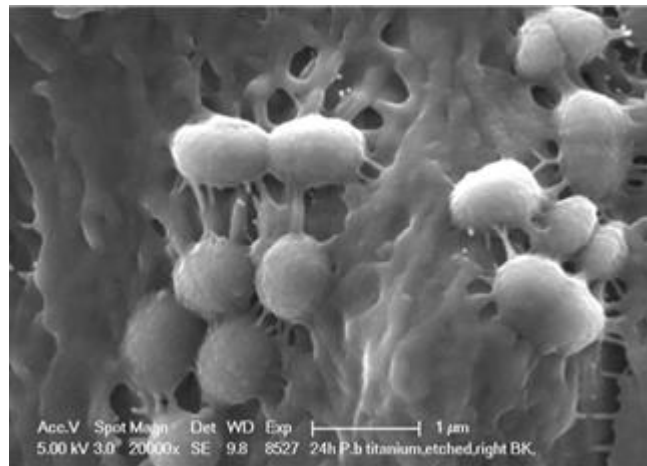
Figure 3.9: SEM micrographs of the microbial diversity of an in situ biofilm.
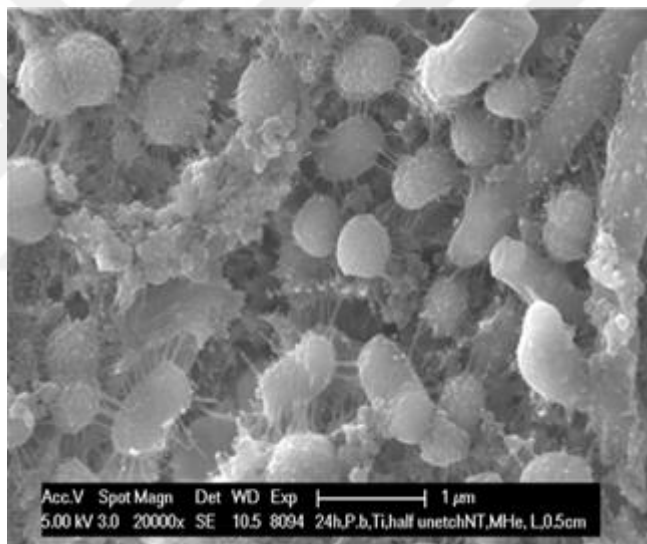
Figure 3.10: The different bacterial cell shapes, including cocci and rods, adherent to the 24-h in situ pellicle biofilm.
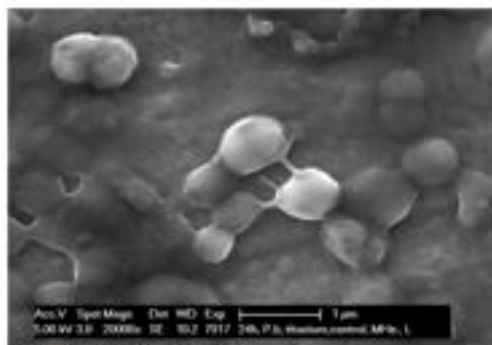
a)Polished (control)

b)Polished after coated with NWs

c)Etched after coated with NWs
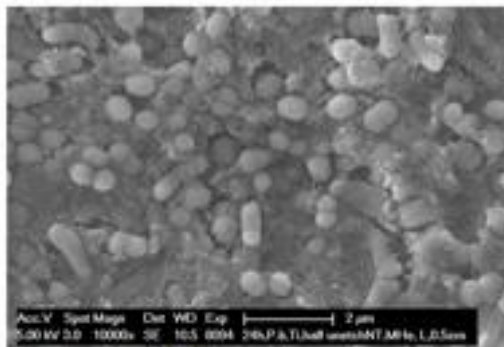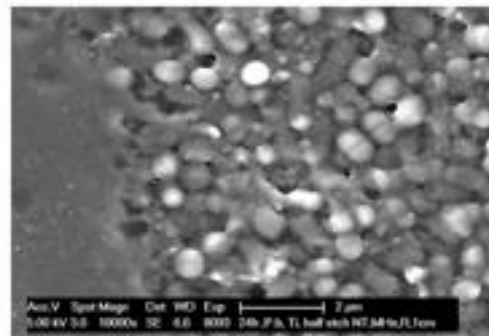
d)Coated with NTs

d)Etched after coated with NTs

Figure 3.11: SEM micrographs for MHe: biofilms on untreated and treated Ti.
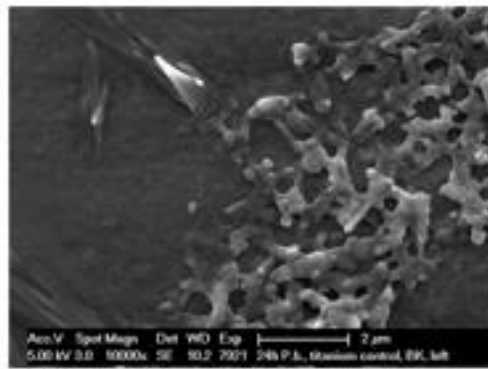
a)Polished (control)
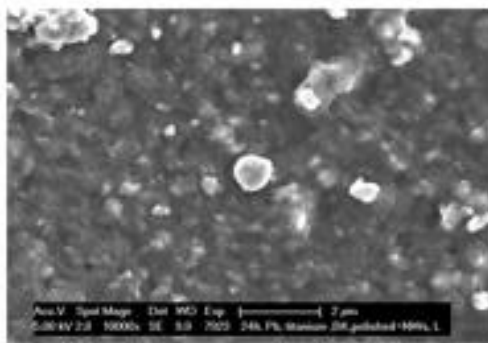
b)Polished after coated with NWs
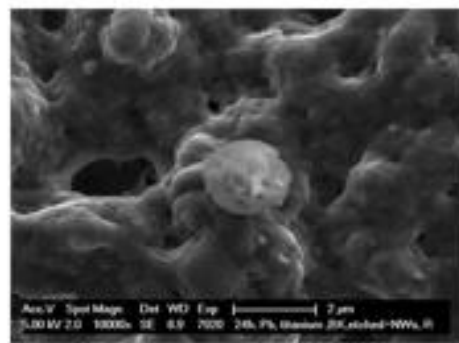
c)Etched after coated with NWs
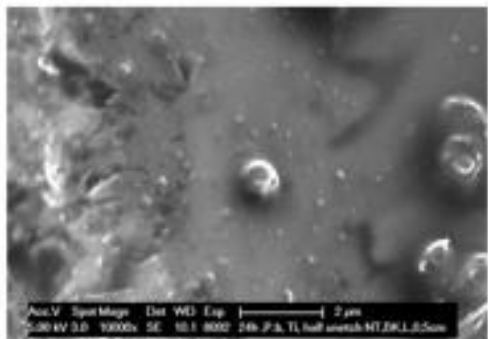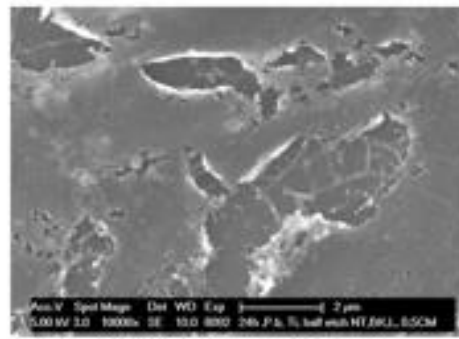
d)Coated with NTs

e)Etched after coated with NTs

Figure 3.12: SEM micrographs for volunteer BK.

a)Polished (control)

b)Etched (control)

b)Polished after coated with NWs

c)Etched after coated with NWs

d)Coated with NTs

e)Etched after coated with NTs
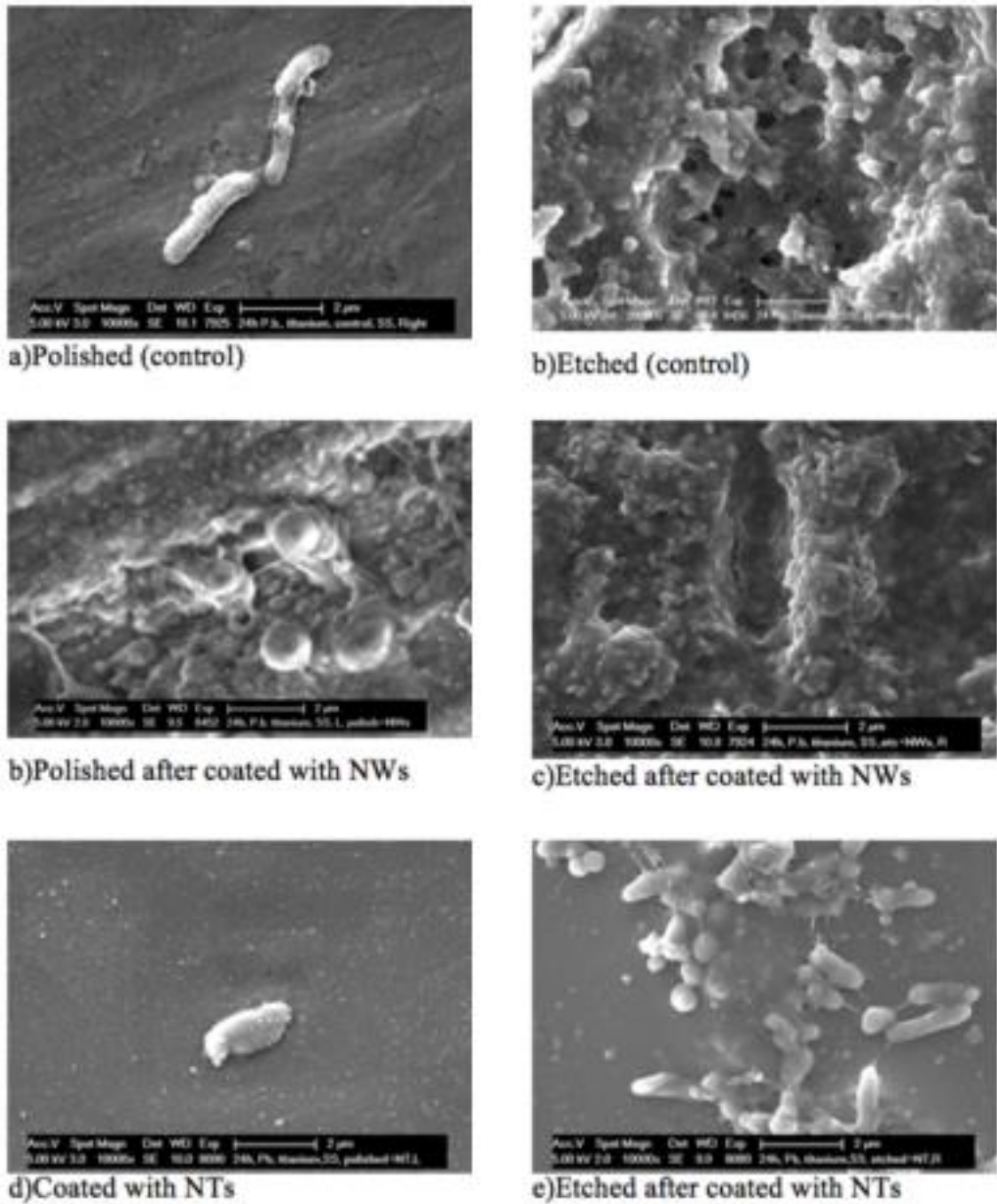
Figure 3.13: SEM micrographs for volunteer SS.

Biofilms on untreated and treated samples. Fewer bacteria are evident in the (a, d and e) 24-h biofilms.
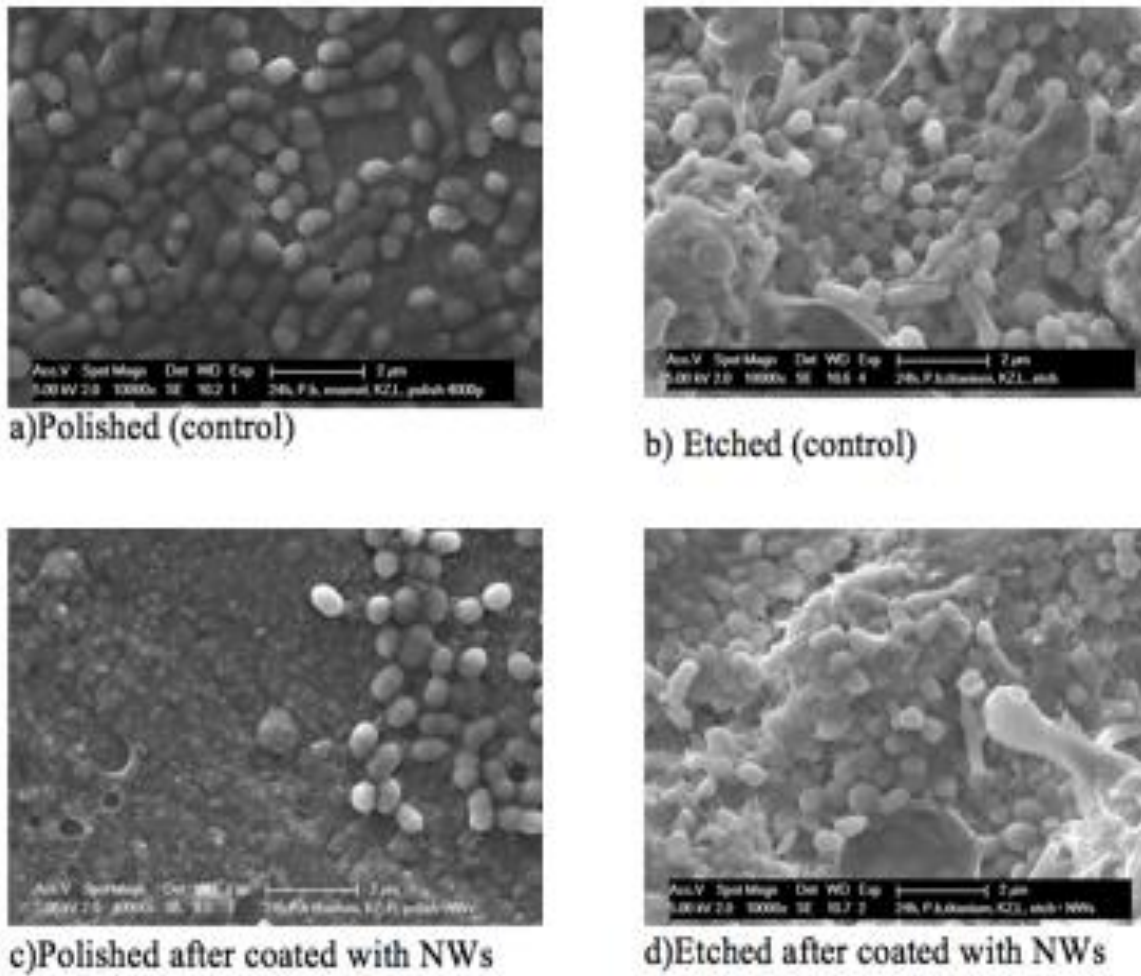
Figure 3.14: SEM micrographs for volunteer KZ.

Biofilms on untreated and treated samples. Fewer bacteria are evident in the (a and c) 24-h biofilms. Original magnification: 10.000-fold.

a) Etched (control)

b)Polished after coated with NWs

c)Etched after coated with NWs
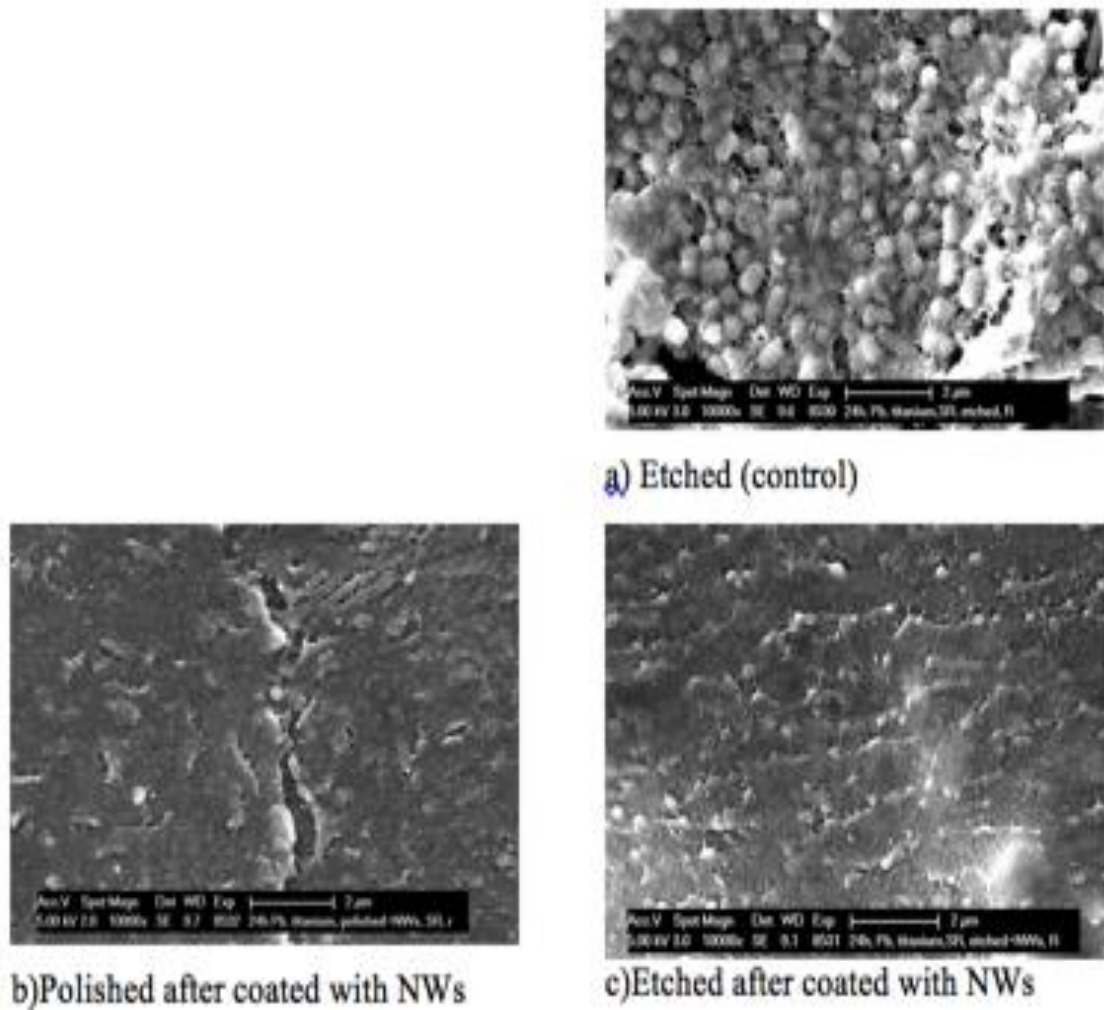
Figure 3.15: SEM micrographs for volunteer SR.

Biofilms on untreated and treated samples. Fewer bacteria are evident in the (c) 24-h biofilm. Original magnification: 10.000-fold.

a) Etched

b)Polished after coated with NWs

c) Etched after coated with NWs
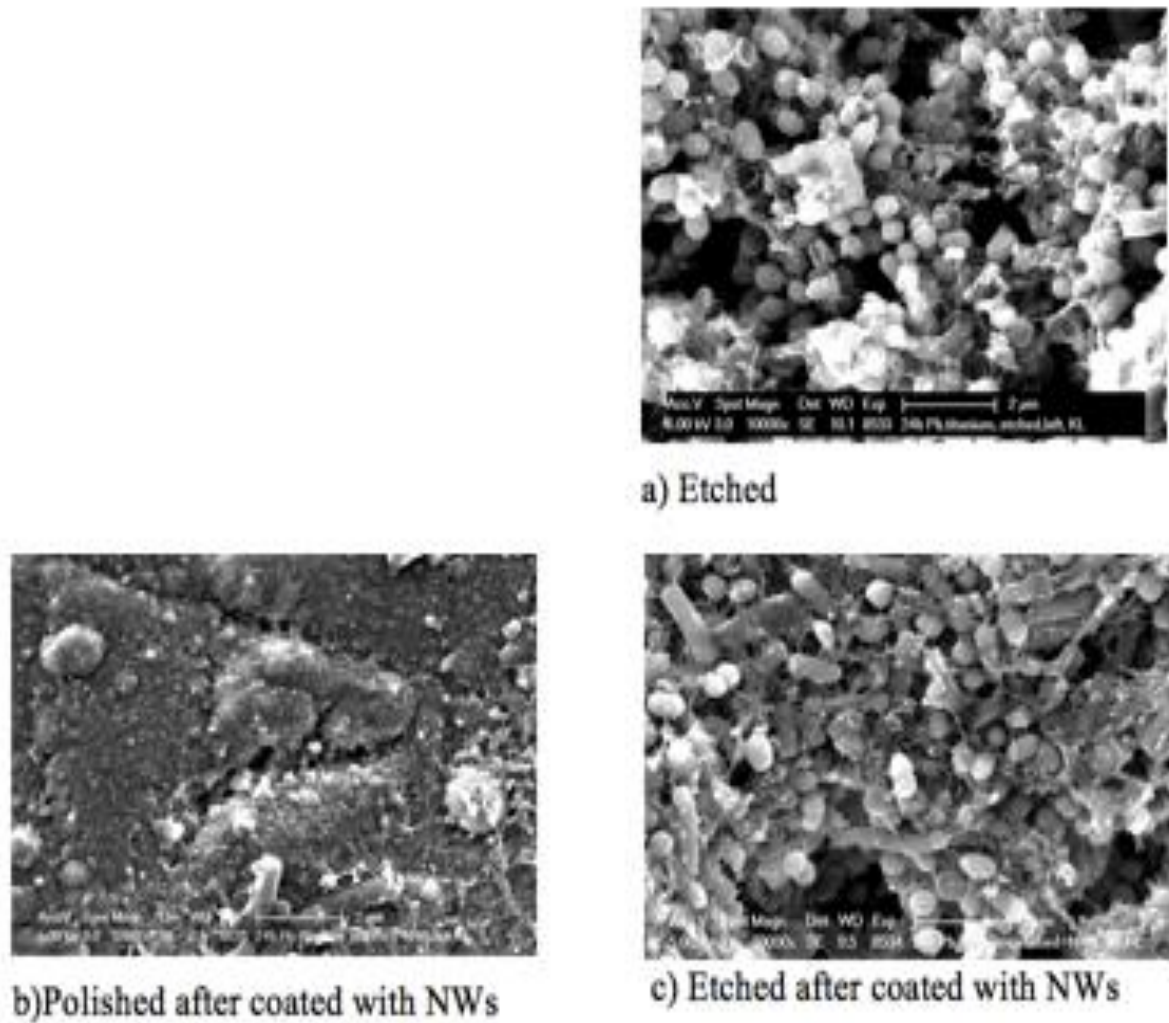
Figure 3.16: SEM micrographs for volunteer KL.

Biofilms on untreated and treated samples. There is no evidence of fewer bacteria in these 24-h biofilms. Original magnification: 10.000-fold.
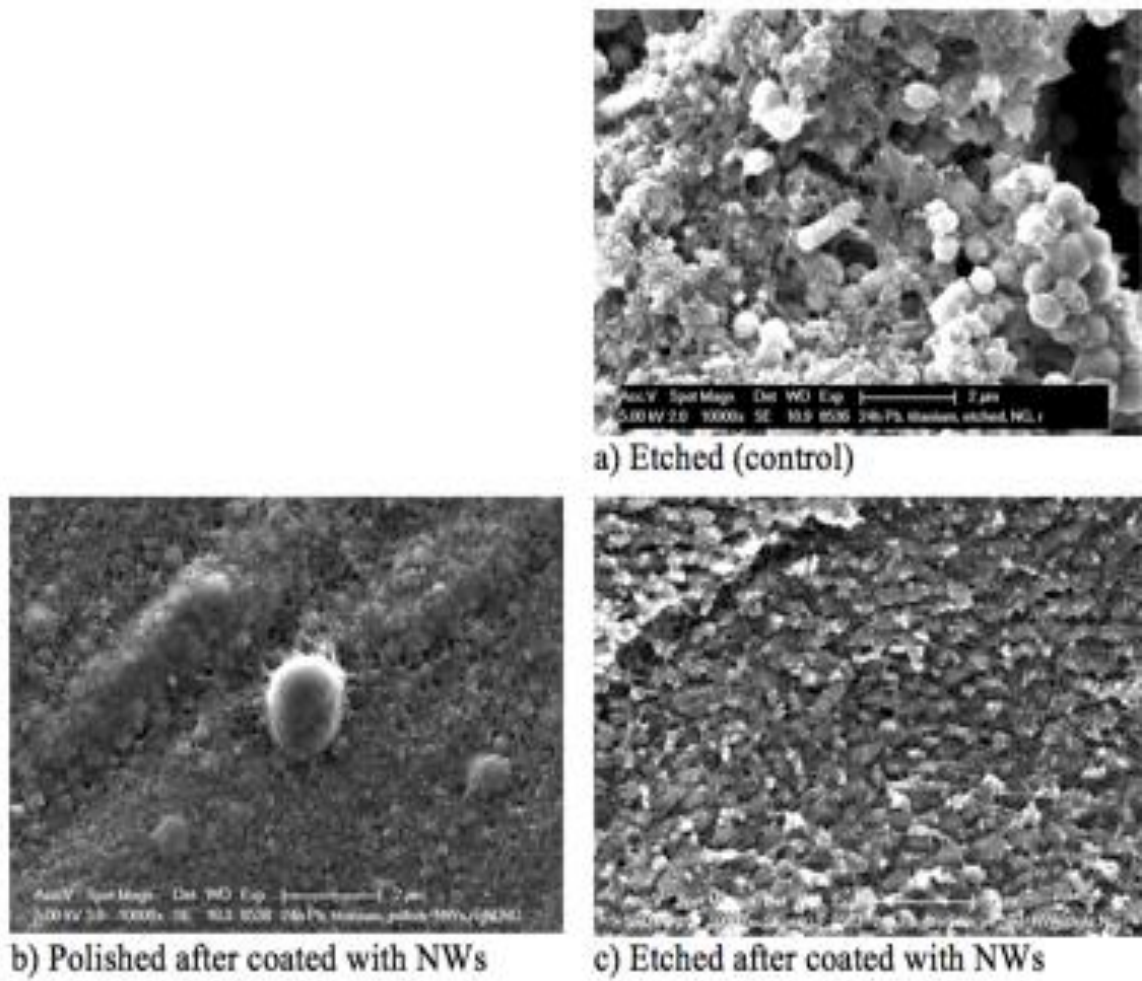
Figure 3.17: SEM micrographs for volunteer NG.

Biofilms on untreated and treated samples. There is no evidence for fewer bacteria in these 24-h biofilms. Original magnification: 10.000-fold.

a)Polished after coated with NWs   b)Etched after coated with NWs
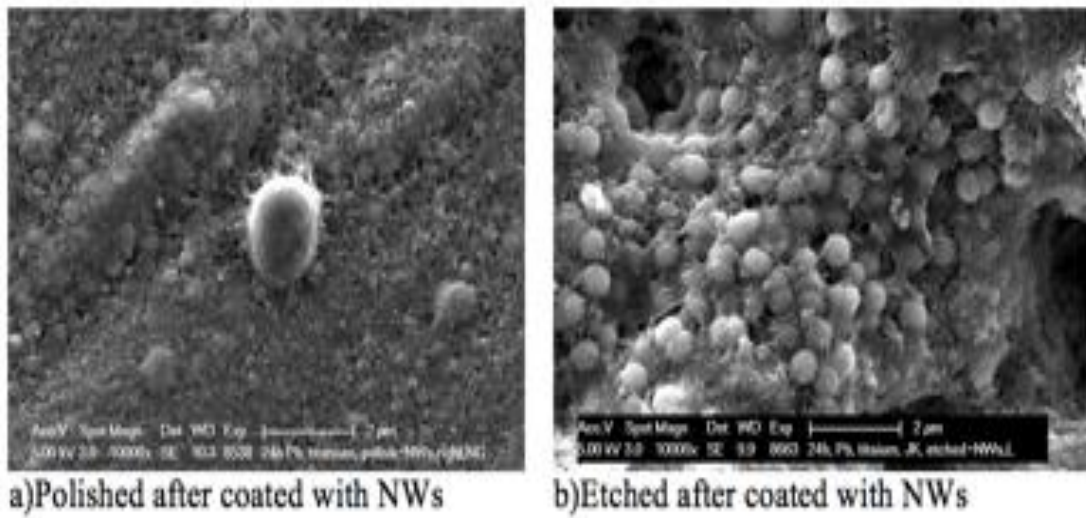
Figure 3.18: SEM micrographs for volunteer JK.

Biofilms on untreated and treated samples. Fewer bacteria are evident in the (a) 24-h biofilm. Original magnification: 10.000-fold.

a) Polished after coated with NWs   b)Etched after coated with NWs
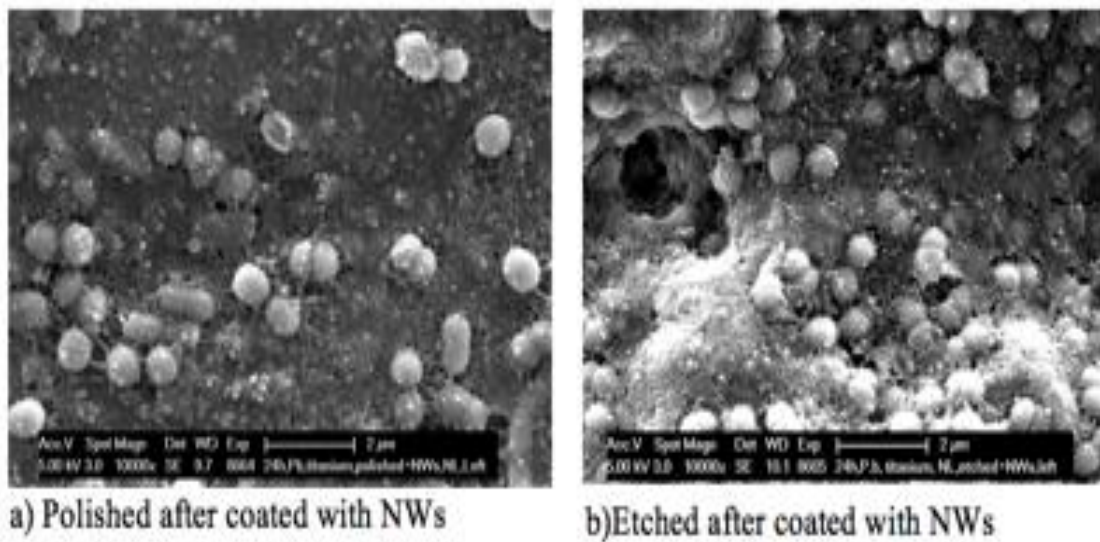
Figure 3.19: SEM micrographs for volunteer NL.

Biofilms on untreated and treated samples. Fewer bacteria are evident in the (a) 24-h biofilm. Original magnification: 10.000-fold.

Different amounts of bacteria were detected for all of the volunteers for the control surface and the raw, polished Ti surface (Figure 3.20).
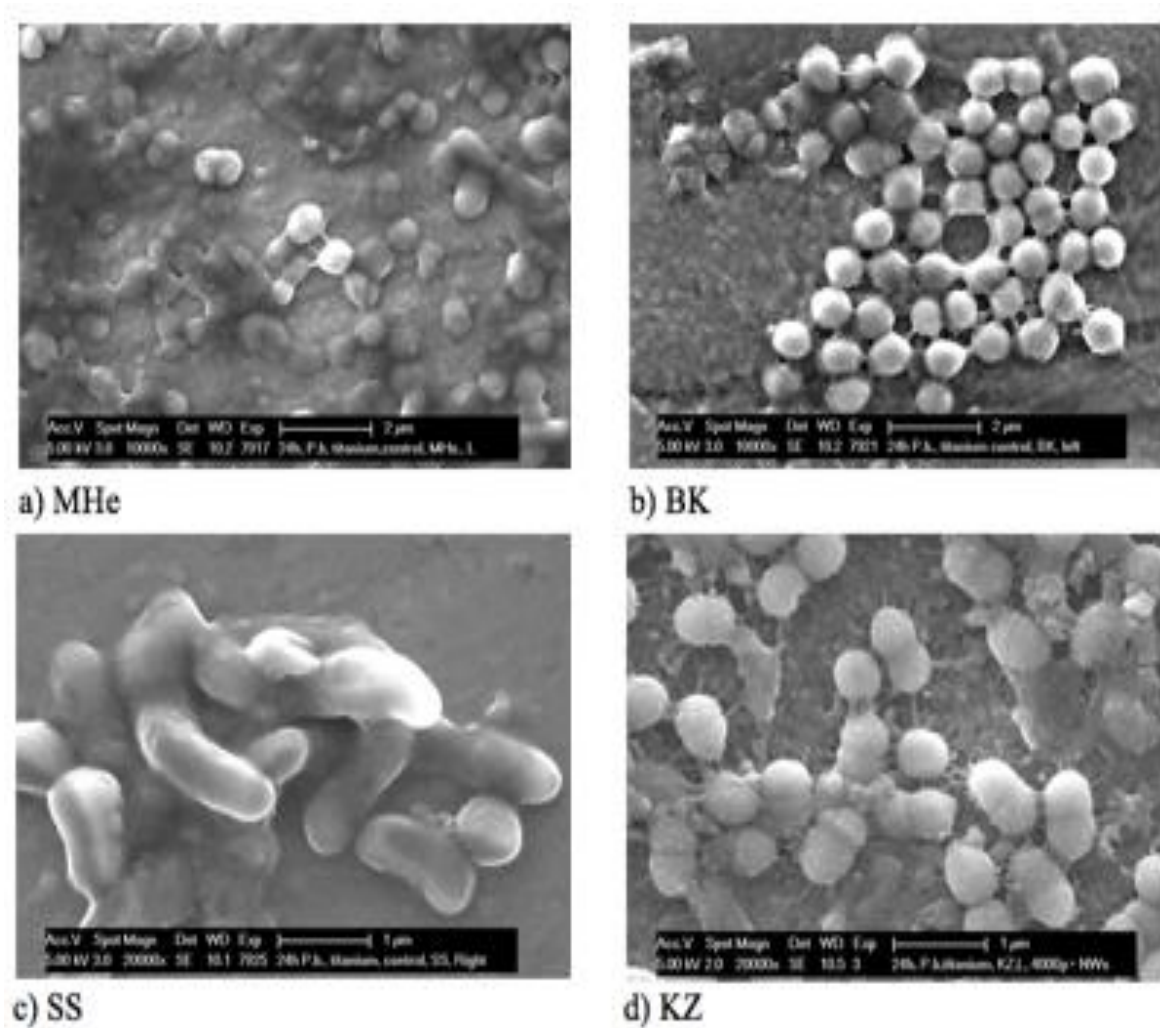
Figure 3.20: SEM micrographs for volunteers MHe, BK, SS and KZ.

Biofilms on polished titanium surfaces. Fewer bacteria are evident in the (c) 24-h biofilm. Original magnification: 20.000-fold. The results of all the volunteers were compared, and the Ti surfaces coated with NWs did not demonstrate increased bacterial attachment.
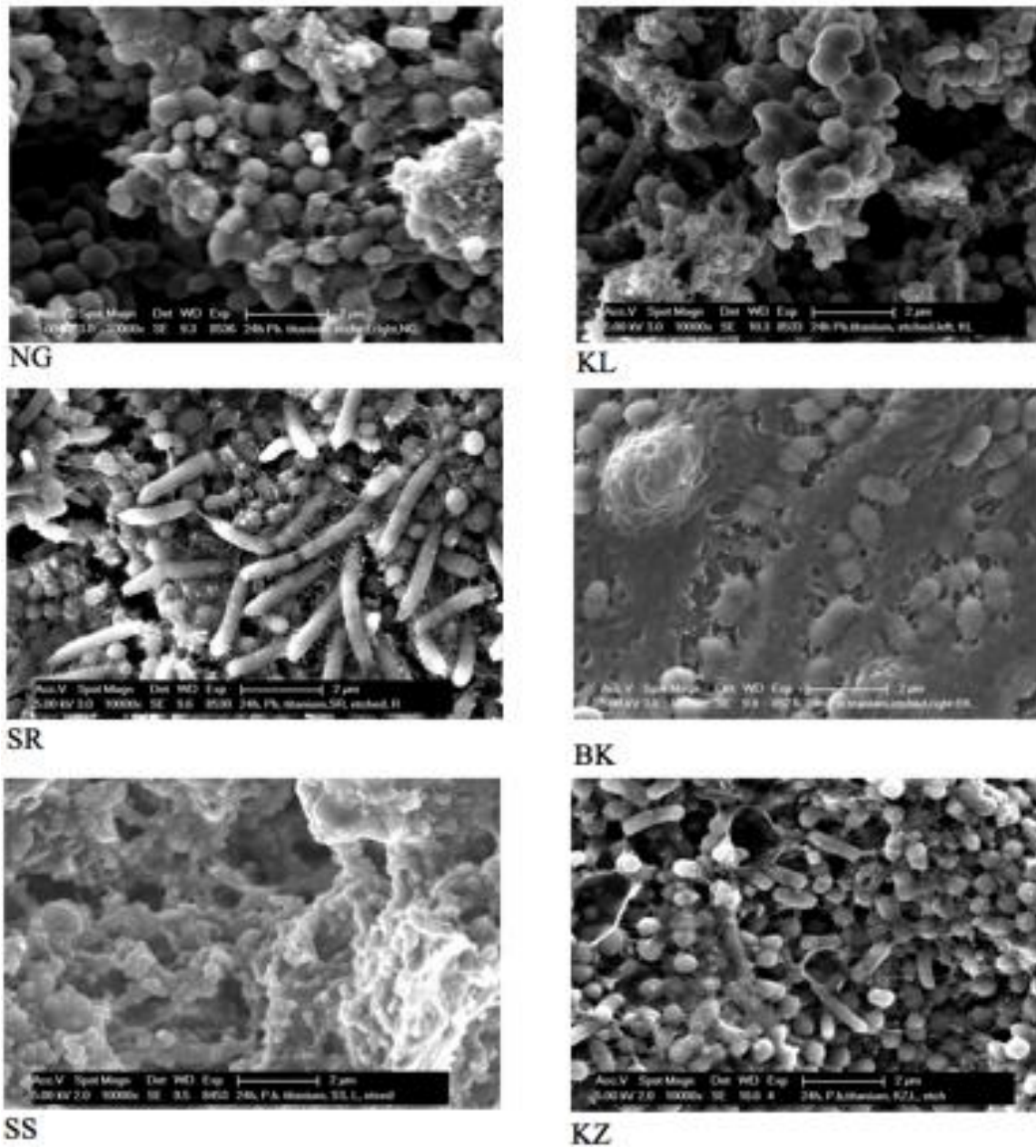
Figure 3.21: SEM micrographs for volunteers NG, KL, SR, BK, SS and KZ.

Biofilms on etched titanium surfaces. Original magnification: 20.000-fold (Figure 3.21).
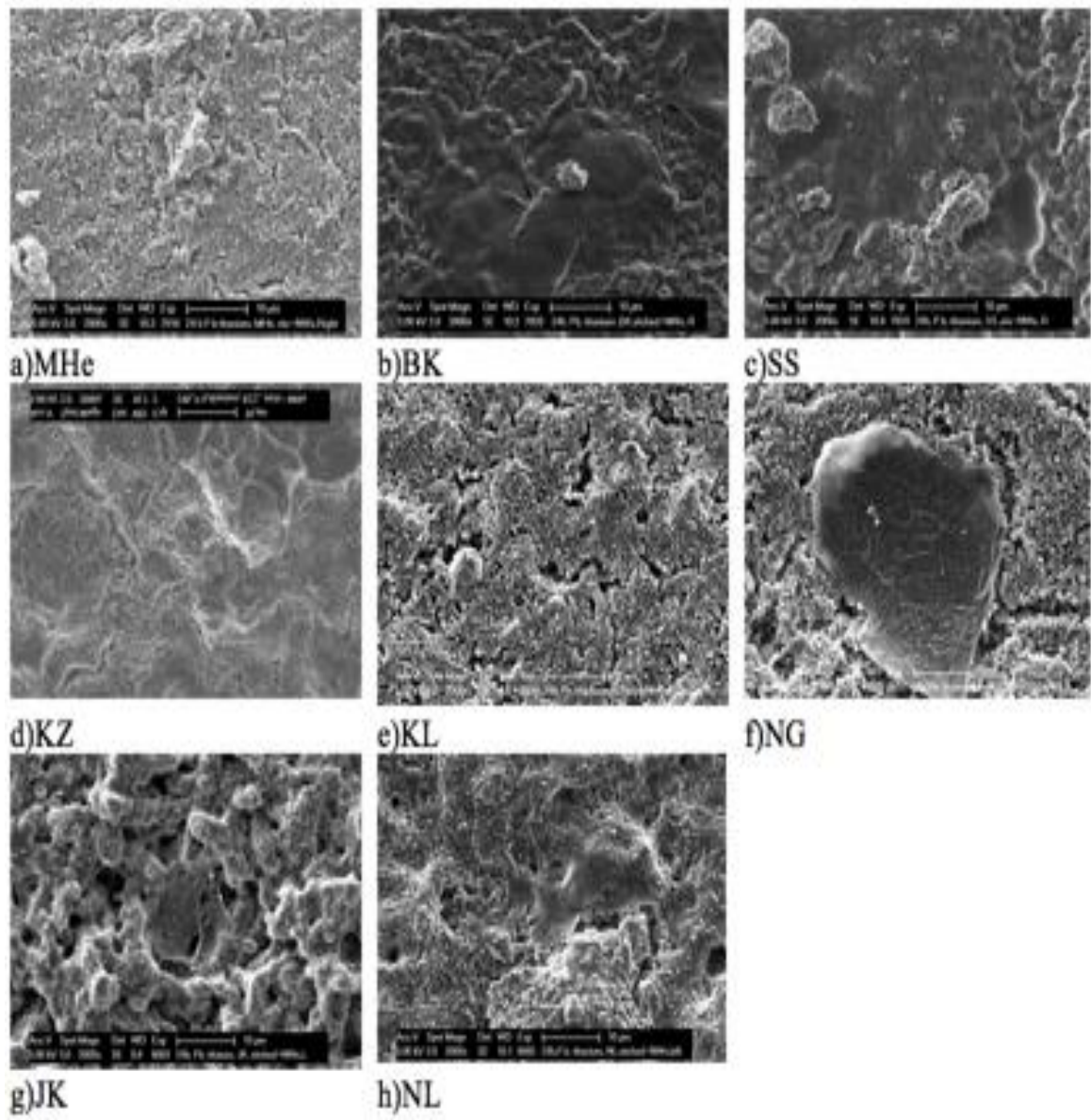
Figure 3.22: SEM micrographs for volunteers MHe, BK, SS, KZ, KL, NG, JK and NL.

Biofilm on etched titanium surfaces with NWs. Magnification: 20.000-fold (Figure 3.22).
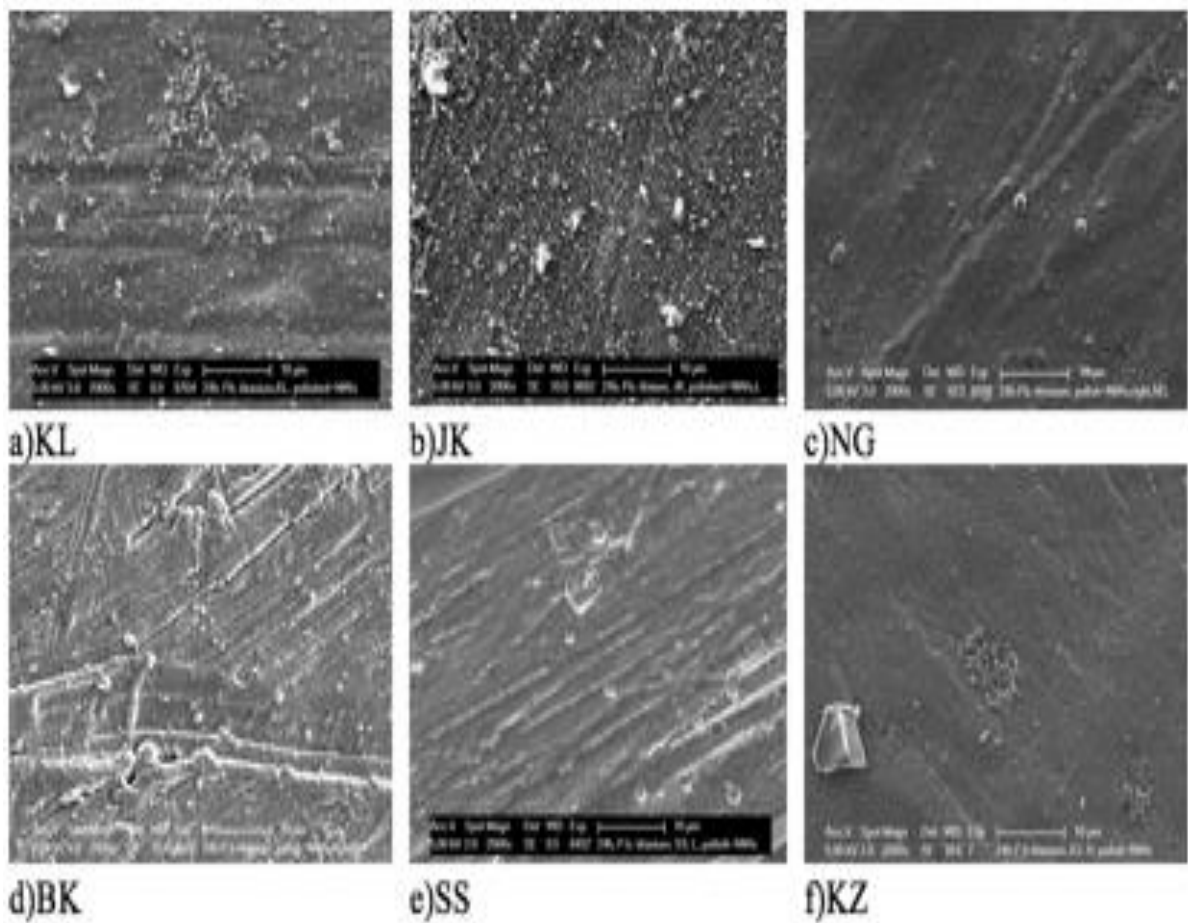
Figure 3.23: SEM micrographs for volunteers KL, JK, NG, BK, SS and KZ.

Biofilms on polished titanium with NWs. Fewer bacteria are evident on all of the biofilm surfaces. Original magnification: 20.000-fold. The results of all the volunteers were compared, and they showed that Ti coated with NTs had less bacterial attachment.

Bacteria lost their cell wall structures, and their cell outlines were unrecognizable (Figure 3.24).

Figure 3.24: SEM micrograph: rods adherent to the 24-h in situ pellicle biofilm.

Original magnification: 20.000-fold. Another interesting observation was that epithelial cells were detected on polished titanium surfaces, as shown in Figure 3.25.
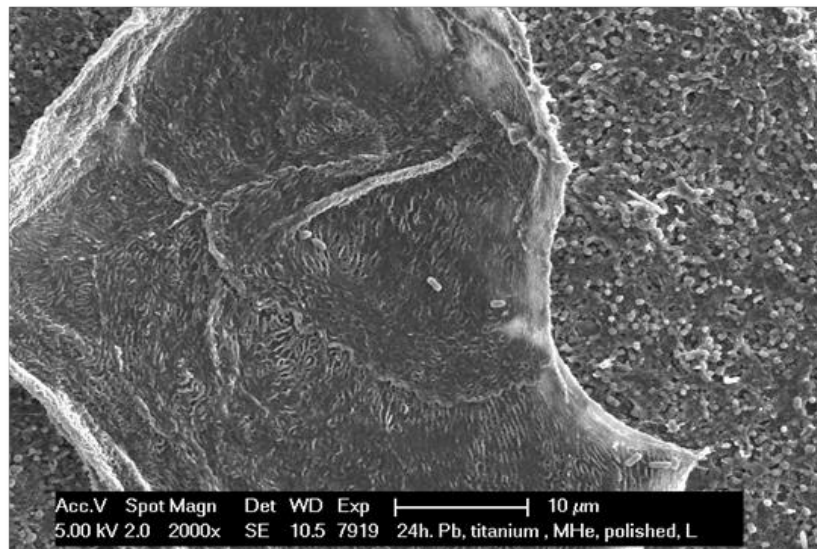
Figure 3.25: SEM micrographs: an epithelial cell adhering to the 24-h in situ pellicle biofilm.

a)Titanium Surface   b)Titanium surface covered   c)The streptococci attached

with salivary proteins   on the salivary proteins
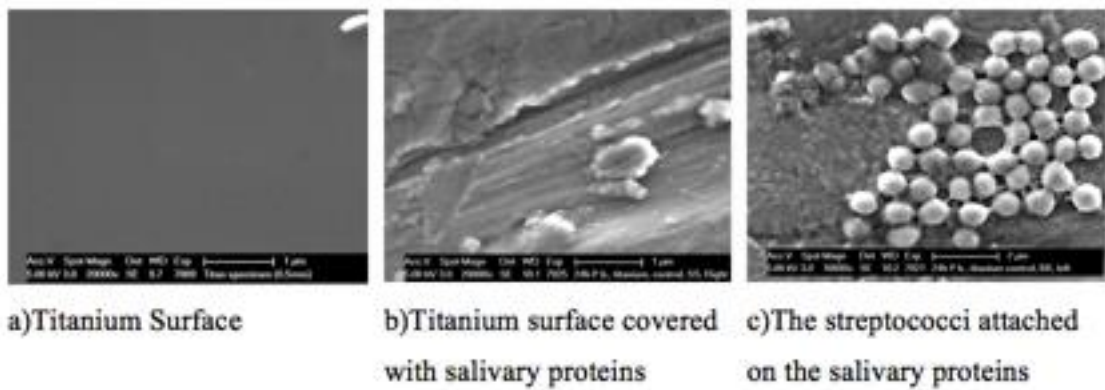
Figure 3.26: The mechanisms of biofilm formation.

SEM micrographs: the image in a) shows a titanium surface without in situ biofilm formation. The image in b) shows salivary proteins adhering to a 24-h in situ pellicle biofilm. The image in c) shows streptococci attached to the salivary proteins in the in situ pellicle. Original magnification: 2.000-fold.

Most of the bacterial species found in the oral biofilm belong to microbial communities, some of which are shaped differently than streptococci such as *Streptococcus salivarius*, *Streptococcus mutans* and *Streptococcus sanguinis*. The first layer of bacteria commonly includes *Streptococcus* species (Figure 3.27-a.). Other recognizable bacteria are *Fusobacterium nucleatum* due to its shape; this bacterium is bacilli shaped during late biofilm formation (Figure 3.27-b.).
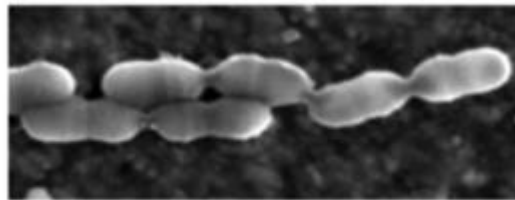
a) Streptococcus on a biofilm surface
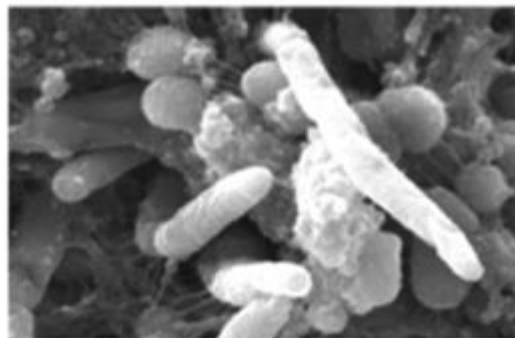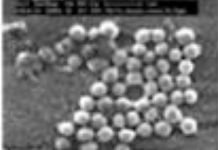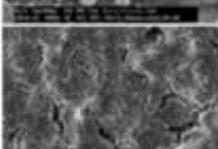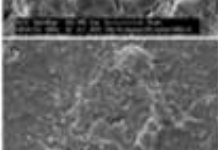
b) Fusobacterium nucleatum on a late biofilm surface

Figure 3.27: The different types of bacteria on the biofilm surface.

SEM micrographs: the image in a) shows a titanium surface without in situ biofilm formation. The image in b) shows salivary proteins adhering to the 24-h in situ pellicle biofilm. The image in c) shows streptococci attached to the salivary proteins in the in situ pellicle. Original magnification: 2.000-fold.

Formation of a biofilm begins with attachment to a Ti surface. (Figure 3.28).

Biofilm Stage	Surface	Explanation
0 Raw surface		Reversible attachment of free swimming microorganisms to the Ti surface.
1 Initial attachment		To reversible attachment pf free swimming microorganisims to the Ti surface.
2 Irreversible attachment.		Bacteria that can weather shear forces maintain a steadfast grip on the Ti surface". Please change the fourth explanation to
3 Maturation I		Complex architecture, channels, and pores are generated, and bacteria are redistributed away from the substratum
4 Dispersion		Bacteria detach from the surface and attach to other areas

Figure 3.28: The five stages of biofilm development.

Stage 0: A raw surface without any biofilm formation. Stage 1: Initial attachment in which a few bacteria can be detected on the surface. Stage 2: Irreversible attachment, where one layer of bacteria accumulates on the surface; this attachment becomes irreversible. Stage 3: A biofilm is formed and matures; cells form multi-layered clusters with 3-D growth, leading to further maturation of the biofilm on the Ti surface.

3.3 EDX SURFACE ANALYSIS

EDX detected the different biofilm layers as titanium, modified surface (machined, nanostructure), artifacts and carbon (Figure 3.29).
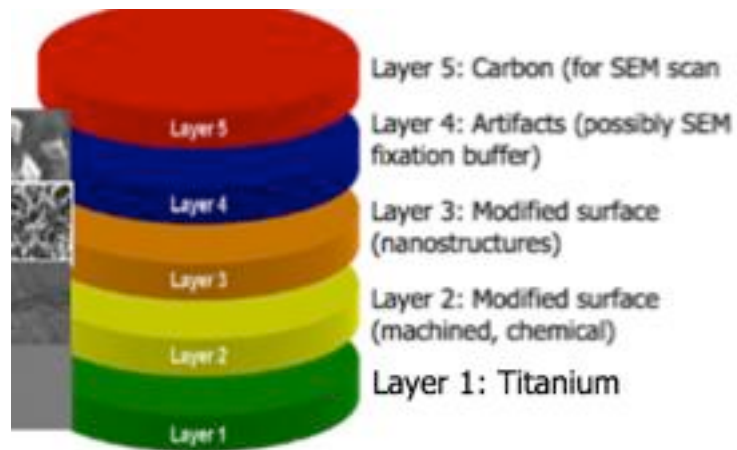
Figure 3.29: The sample layers of biofilm formation.

The layers could be categorized as layers 1 to 5, and SEM images of all the layers are shown on the left side of the figure. Backscatter images taken under low, medium, and high eV showed apparent differences in the elemental compositions of the polished surface. Ti had the highest amount, followed by oxygen and carbon. Each polished surface was analyzed using 5, 10, and 20 eV channels.

Table 3.1: Composition at 5, 10, and 20 eV for the polished Ti surface.

Elements % / eV	5	10	20
C	71	57	31
Ti	7	14	45
O	16	18	21
Si	6	8	2
Al	0	0	0
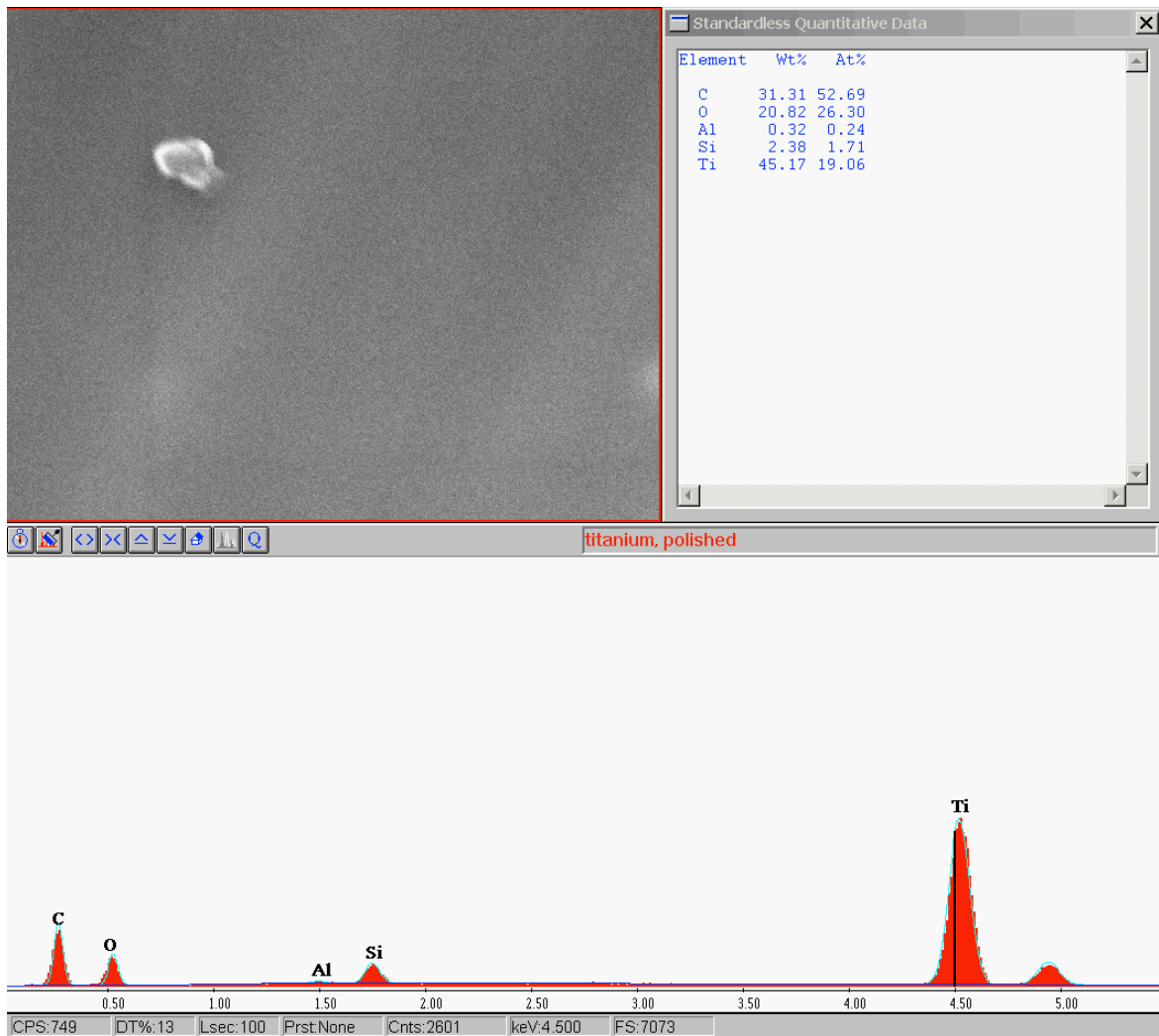
Figure 3.30: EDX spectra of a polished Ti surface.

The upper left panel shows a wide view of a Ti polished surface. The upper right panel shows the elemental amounts. The lower graph shows the EDS results. C, O, Si, Al, and Ti were the main elements at the surface.
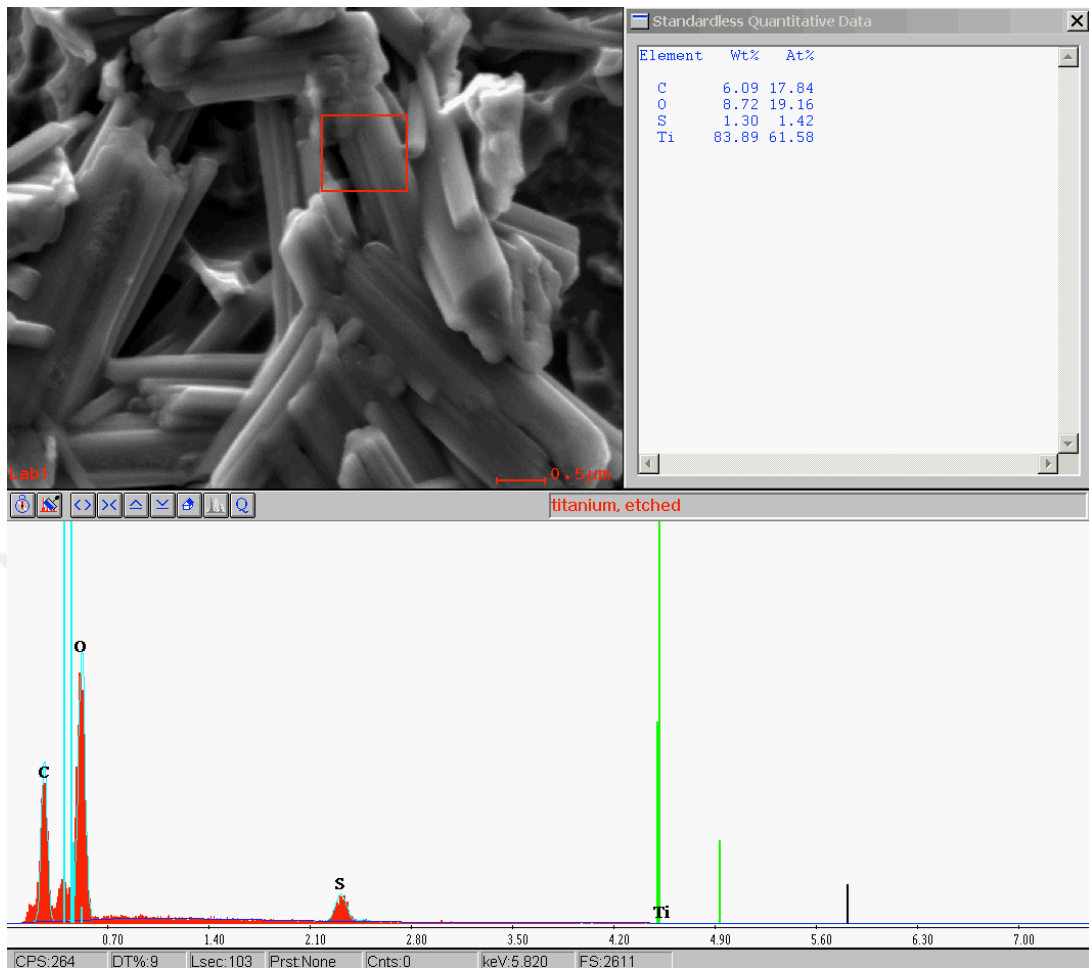
Figure 3.31: EDX spectra of an etched surface.

The upper left panel shows a wide view of an etched Ti surface. The upper right panel shows the elemental amounts. The lower graph shows the EDS results.
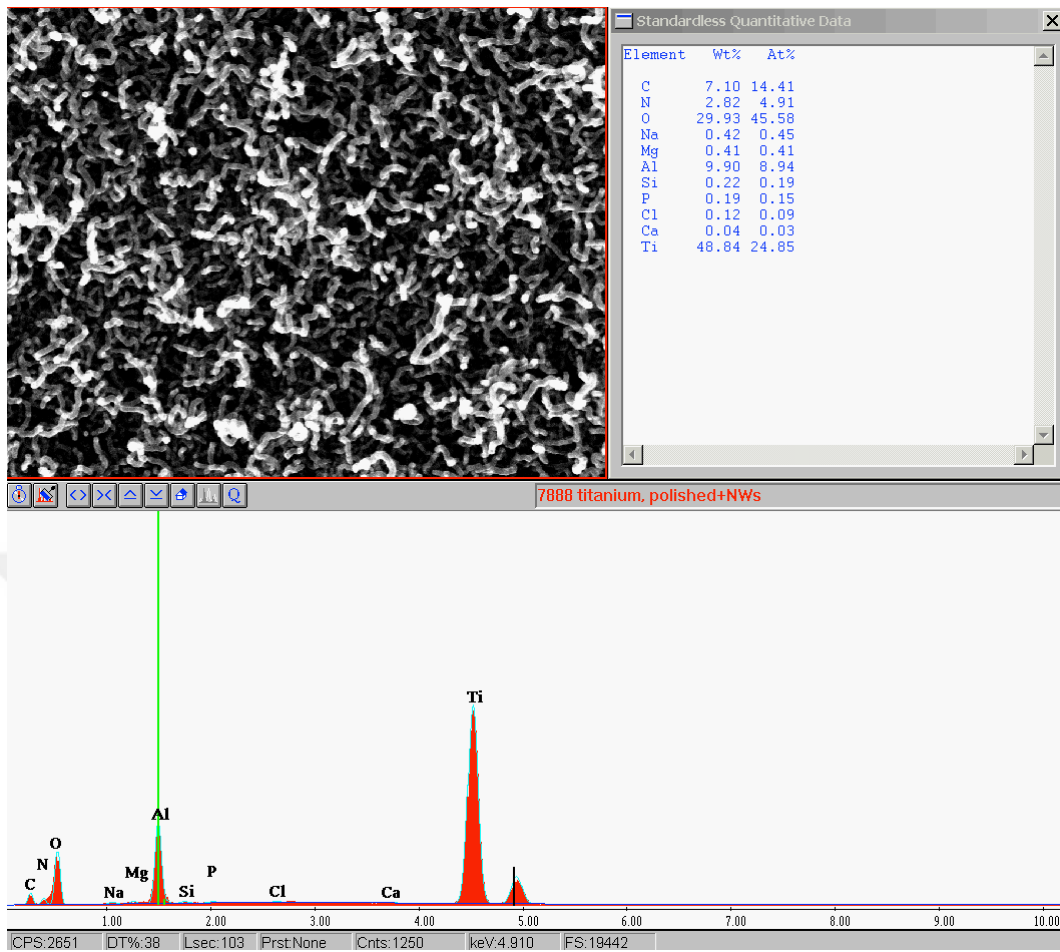
Figure 3.32: EDX spectra of a polished Ti surface with NWs.

The upper left panel shows a wide view of a polished Ti surface with NWs. The upper right panel shows the elemental amounts. The lower graph shows the EDS results. The surface was composed of C, O, S, and Ti elements.
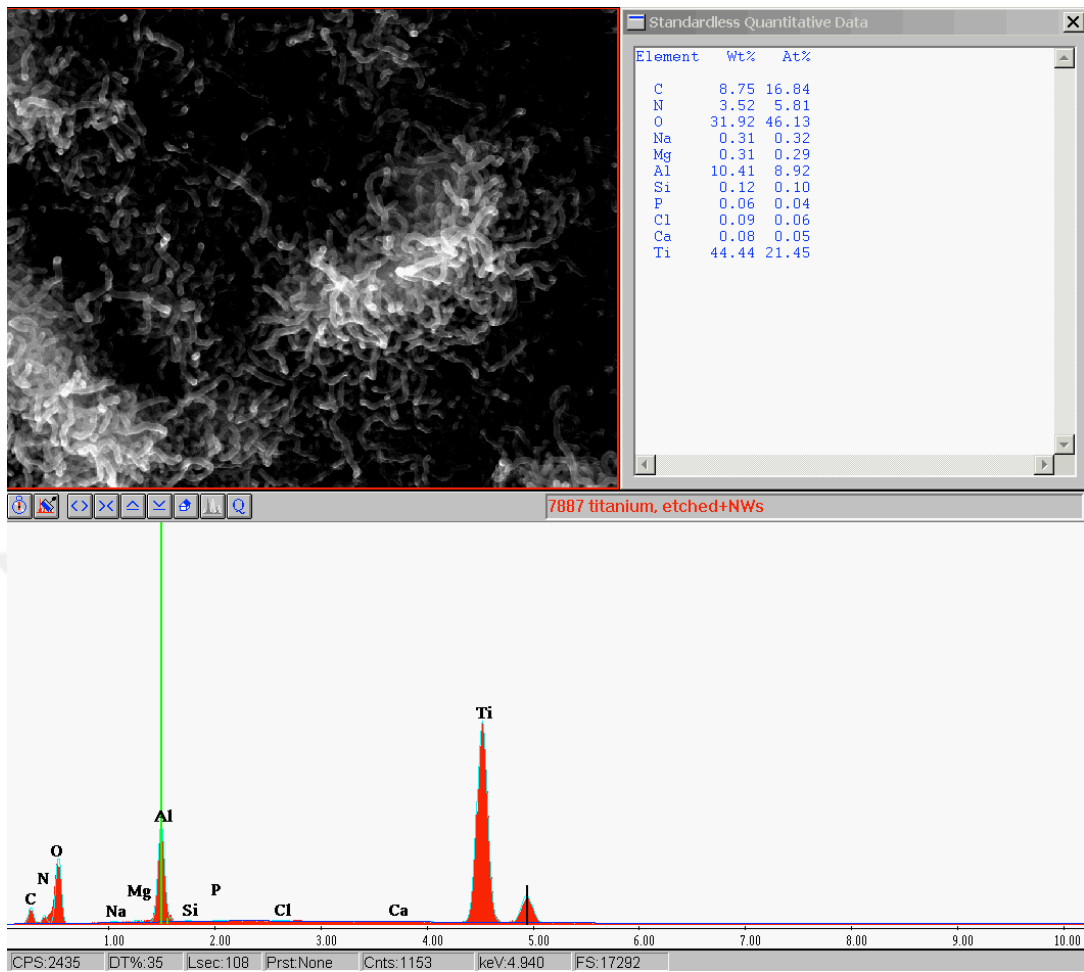
Figure 3.33: EDX spectra of an etched Ti surface with NWs.

The upper left panel shows a wide view of an etched Ti surface with NWs. The upper right panel shows the elemental amounts. The lower graph shows the EDS results. C, O, S, and Ti were the main elements.

Tables 3.2 and 3.3 show the EDX results for each prepared surface in 5, 10 or 20 eV channels.

Table 3.2: Composition at 5, 10, and 20 eV for the etched Ti surface.

Elements % /eV	5	10	20
C	6	6	8
Ti	83	83	63
O	8	8	16
Si	1	1	2
Al	0	0	0

Table 3.3: Composition for the polished Ti surface with NWs and the etched Ti surface with NWs.

	Polished+NWs			Etched+NWs		
Elements % / eV	**5**	**20**	**20**	**5**	**10**	**20**
C	29	14	7	8	15	8
O	28	34	29	31	30	31
Ti	0	21	48	44	24	44
Si	42	29	9	10	25	10
Al	0	0	2	3	2	3

Table 3.4: Composition of the polished Ti surface with NTs and the etched Ti surface with NTs.

Elements eV/Wt%	Polished+NTs			Etched+NTs		
	5	10	20	5	10	20
Tİ	51	51	58	40	40	57
o	12	12	12	13	13	10
N	6	6	7	4	4	4
C	21	21	17	37	36	24
Sİ	3	3	1	4	4	2

This technique provides elemental details for in situ biofilm formation. The eV level of the channel explains the percentage of the elements for the 24-h in situ biofilm formation of volunteer MHe (Figure 3.34).

	Polished			Etched+NWs			Polished+ NTs			Etched+NTs		
	5kv	10kv	20kv	5kv	10kv	20kv	5kv	10kv	20kv	5kv	10kv	20kv
N	28	28	8	0	0	0	6	9	5	7	9	8
O	25	19	10	7	14	16	17	10	9	7	6	6
Al	0	0	0	5	19	9	0	0	3	0	0	0
Si	0	0	0	0	0	0	5	0	1	6	0	5
P	0	0	0	0	1	0	0	1	0	0	1	0
Cl	0	0	0	0	0	0	0	0	0	0	0	0
Ti	0	19	65	15	4	42	5	0	24	0	0	6
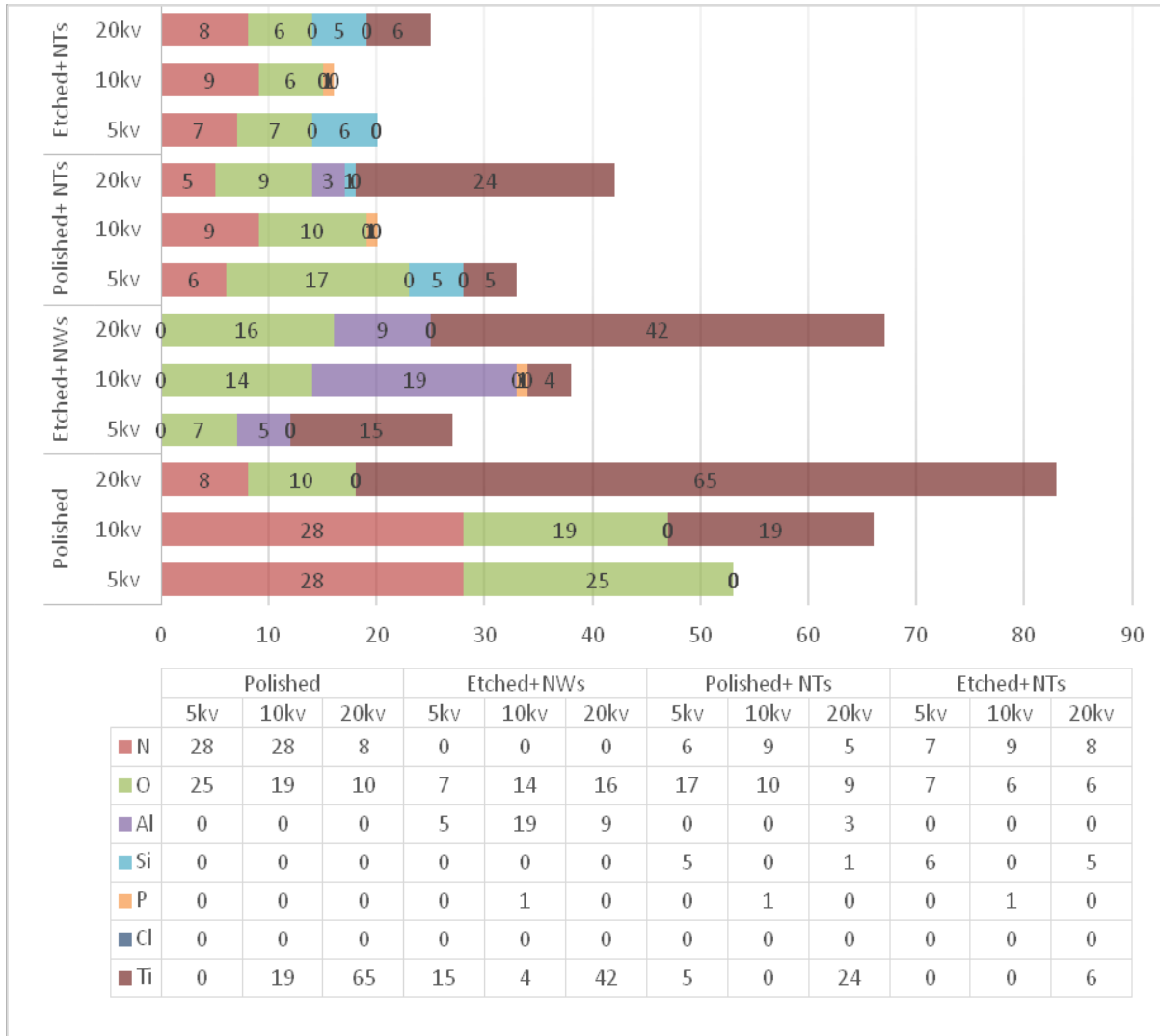
Figure 3.34: EDX results for MHe.

Complete surface analysis for 5, 10 and 20 eV wide channels. The EDX results of the other volunteers confirm each other, for example, BK and SS 3.

Table 3.5: EDX results for volunteer BK for 5, 10 or 20 eV wide channels.

	Polished			Etched			Polished+NWs			Etched+NWs		
Elements eV/Wt%	5	10	20	5	10	20	5	10	20	5	10	20
C	13	12	10	58	5	7	46	34	24	71	51	30
N	8	10	10	7	2	4	0	0	0	9	4	0
O	10	11	6	9	2	2	24	29	29	9	16	16
Al	0	0	0	0	0	0	7	8	10	0	20	9
Si	0	0	0	0	0	0	17	0	7	0	0	0
Ti	68	66	72	8	83	83	0	6	21	0	7	42

Table 3.6: EDX results for volunteer SS for 5, 10 or 20 eV wide channels.

	Polished			Etched			Polished+NWs			Etched+NWs		
Elements eV/Wt%	5	10	20	5	10	20	5	10	20	5	10	20
C	63	20	17	49	24	22	8	5	3	42	24	18
N	20	10	8	5	4	4	2	2	1	2	2	2
O	16	9	9	8	7	5	38	44	41	21	32	36
Al	0	0	0	0	0	0	41	33	17	25	25	18
Si	0	0	0	5	1	0	0	0	0	1	0	0
Ti	0	60	64	26	59	65	1	11	34	2	10	22

3.4 BACTERIA IN THE BIOFILMS

Total bacteria determined by SEM Imaging

BacLight viability assays were used to study the microorganisms on the samples at the buccal sites of the upper 1st and 2nd molars after 1 day. Significant differences between the surface conditions (treatments) were found using ImageJ software.
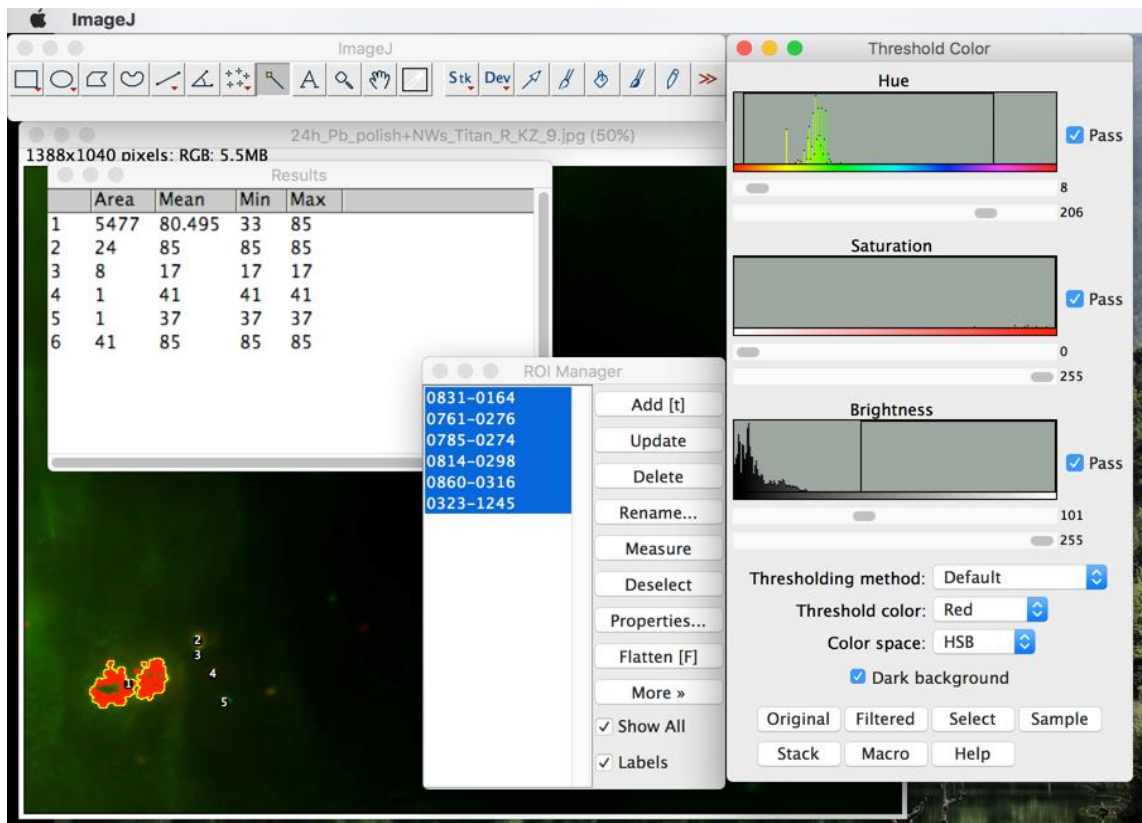
Figure 3.35: Bacteria and the minimum and maximum biofilm values.

ImageJ was used to set the color threshold and to calculate the means. Inter-subject variability was observed.
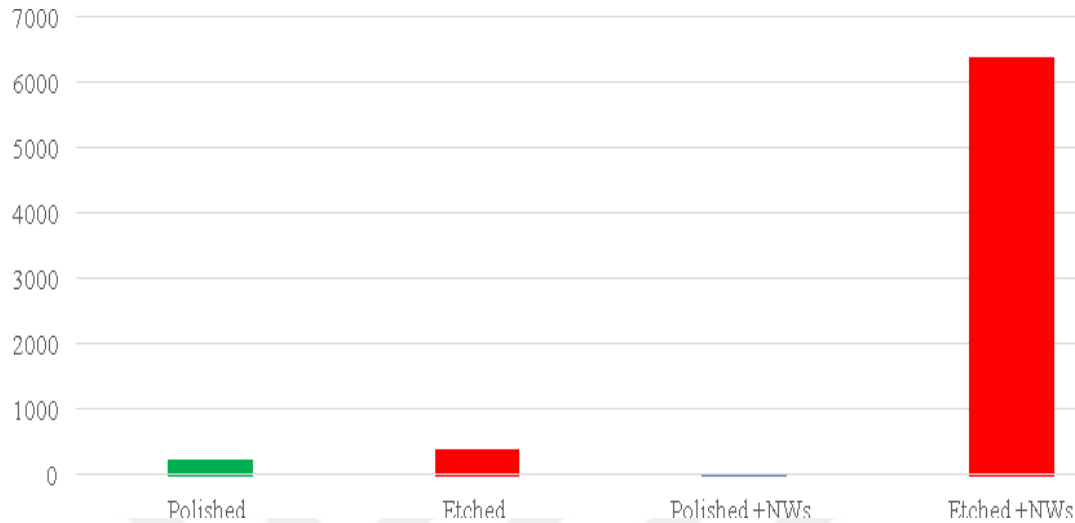
Figure 3.36: Bacteria on the polished, etched, polished+NWs, and etched+NWs surfaces.

A significant difference was observed using ImageJ software. The Y axis indicates the quantity of bacteria, and the X axis denotes the surface properties. Compared to the controls, bacterial growth on polished surface specimens was reduced after treatment.

Live/dead analysis of total bacterial colonization

Using BacLight tests, the adherence of live and dead bacteria in the biofilm was assessed.

Table 3.7: Live/dead bacterial biofilm colonization assessed by BacLight assays.

Volunteer/ Surface	Polished		Etched		Polished+NWs		Etched+NWs	
	Live	Dead	Live	Dead	Live	Dead	Live	Dead
KZ	196	65	317	158	13	4	780	230
SS	177	69	297	29	10	6	2842	8927
Average	186	67	307	93	12	5	1811	9157
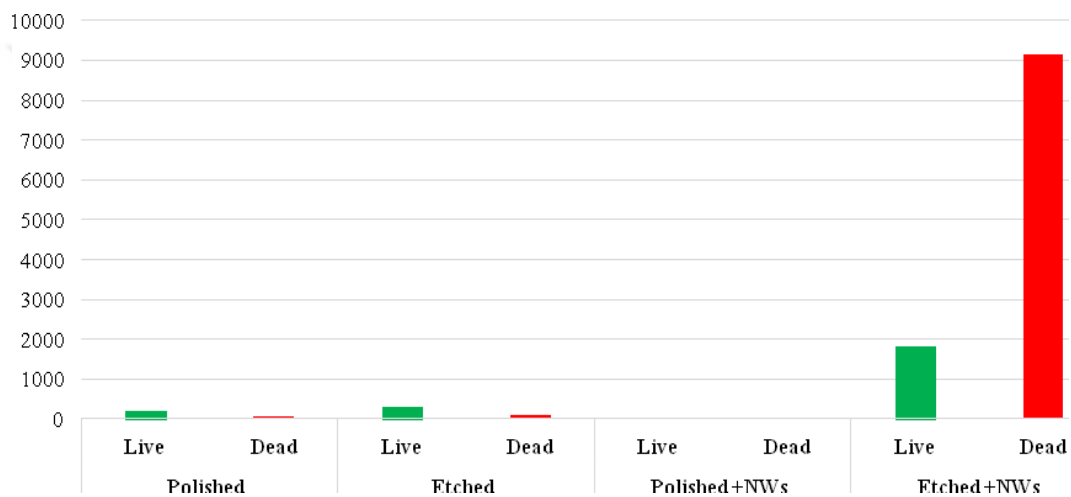
Figure 3.36: Live and dead bacteria in the biofilms on different surfaces.

Median scores of biofilm formation were analyzed using ImageJ software. Figure 3.36 summarizes the data in Table 3.8. Bacteria were not detected on the other surfaces. The Y axis indicates the quantity of bacteria, and the X axis denotes the surface properties.

Bacteria in the in situ biofilms (semi-quantification)

Significant differences in the biofilm formation time were observed among the subjects for the polished surface with NWs compared to the etched surface with NWs (Table 3. 9). Thus, inter-subject variability was suspected.

Table 3.8: Bacterial colonization evaluated by SEM

Volunteer/Surface	Polished	Etched	Polished+NWs	Etched+NWs	Polished+NTs	Etched+NTs
MHe	21	78	14	138	63	158
BK	12	45	6	298	12	9
SS	2	62	4	448	8	26
KZ	87	129	26	164		
SR	94	194	96	184		
KL	37	64	6	108		
NG	54	175	2	316		
JK	22	97	12	324		
NL	32	76	17	109		

SEM showed that biofilm formation was inhibited by all of the surface applications. Single bacteria were rarely observed on the polished surface with NWs, whereas bacterial growth was detected on both the etched surface and the etched surface with NWs.
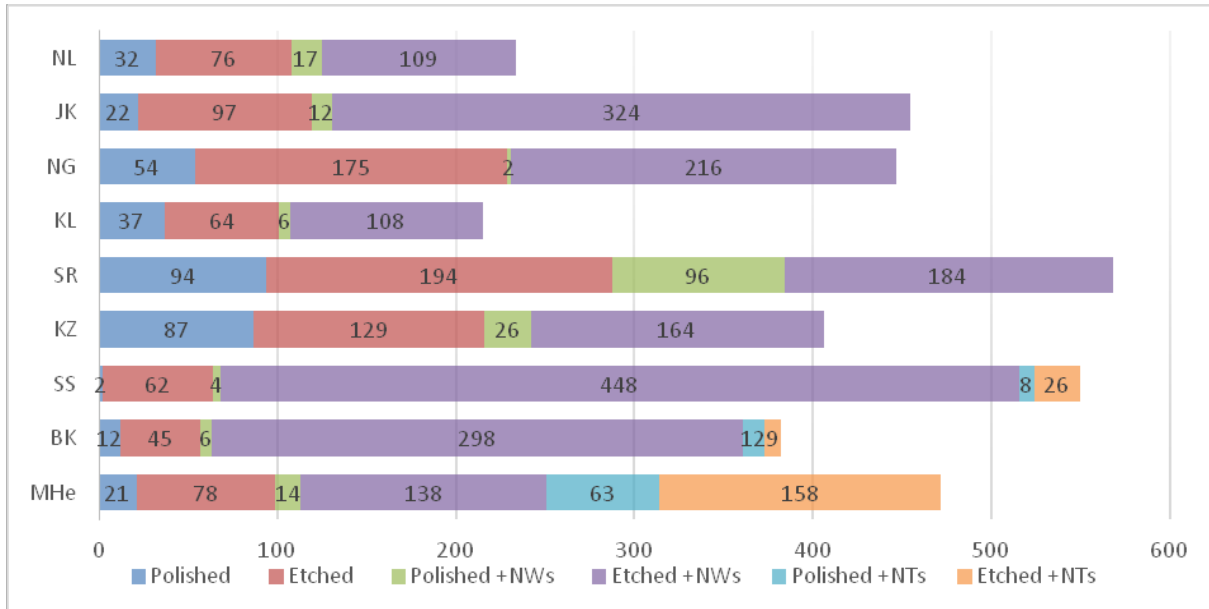
Figure 3.37: SEM determination of bacteria in biofilms on surfaces.

Bacteria were not detected on the other surfaces. The Y axis indicates the names of the volunteers, and the X axis denotes the surface properties (Figure 3.37).

Image Analysis for the Detection of Biofilm Stages in 24-h in situ Specimens

The convention for measuring the zone of biofilm evacuation using SEM discoverer frameworks and picture handling is a novel application for the quantitative examination of SEM images prior to and after a trial treatment on 24-h in situ biofilm specimens.

Likewise, this strategy could possibly be utilized to assess biofilm development on a surface over time, and though is restricted to SEM images, it could also be utilized to assess biofilms from different types of microscopic images.

To the best of our knowledge, we are the first to propose a strategy for precisely fragmenting biofilms from SEM images to ascertain the rate of biofilm loss/maintenance. This strategy

can easily be adapted to different studies, empowering analysts to utilize SEM as both a subjective and quantitative instrument for the assessment of biofilm interruption.

In this method, the SEM image is analyzed using the open source image editing software ImageJ, as shown in Figure 3.39.
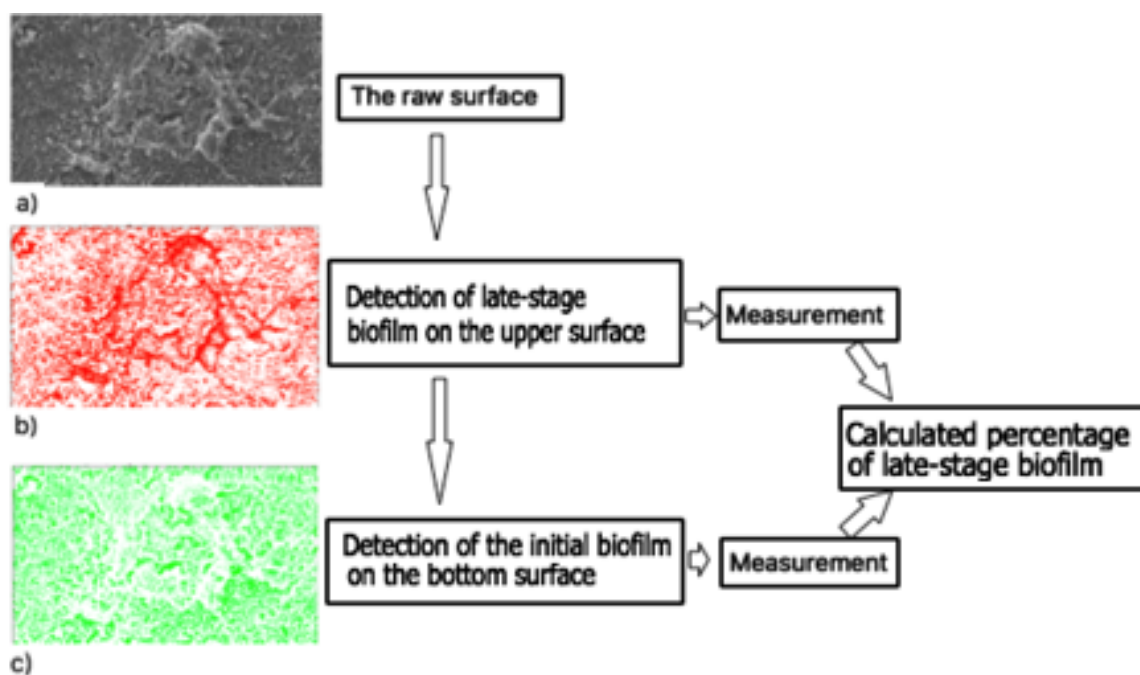
Figure 3.38: SEM images evaluated by ImageJ.

The picture in a) is a raw image, and the image displayed for late-stage biofilm formation is from 24-h in situ etched Ti with NWs. The image in b) is the late-stage biofilm labeled in red, and that of c) is the initial biofilm labeled in green.

Objects smaller than 20 pixels were considered noise and were eliminated from the sectioned pictures utilizing the 'Analyzed Particles' module. Double pictures were rearranged if necessary such that the surface was dark, and the biofilm regions were white. A histogram of every picture was computed to locate the quantity of white pixels, which were compared to the biofilm range. The rate of biofilm maintenance was initially calculated as:

$$\text{Amount of late biofilm mass \%} = \frac{\text{Late Biofilm mass}}{\text{Total biofilm mass (Initial biofilm + late biofilm)}} \times 100$$

The measurement of the initial biofilm (mean) = 80,233

The measurement of the late biofilm (mean) =77,235

Amount of late biofilm (mass) = 49.04%
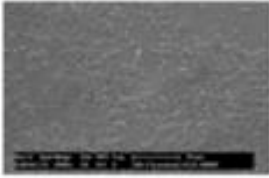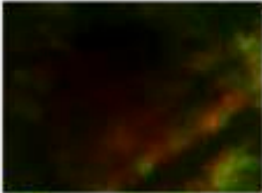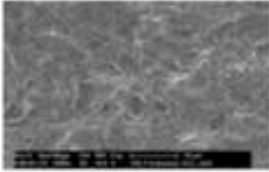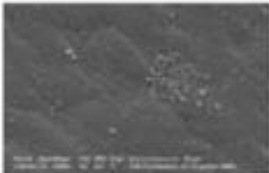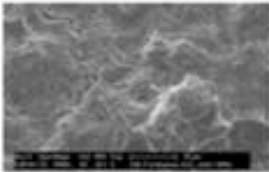
The pixel tests selected by the client for image preparation can be free-drawn, for instance with the tether apparatus in ImageJ, yet to guarantee consistency and reproducibility, an arrangement of square districts of interest measuring 300×400 pixels were utilized. This size was ideal as it was sufficiently extensive to allow high-quality pixel preparation and sufficiently small enough to fit over small masses of biofilms and individual microorganisms.

Approximately 24 to 18 regions of interest (ROIs) were selected in the picture by the client and were then categorized into one of two classes - initial biofilm or late biofilm.

The following analyses were included in a classifier to assess the images: Gaussian obscure, Sobel channel, Hessian, Difference of Gaussians, Membrane projections, Variance, Mean, Minimum, Maximum, Median and Bilateral. This combination provided the best analysis for all measures of time. This strategy was developed using images of scratched surfaces with NWs as they had more microbes and more biofilm mass

3.5 COMPARISON OF THE BACLIGHT AND SEM TECHNIQUES

Table 3.9: Amount of biofilm detected via BacLight assay and SEM for KZ.

SEM	BacLight™	Explanation
		Bacterial colonies, which cover more than 70% of the surface area.
		Monolayered bacterial colonies, which cover approximately 50% of the surface area, or large multi-layered agglomerates.
		Monolayered bacterial chains or isolated bacterial agglomerates.
		Multi-layered bacterial biofilm covering the entire surface (>90%).

As described above, the fluorescence technology provides insights into the bacterial colonization and viability patterns. Therefore, the combination of the fluorescence technique and the electron/fluorescent microscopic technology allows investigation of the effects of mouthwashes on biofilm quantity and quality, which is of considerable relevance for assessing the efficacy of oral health care products in biofilm management, as shown in Table 3.10.

4. DISCUSSION

The present study demonstrated that machined, chemically treated and nanofabricated polished surfaces coated with NWs are suitable due to their lack of attachment, but they are unacceptable implant surfaces because substantial oral biofilms formed on discs after 24 h in situ. The efficacy of each surface treatment was evaluated using two different microscopic techniques, SEM and BacLight, and two different data analyses, statistical and morphological. The polished and etched surfaces served as negative controls and the treated surface groups (polished+NWs, etched+NWs, polished+NTs and etched+NTs) were used as positive controls.

4.1 DISCUSSION OF MATERIALS AND METHODS

Analysis of titanium discs

Titanium and some of its compounds are utilized as biomaterials for dental and orthopedic applications. The most widely recognized formulations utilized are economically pure titanium and the Ti6Al4V composite obtained from aviation applications.

Different methodologies can be used to change the surface of metallic materials (including nanophase materials) to enhance their applications compared to routine micro-rough materials. For the most part, nanoscale surfaces have high surface strength, which expands initial protein adsorption and is critical for managing cell associations on implant surfaces. Surface properties likewise affect bonding, charge conveyance and the behavior of the material [71-73].

The types of samples included:

- Polished surface

- Etched surface

- Polished surface after being coated with NWs, LASER treated

- Etched surface after being coated with NWs, LASER treated

- Polished surface after being coated with NTs, LASER treated

- Etched surface after being coated with NTs, LASER treated

The flow chart shows the preparation of the surfaces (Table 4.1).

Table 4.1: All types of surface modifications.
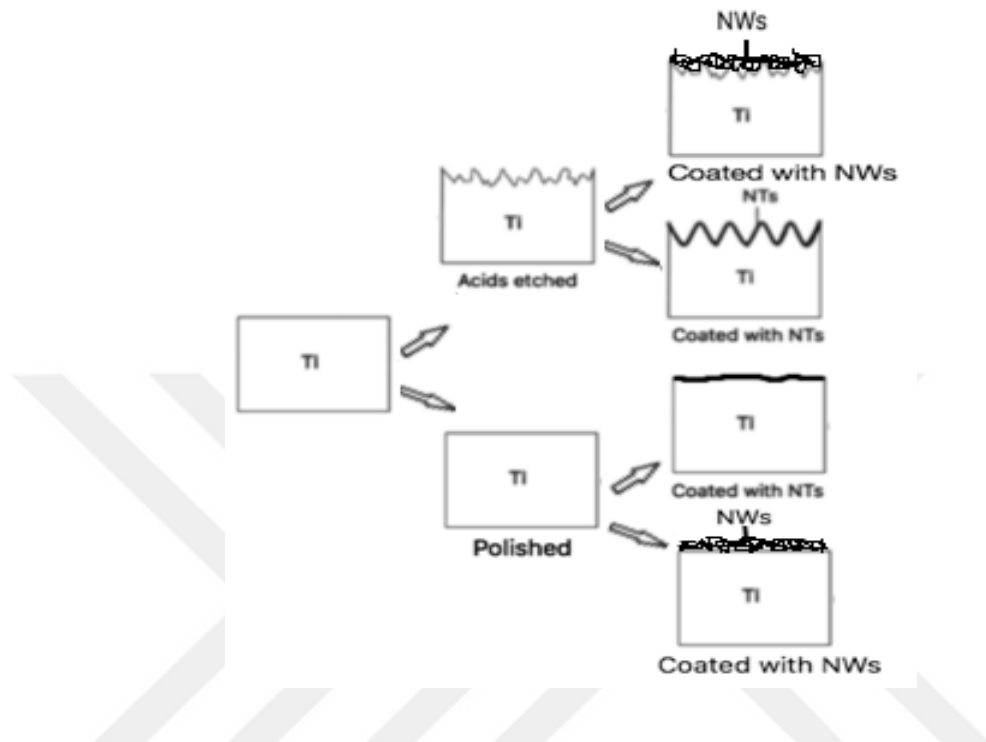
Polishing involves machine modification of a surface, while etching is a chemical (acids) modification of a surface, and both methods served as negative controls. Subsequently, both control surfaces were further treated via nanofabrication with NWs or NTs. The surface topology of all of the treatments, i.e., the surface roughness and adhesive interactions, were different, as shown in Figure 4.1.
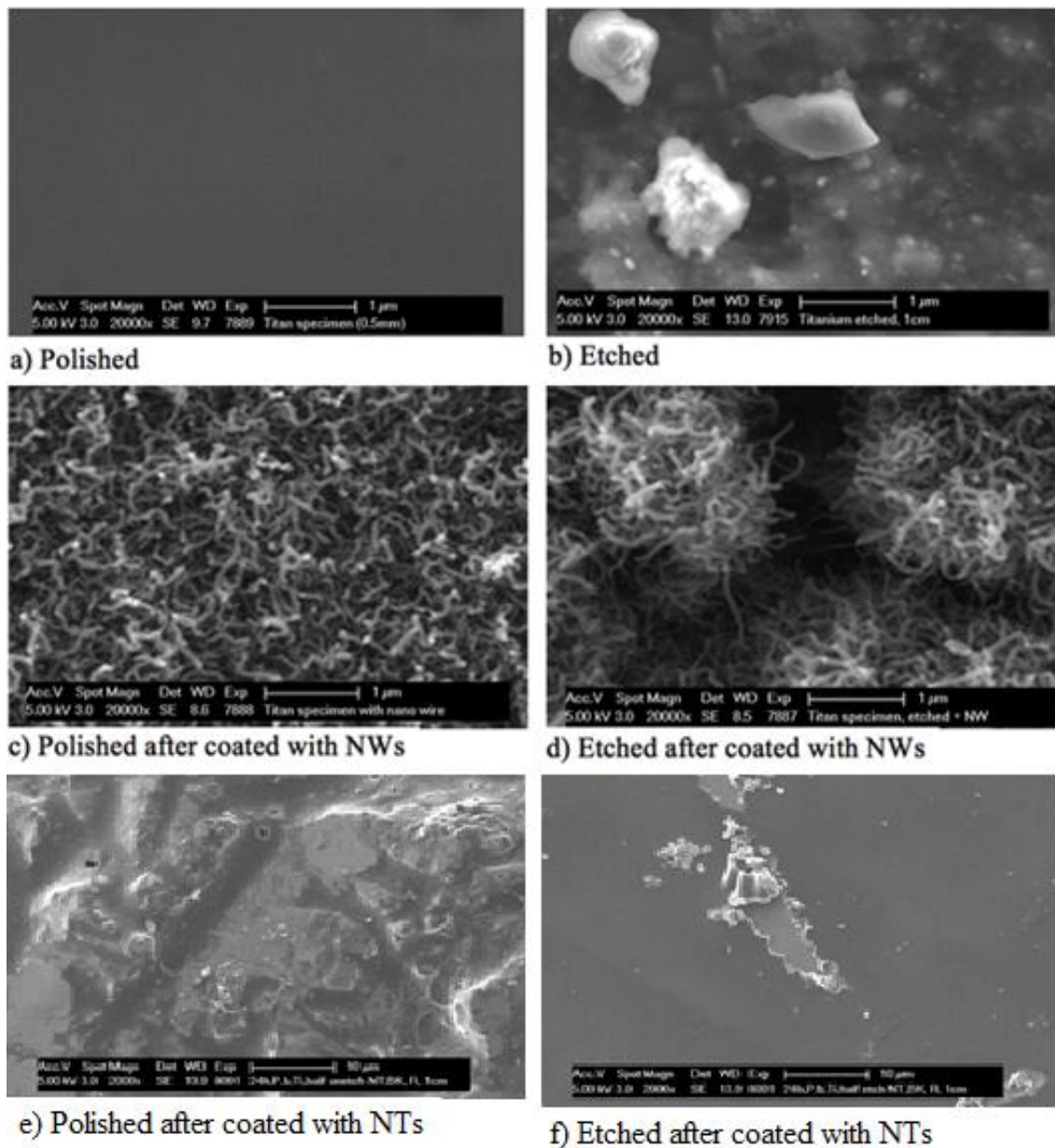
Figure 4.1: Scanning electron microscopy images of various surface nanostructures.

(a) Control (Ti with a polished surface); (b) control (Ti with an etched surface); (c) Ti with polished surface, coated with NWs; (d) Ti with an etched surface, coated with NWs; (e) Ti with a polished surface, coated with NTs; (f) Ti with an etched surface, coated with NTs. Volunteers adjusted their cleanliness to measure practical biofilms such as those that form around dental implants in the oral cavity. They ceased using mouth wash 2 h before beginning the study. Furthermore, oral cleanliness activities were performed without toothpaste, and the Ti samples were not brushed. The Ti discs were situated 1 mm into silicon to avoid any self-cleaning (Figure 4.2).

Figure 4.2: Individual removable custom-made maxillary splints.

Experimental Design

Numerous in vitro studies (Figure 4.3) have been performed to explore biofilm arrangement and the effect of different materials on biofilm progression.

Figure 4.3: Picture of titanium discs fixed with silicon.

When comparing in vitro and in situ research models to explore biofilm structure, in situ models are better as they capture the organisms involved in biofilm progression. Nonetheless, in vitro studies are initially necessary to examine the biofilm activity and to assess the adequacy of its dynamic elements, which are difficult to decode. However, as they cannot mimic salivation, in vitro studies are impractical for emulating bio-adhesion. Adhesion in vitro is unmistakably different from adhesion in vivo [74]. In over 100 different circumstances, in vivo/in situ

biofilms have demonstrated higher imperviousness to oral chemotherapeutics than their constituent planktonic or scattered microscopic organisms [75]. Additionally, a microbial community with metabolic cooperativity and cell-to-cell-flagging [66] could not be constructed via plate culture innovation in vitro. Studies on biofilm design have illustrated that in vivo discoveries do not agree with the results of in vitro models.

BacLight viability assays

Evaluations of bacterial colonization and the antimicrobial movement of oral chemotherapeutics were performed utilizing microbiological plate culture innovation in combination with the quantification of colony forming units [75].

1- Strategy (CFU): only half of the oral bacterial strains are cultivatable.

2- Ultra-sonication was performed to remove the secondary bacterial groups from the sample surface, lowering the bacterial totals and, in this way, prompting potential overestimation [70].

These difficulties can be overcome with fluorescence recoloring systems after fluorescence microscopy investigations.

Additionally, fluorescence-based, 2-shading measures, which depend on the effects of the fluorochromes on either the film porousness or metabolic movement, can distinguish live and dead cells, thus giving new understanding to the evaluation [76-77].

For the aggregate sums of microorganisms, this LDS has uncovered a connection by comparing the results of DAPI recoloring [74]. With the improvement of fluorescent colors, various fluorescence microscopy measurements can be made with different blends of fluorochromes. BacLight^{TM} viability assays have been used in previous studies due to its rapidity, high reliability and simplified preparation procedures [70, 74].
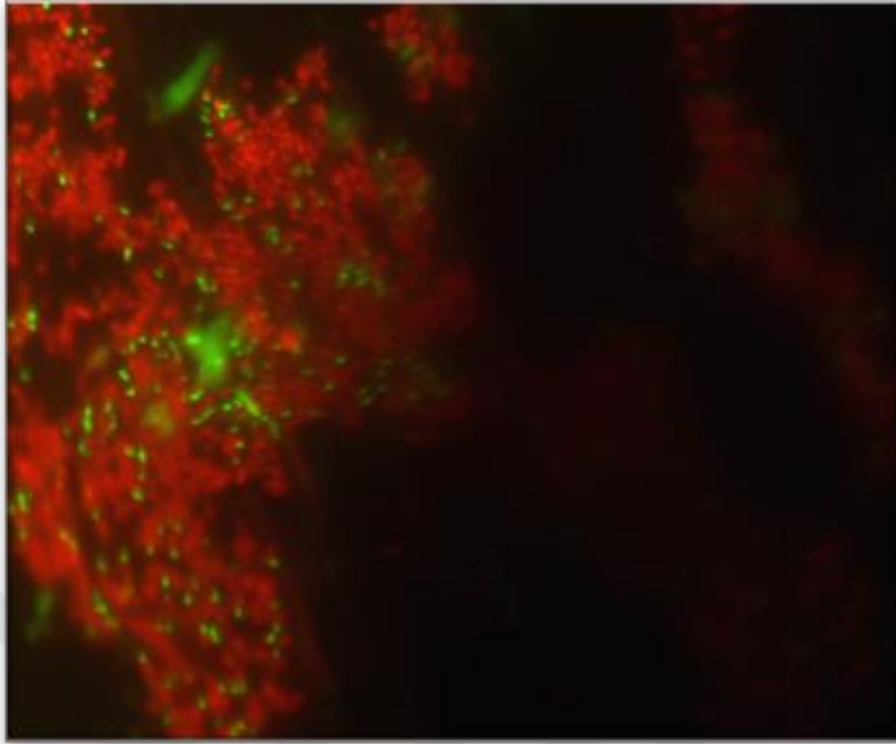
Figure 4.4: Differentiation of live and dead bacteria during biofilm formation.
Green: live bacteria; red: dead bacteria.

Despite the quickness with which this system can be connected and performed even with practical changes, there are a few restrictions that need to be considered:

(1) Bacteria that are neither live nor dead but somewhere in between, i.e., lethargic or pre-lytic cells, may appear green, yet they are not viable or cultivable [78];

(2) Imaging isolated microorganisms on planar surfaces is simple, yet the quantitative translation of images is progressively troublesome with unpredictable surfaces containing various quantities of smaller bacterial loads, as was the case in this investigation of characteristic biofilms shaped in situ; and

(3). Taking everything into account, red fluorescence can be expected to indicate dead microscopic organisms, but green fluorescence does not truly signify all viable microorganisms.

Therefore, utilizing another procedure to examine the viability of microscopic organisms in the remaining biofilms is practical. For this reason, contact inoculation of the control and treated samples were performed on blood agar, a non-specific development medium, to provide a

supplementary environment for the microorganisms, thus supporting the development of an extensive variety of life forms.

Electron microscopy investigations

SEM is the most commonly used microscopic examination technique for biofilms as it permits the immediate recognition of their morphological structure at high magnification. At the smaller scale, the bacterial loads, the biofilm network and the bacterial interactions are strikingly represented. Moreover, the morphogenesis of biofilms at the dentinal surface as opposed to the subsurface and profound parts of the tubules is available.

Biofilms on Ti surfaces
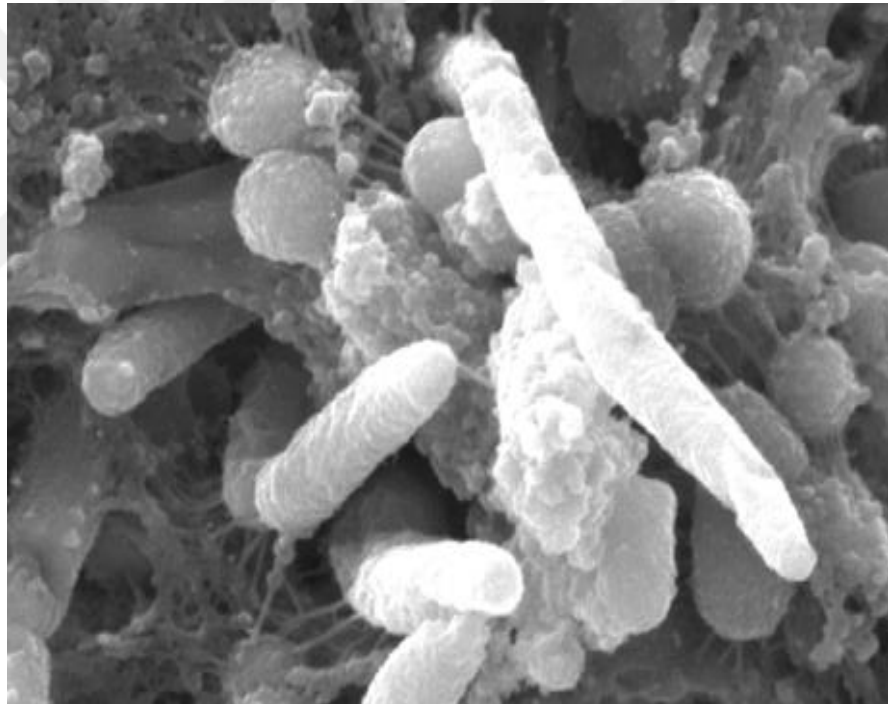
Figure 4.5: *Fusobacterium nucleatum* on a late-stage biofilm surface.

Early colonization and biofilm formation displayed on titanium (polished and polished with NWs surfaces) (Figure 4.6).
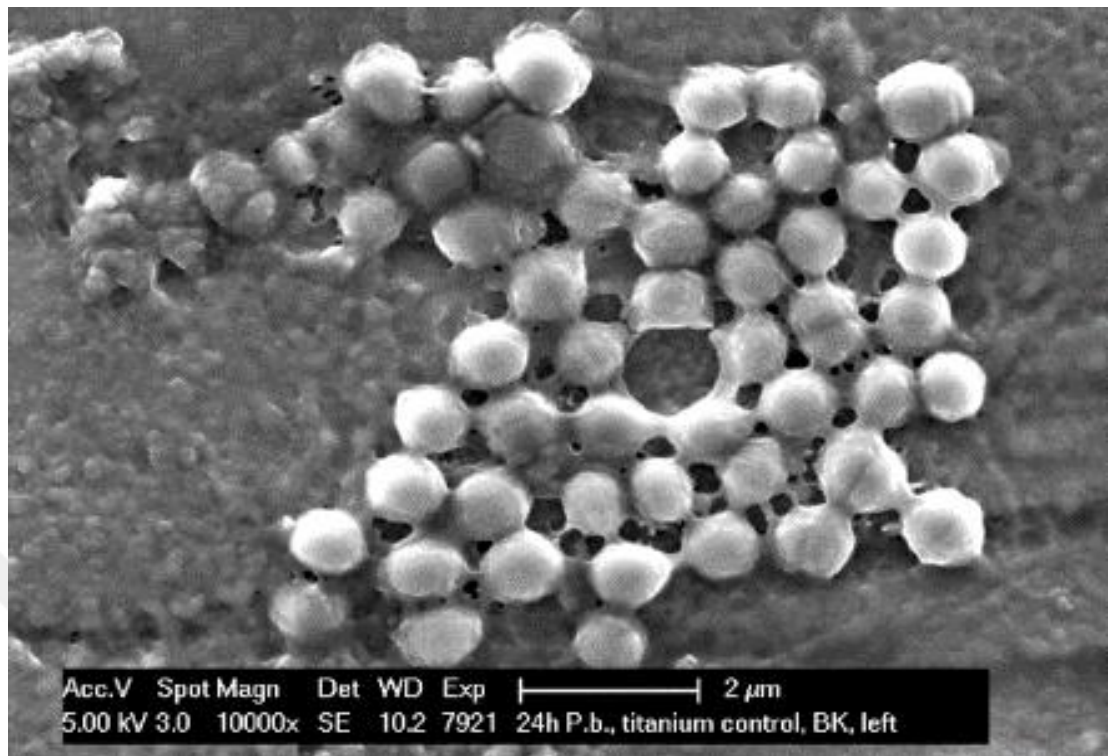
Figure 4.6: The main bacteria found in early biofilms on polished surfaces are streptococci.

In the SEM study, all of the Ti discs with etched surfaces were entirely covered by biofilms, which were visually detectable after being treated with NWs, while the covered areas on the Ti discs increased biofilm formation on the surface in situ after 24 h [79, 80].

Scanning electron microscopy has many benefits over optical microscopy, including its wide depth of field. The specimen surface can be clearly visualized no matter the surface raggedness [82]. SEM can be performed at magnifications up to its maximum of 1,000,000x, with a final resolution of 1 nm or higher. Moreover, it is feasible to obtain more data to provide detailed surface topography [83]. In Scanning Electron Microscopy, the electrons have energies between 2 and 40 keV; how the electrons permeate the specimen is defined by the energy of the electron beam, the atomic bulk of the elements in the sample and the angle at which the electron beam hits the sample [81-82].

4.2. DISCUSSION OF RESULTS

Different results were observed on the same surfaces. For example, on the titanium surface that was machine polished, a few volunteers had extraordinary biofilm formation, as visualized with SEM.

Surface abnormalities are important for the beginning stages of underlying pellicle development and bacterial adherence [85]. Additionally, anomalies over the basic surface roughness of 0.2 μm should be advantageous for microbial maintenance [86]. Most likely, tubules served to protect microorganisms from shear forces and thus led to bacterial biofilm development. Along these lines, the nearness of the dentinal tubules encourages early pellicle arrangement and bacterial colonization. Tubules free of microscopic organisms were not observed in any of the test subjects, who were subjected to a test for antimicrobials. Be that as it may, care should be taken when translating the present outcomes, since cow-like dentin uncovers less thick tubules that are larger than dentin [87].

4.2.1. Polished Ti surface

The topology of oral restoration frameworks upheld by inserts is of significance for microbial colonization considering that harsh surfaces are more defenseless to colonization by microorganisms than smooth surfaces. In this study, the results of all the volunteers supported previous studies.

According to previous studies:

-A decline in biofilm development connected with low estimations of surface harshness was uncovered [89]. Providing mechanical security against shear forces from the encompassing environment helps the underlying adherence of a biofilm [90].

-Generating an extracellular grid composed of polysaccharides (e.g., glucan and fructan) and glycoproteins expands biofilm development on surfaces as well as microbial agglomeration. Retentive zones such as scratches or surface anomalies can create a flawless microscopic scale environment for underlying microbial attachment [91].

-Biofilm colonization declines on surfaces with Ra values beneath an edge estimation of 0.2 μm [86].

The mechanical sliding contact of grating particles from sustenance and toothpastes and the contact from dental Pilgrim instruments are detrimental for biofilm maintenance [92-94].

Surface Chemistry: Surface elemental analysis of the titanium polished discs was performed with EDX, providing a mean percentage of each element. Among the elements considered,

titanium was present in the highest amounts, followed by oxygen and carbon. Backscatter images taken under low, medium, and high magnifications did not show any apparent differences in the polished surfaces. However, the backscatter images taken under low, medium, and high eV showed apparent differences in the elemental compositions of the polished surfaces. Ti was present in the highest amounts, followed by oxygen and carbon.

The EDX results of the polished titanium surfaces are shown in Figure 4.34. The surfaces were analyzed for each channel at 5, 10, and 20 eV. The EDX analysis at 20 eV provided the best results for high surface depth as Ti was dominant, but the 5 eV analysis was best for the top surface because carbon was most prevalent.
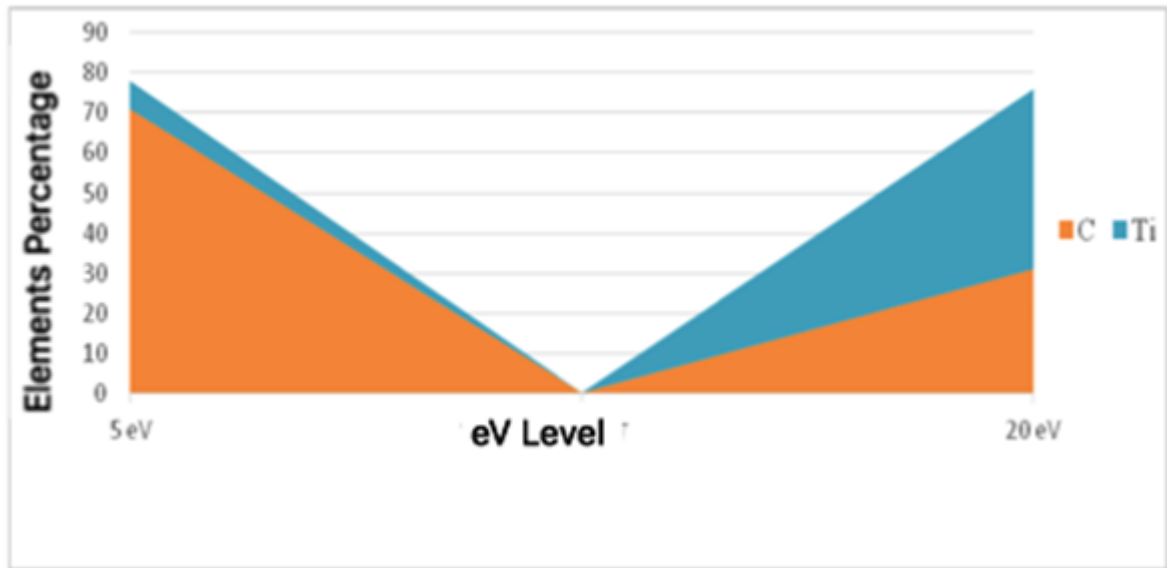
Figure 4.7: Evaluation of the deep and top surfaces of polished Ti.

Biocompatibility: After each surface experiment, the microorganisms detected by BacLight viability assays were evaluated according to the scores defined in Table 4.8. The Ti control surface was covered with salivary proteins.

The results confirmed that the polished titanium surface with in situ 24-h biofilms can be analyzed by BacLight assays in combination with live/dead fluorescence staining and SEM images. The polished surface had monolayer biofilm formation as the live bacteria outnumbered the dead bacteria. The live and dead bacteria covering the titanium polished discs were quantified, and their proportions are shown in Figure 4.9.
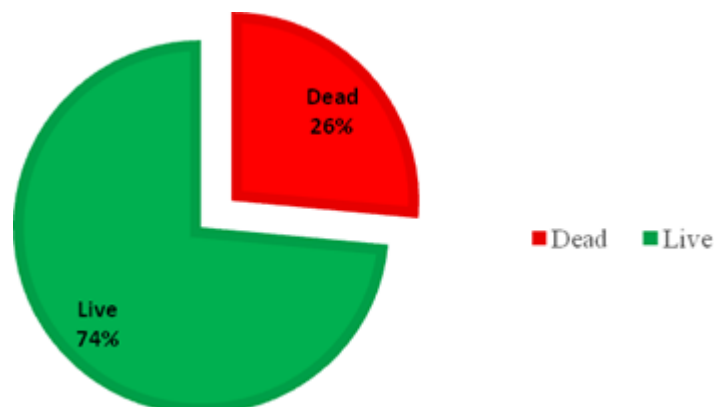
Figure 4.8: Quantification of live and dead bacteria on a polished Ti surface via a BacLight assay.

Biofilm Removal: SEM images of the control and treated (polished) smooth titanium surfaces were captured. The smooth control surfaces exhibited pronounced circumferential machining

marks, whereas the rough control specimens showed regular topography due to their surface porosities. Surface imperfections that appeared as metal scratches or tags were commonly observed in the smooth control disks and were irregular in size, shape, and distribution. SEM images of the treated titanium specimens also revealed changes in the amounts of biofilm present.

Images of the polished discs captured under different magnifications between 500x and 100000x showed that the entire disc surface was colonized by a dense network of multiple layers of streptococcal chains enmeshed in polysaccharide fibrils. The SEM images were analyzed using ImageJ. The polished surfaces displayed different amounts of bacterial colonization for each volunteer.
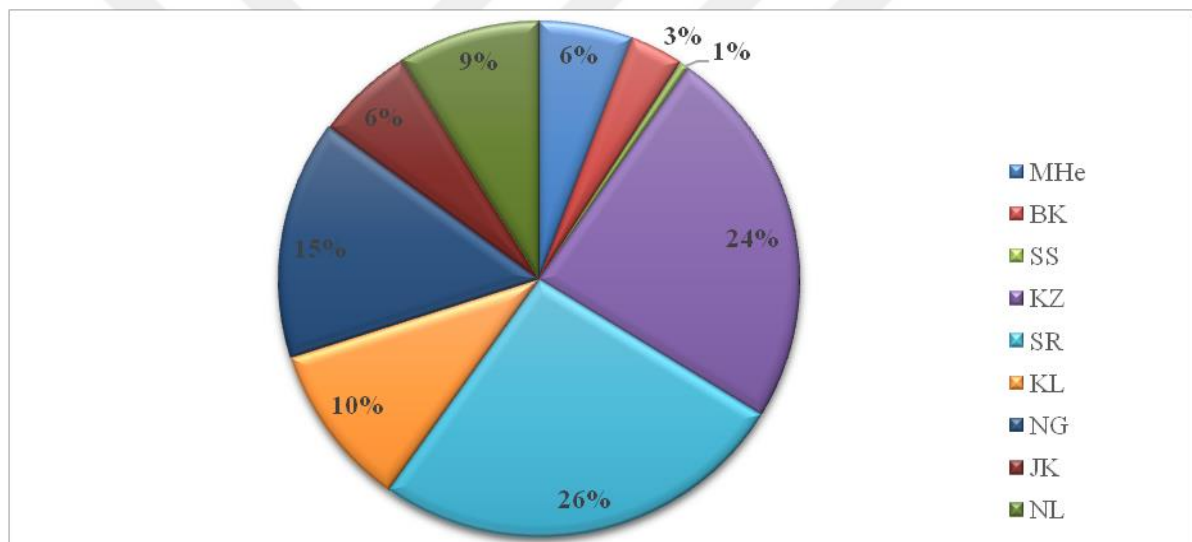
Figure 4.9: ImageJ software measurement of SEM images for each volunteer.

Each color represents a volunteer, including MHe, BK, SS, KZ, SR, KL, NG, JK and NL.

4.2.2. Etched Ti surface

Biofilm examinations uncovered a thicker biofilm arrangement and cell density on titanium with rough, scratched surfaces than on cleaned ones.

Studies in the literature have reported that bacterial biofilms may be noticeable and partly responsible for implant disfigurement [95]. The microorganisms must interact with an implant surface and adhere to develop a biofilm. Altered materials have antibacterial activity, while others initiate bacterial development [96]. The surface roughness is an imperative parameter

that may affect the interaction between biomaterial surfaces and proteins and cells. Protein adsorption and bacterial adherence in vivo may be controlled by an edge surface roughness of 0.2 μm [97]. The in vivo, in situ, and in vitro tests provided clear results, and the variables that contribute to in vivo and in situ studies include various considerations regarding the selection of patients, while the numbers and types of microorganisms used for biofilm formation are the most pertinent variables for in vitro investigations [98].

The etched surface roughness seemed to promote increased amounts of plaque, but the biofilm composition was not substantially different nor was the establishment of irreversible attachment in the surface irregularities, where microorganisms are protected from mechanical shearing. Despite these findings, the results of our study demonstrated that biofilm formation increases markedly on rougher surfaces.

The SEM results of the volunteers were compared, and bacteria were found to adhere to the pellicle layer and to be embedded in the matrix as well all of the implant surface in the 24-h biofilms, as shown in Figure 4.21.

Surface Chemistry: The EDX spectral analysis of a Ti etched surface is shown in Figure 4.35. C, O, S, and Ti were the main elements detected. Among them, a very high percentage of Ti was found. Backscatter images taken under low, medium, and high eV showed apparent differences in the elemental composition of the acid etched surface. Ti was present in the highest amount, followed by oxygen and carbon. Carbon was the principle element of the conductive layer. The etched surface was analyzed with 5, 10, and 20 eV channels. The EDX analyzed at 20 eV gave the best results for the surface given that Ti was most abundant, while 5 eV gave the best results for the top surface as carbon was most prevalent.
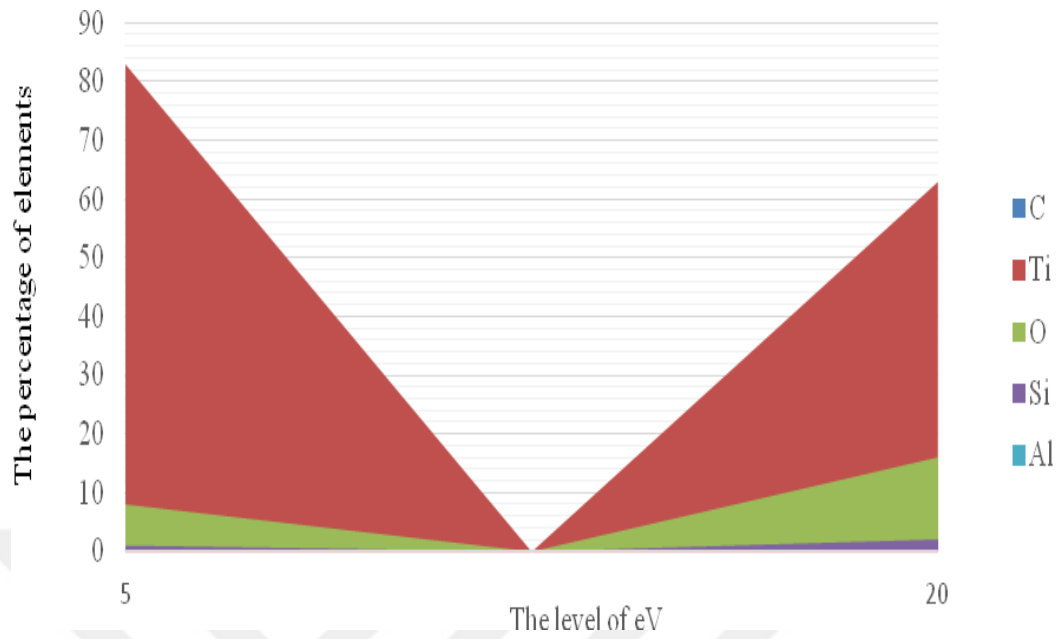
Figure 4.10: Evaluation of the deep and top surfaces of etched Ti.
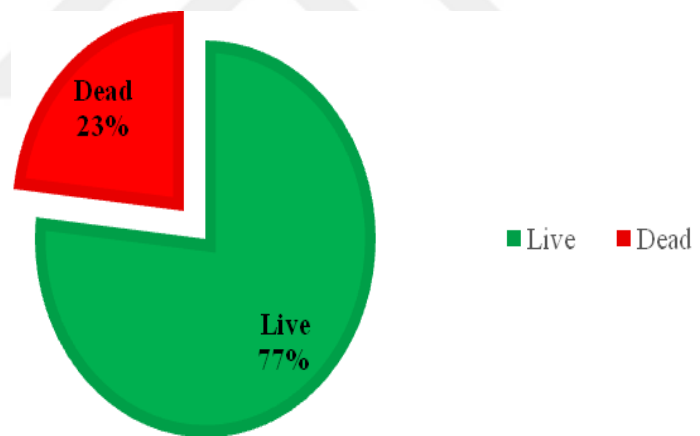
Figure 4.11: Quantification of live and dead bacteria for all volunteers.
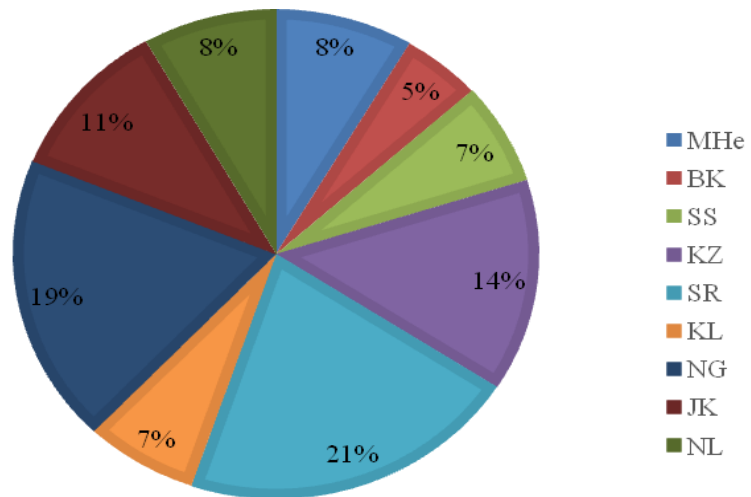
Figure 4.12: Bacterial colonization evaluated by SEM with ImageJ measurements.

Each color represents a volunteer, including MHe, BK, SS, KZ, SR, KL, NG, JK and NL. Some volunteers experienced more biofilm formation than others, indicating that biofilm thickness is specific to each individual. The biofilm of the volunteer MHe attained more mass than that of the others for the different in situ surfaces after 24 h.

4.2.3. Ti surface coated with NWs

The bacterial contamination of implants and prosthetics stands out among the most recognized reasons for implant failure. The nanostructured surface of biocompatible materials unequivocally impacts the adherence and growth of mammalian cells on strong substrates. This perception has prompted the development of new procedures to avoid bacterial adhesion and biofilm development, most of which use nanoengineering to alter the topology of the materials utilized as a part of implantable devices. While a few reviews have shown the impact of nanoscale surface morphology on prokaryotic cell adhesion, none have provided quantitative data. Utilizing supersonic cluster beams, we created nanostructured titanium thin films with controlled and reproducible nanoscale morphology individually [99-102].

The titanium surfaces that were produced imitated the surface engineering of dragonfly wings, with the presumption being made that this surface design would have similar antibacterial properties as those displayed by dragonfly wings. The nanowire surfaces were manufactured using a simple covered process. The subsequent surfaces were extensively analyzed. The outcomes reported herein provide additional confirmation that titanium

surface nanocomponents can be designed with the aim of controlling the degree to which bacterial adherence occurs on such surfaces.

Two different Ti surfaces were prepared with NWs: a Ti surface that was polished after being coated with NWs and a Ti surface that was etched after being coated with NWs.

Topology: The two surfaces were observed using Electron Microscopy, and the surface that was polished after being coated with NWs is shown in Figure 3.8, c and d. The etching and polishing modifications that occurred after being coated with NWs significantly affected the surfaces. The polished surface with NWs was more homogenously smooth than that of the etched surface with NWs, indicating that the raw titanium surface was extremely effective. As the top surface was rough, more biofilm formation occurred in situ over the 24-h period.

Surface Chemistry: The EDX spectral analyses of the polished Ti surface with NWs and the etched Ti surface with NWs are shown in Table 3.3.
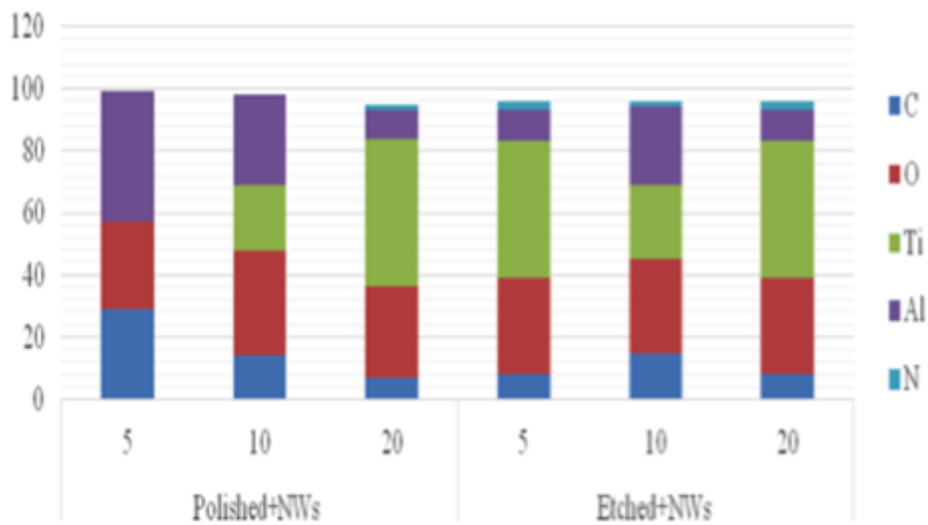
Figure 4.13: Evaluation of the deep and top surfaces of the Ti surfaces treated with NWs.

Backscatter images taken under low, medium, and high eV showed apparent differences in the elemental composition of the acid-etched surface. Ti was present in the highest amount, followed by oxygen and carbon. The etched surface was analyzed with 5, 10, and 20 eV channels (to compare to the data in the Table 3.2). The EDX analysis at 20 eV gave the best results for the highest depth surface on which Ti was most abundant, while 5 eV gave the best

results for the top surface where carbon was most prevalent (Figure 4.14). The elements aluminum and oxygen indicated the presence of the nanowires.

The amounts of bacteria on the polished Ti surface with NWs and the etched Ti surface with NWs were analyzed with ImageJ software. The polished surface with NWs had fewer adhered bacteria compared to the etched surface with NWs. The latter had both live and dead bacteria attached it, and the dead bacteria were more prevalent than the live bacteria, as shown in the bar graph in Figure 3.15.
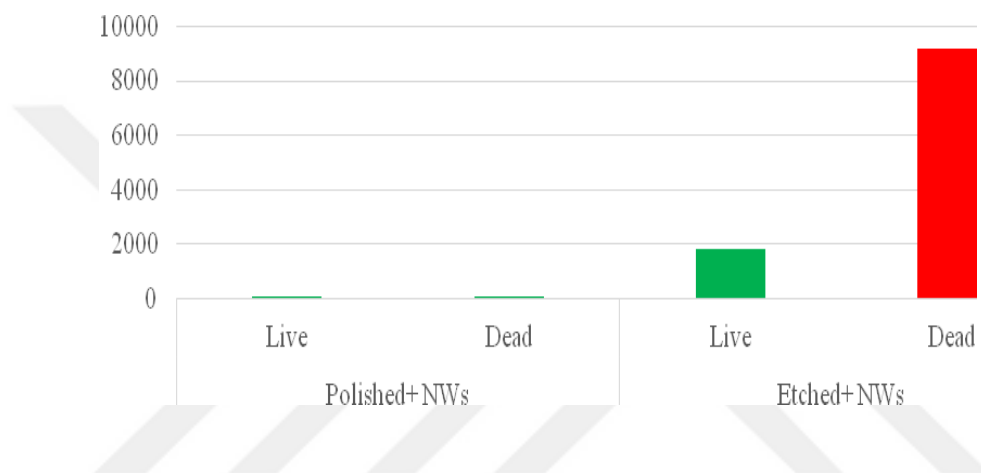
Figure 4.14: Quantification of the bacteria on the polished surface with NWs and the etched surface with NWs

Biofilm Removal: The biofilm thickness on the specimens exposed to the oral cavity in situ for 24 h was determined using ImageJ software for each volunteer. For the polished surface with NWs, all the volunteers showed decreased bacterial adherence to some degree. For the etched surfaced with NWs, all the volunteers showed increased bacterial adherence to some degree.

Compared with the polished and etched surface controls, the surface that was polished after being coated with NWs had varying levels of reduced bacterial adherence, as shown in Figures 3.21 and 3.22.
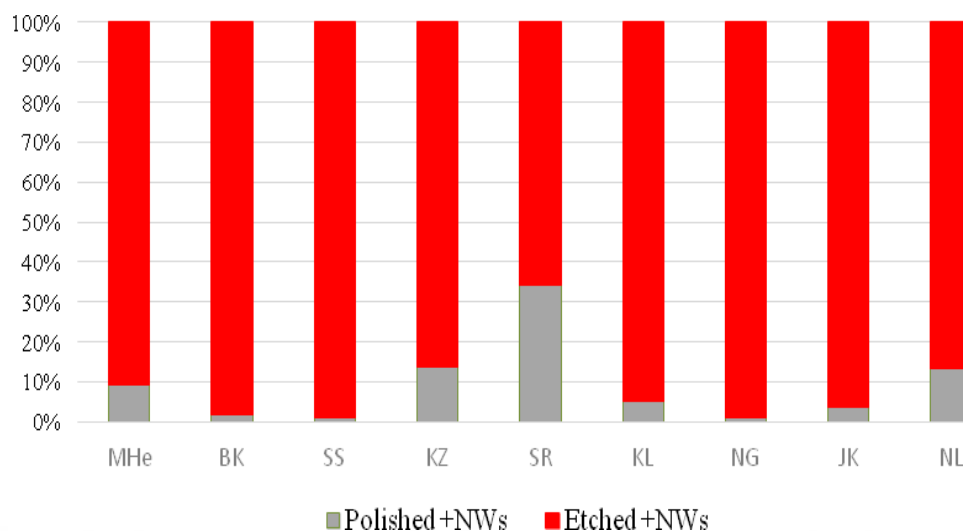
Figure 4.15: Bacterial colonization on NW surfaces evaluated using ImageJ software.

The volunteers are indicated as MHe, BK, SS, KZ, SR, KL, NG, JK and NL.

4.2.4. Ti surfaces coated with NTs

Biofilm coatings have focused on changing the surface of therapeutic devices to discourage bacterial attachment and to develop high imperviousness to biofilm formation. These innovations for preventing biofilms could quickly prove hostile to biofilm treatments. The manufacture of surface-finished structures has been a key issue in different research fields including superhydrophobic surfaces, anti-reflective structures, microlens displays, photonic precious stones, optoelectronic devices, and microscale/nanoscale biotechnology because the improvement of basic functionalities differed and was not straightforward. An assortment of techniques has been used for building surface-finished structures. Bottom-up based techniques are conceivably great means by which to manufacture surface-finished structures because such strategies are basic processes that utilize minimal effort and materials. Be that as it may, these bottom-up based techniques experience issues in controlling the morphology of the finished structure. Moreover, these strategies have difficulty producing uniform structures because of different auxiliary deformities including missing particles and connections. Conversely to bottom-up-based strategies, top-down based techniques can offer effective approaches for creating uniform surface-finished structures with simple to control height and pitch of the finished surface.

Among these strategies, surface-relief gratings have been encouraging devices for manufacturing surface-finished structures since they create expansive finished samples with abundant properly formed structures via an exceedingly basic method. In addition, surface-relief gratings can rapidly produce finished samples, so carving or advancement procedures for photoresist contrast with photolithography and obstruction lithography are not needed. In any case, the greater part of surface-relief gratings can be performed with azopolymer film. Not long ago, there were restrictions for using surface-relief gratings including hard to produce diversiform structures or the requirement of a twofold engraving process for manufacturing a 2-D surface-finished structure. In addition, the mass transport of azopolymer with various obstructions prevents us from comprehending how the instrument shapes surface-relief gratings, which has not yet been demonstrated.

Surface texturing is a procedure that permits us to regulate the surface properties of materials without changing certain parts of the substance. For instance, surface finishing is utilized to adjust the grains of yttrium barium copper oxide in second-era superconducting wires [103], which significantly expands their basic current. Finished Ti surfaces improve bone development in vivo; however, the mechanisms are not fully understood [105]. At first glance, surface science and feasible assemblies appear to impact bacterial adherence. Recently, Anand et al. reported an alternate approach to promote dropwise condensation in which the condensing surface is microscopically textured and impregnated with a lubricating liquid that will not mix with the condensed liquid [106]. Through the selection of appropriate surface geometry, chemistry, and lubricant, the authors demonstrated a surface having enhanced condensation properties with water droplets as small 100 μm in diameter becoming mobile and continuously swept away, creating new areas for droplet nucleation. The textured surfaces studied by the authors were microfabricated posts of silicon (10 μm x 10 μm x 10 μm), which were then solution coated with a low-energy silane to make them hydrophobic. Two kinds of lubricants were investigated, and the impregnation of the surface microstructures was accomplished by dipping the substrate in a bath of the lubricant controlled by a dip-coated system. Utilizing this approach, the surface of the microstructure remains exposed, while the remainder of the surface structure is covered with lubricant.

In characterizing the condensation properties of the lubricant-impregnated surface, the authors found several important parameters that could be used to determine if effective droplet

formation would occur. These parameters included the contact angle, spreading coefficient, density and viscosity of the lubricant, for example. In some cases, the lubricant can promote the formation of cloaked droplets condensed on the surface, where the droplet is covered by the lubricant, and therefore has no means to move. The authors also found that while effective droplet formation occurred, the drops became pinned by the tops of the micropost structure. To resolve this issue, the tops of the microposts were roughened using an etching process, which effectively reduced the capillary forces imparted by this surface, eliminating the pinning of the droplets by the textured surface. Thus, a scalable method has been introduced to promote enhanced dropwise condensation on engineered surfaces for applications that require optimal heat transfer.

Topology: Nano-textured technology. Schematic illustration of Ti disks with polished and acid-etched modifications that were coated with NTs in this study (Figure 4.17). Our previous study revealed that etching in concentrated acid and coating with NWs produced a rougher titanium surface. Thus, these types of modification increased bacterial adherence and the formation biofilms more than polishing and polished after being coated with NWs. Conversely, the surface roughness caused the surface NTs to be stable, meaning that the deformation caused by the NTs was decreased because they were removed from the surface (Figure 4.18).
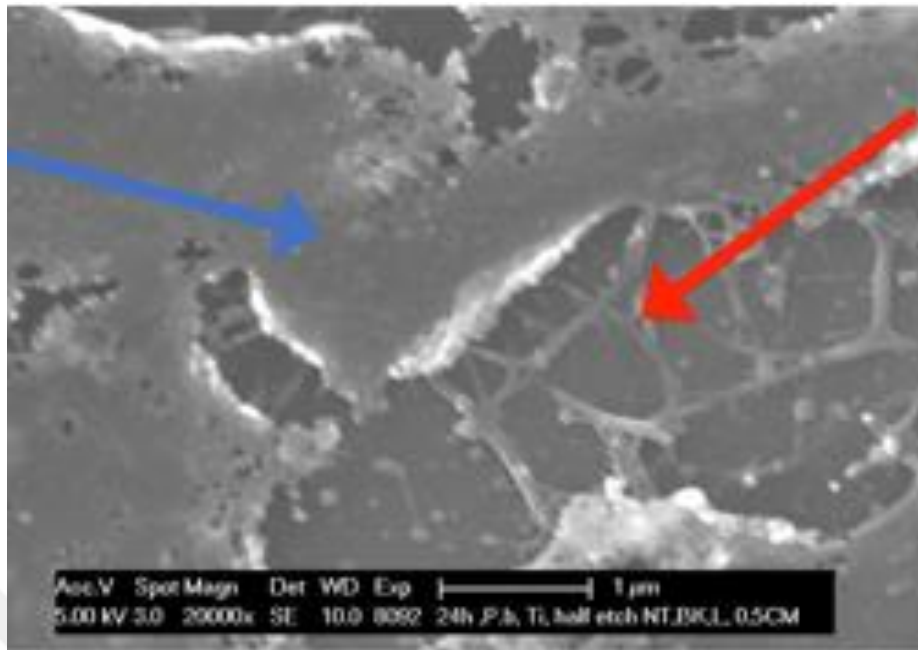
Figure 4.16: SEM image of a Ti surface etched after being coated with NTs.

The red arrow indicates areas with removed NTs, and the blue arrow denotes the areas coated with NTs on the titanium acid-etched surface. The nano-textured layer reduced the degree of roughness even though it could not maintain surface uniformity. The control surface that was acid etched had irregular, unidirectional grooves with some irregular shallow roughness (Figure 4.19). The left half of the surface was smooth from machine modification, and the other half was acid etched and appeared rough.
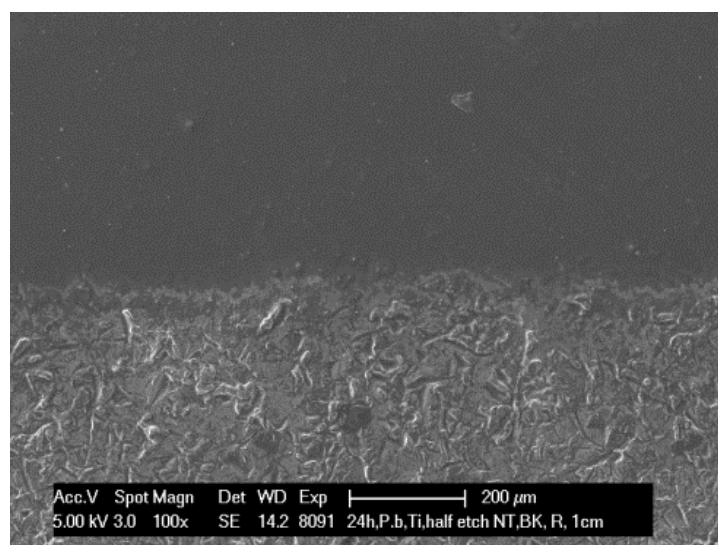
Figure 4.17: SEM image showing the polished and acid-etched control surfaces.

The Ti surface that was polished after being coated with NTs had a poor macrotexture without evidence of micropits and some scratching (Figure 4.20, left); the surface that was acid etched after being coated with NTs had a rather rough surface, but its macrotexture was poor (Figure 4.20, right).
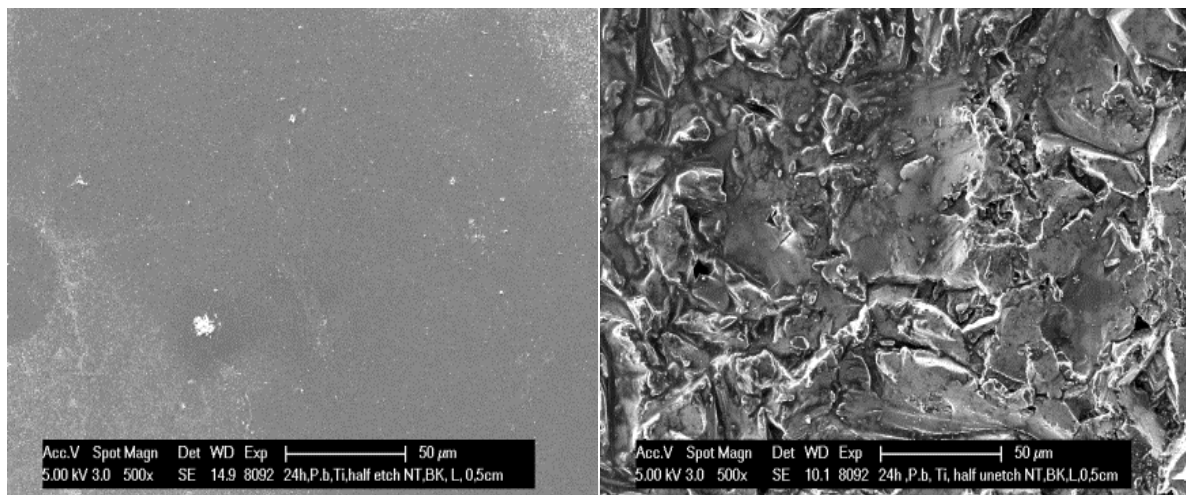
Figure 4.18: Surfaces with NTs.

The left side of the image is a surface that was polished after being coated with NTs, and the right side of the image is a surface that was etched after being coated with NTs. The nano-texture layer on the acid-etched surface could be more stable than the polished surface.

Surface chemistry: EDX spectral analysis of the Ti nanotextured surfaces was performed. Backscatter images were taken under low, medium, and high eV, and they showed no apparent differences in the elemental composition of the acid-etched surface. Ti was present in the highest amounts, followed by oxygen and carbon. The surface was analyzed using 5, 10, and 20 eV channels for both surfaces (to compare to the data in the Table 3.4).
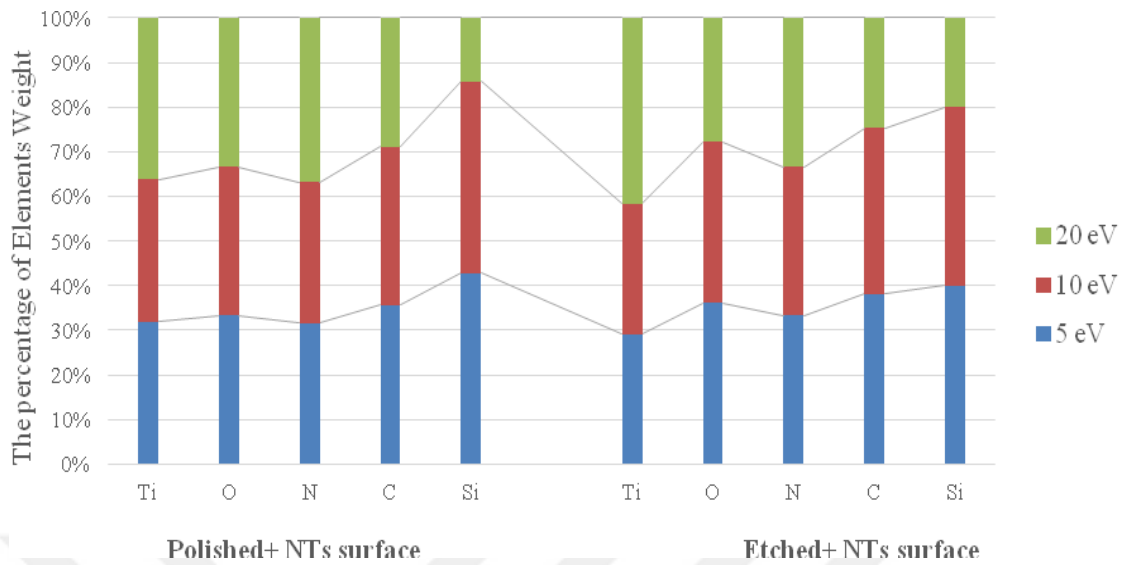
Figure 4.19: The evaluation of etched Ti using 5 to 20 eV channels.

The x-axis represents the elements in the polished surface with NTs and the etched surface with NTs, while the y-axis represents the weight percentages of the elements.

Biofilm removal: When the biofilms structures from the SEM analyses of the volunteers were compared, the modification properties of the NTs inhibited biofilm formation and prevented bacterial adherence.
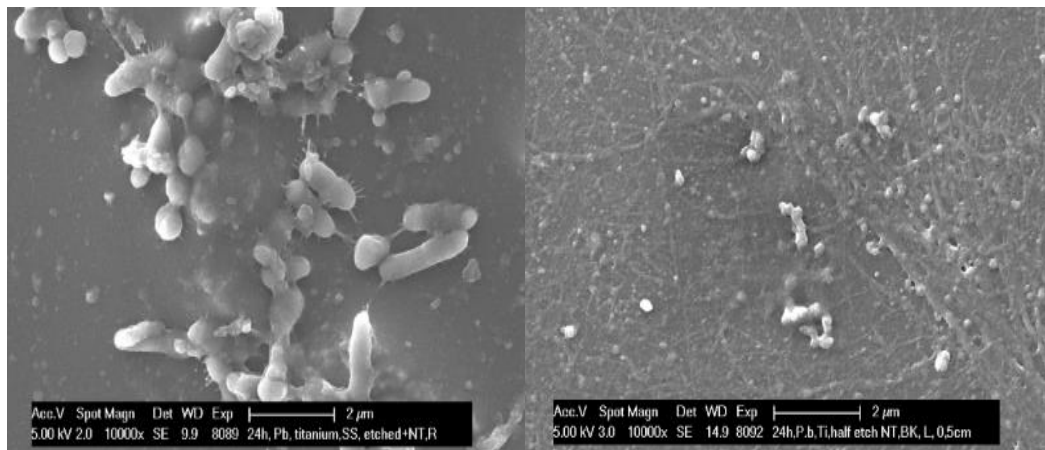
Figure 4.20: SEM images demonstrating the effects of NT modification.

The left side of the image is volunteer SS, while that on the left is volunteer BK; both images show few bacteria attached the surface.

These experiments demonstrate that nanotextured surfaces can be acquired by straightforward substance treatments. Continuous reviews demonstrate that specific morphological properties, for example, normal size and fractal measurements of the nanotexture, can be controlled by shifting the layer of nanotexture as well as its strength. Moreover, the consequences of biofilm thickness demonstrate a reasonable relationship between microorganisms and the morphological properties of nanotextured Ti-based biomaterials. Compared with the polished surface, the etched surface exhibited more biofilm formation for all volunteers. Each color represents a volunteer, including MHe, BK and SS.
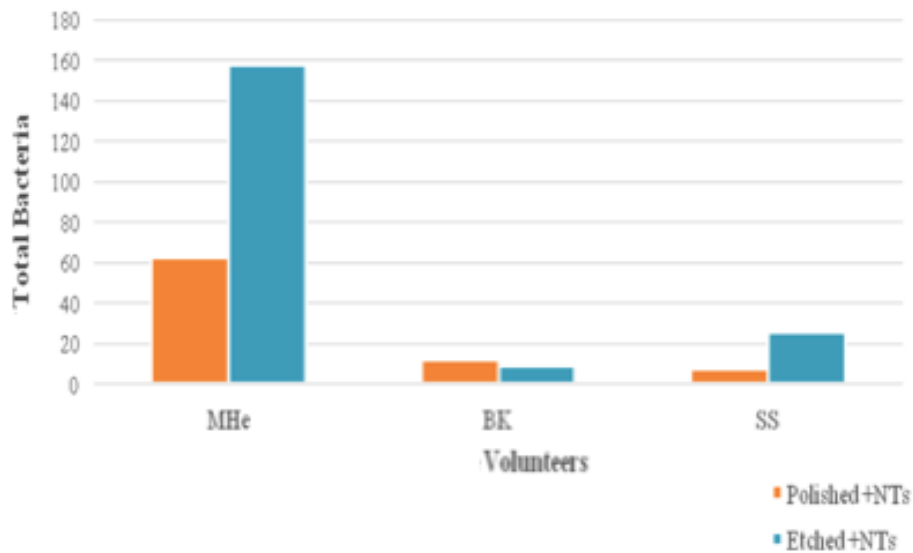
Figure 4.21: Bacterial colonization evaluated by SEM.

5. CONCLUSION AND RECOMMENDATIONS

Over the previous decade, nanotechnology has demonstrated energizing proof that key biological procedures (e.g., osteoblast expansion, osteoblast quality articulation and the initial protein adsorption that control such processes) can be effectively controlled by changing the nanotopography of Ti implants.

Different strategies have been coupled to generate nanostructured Ti surfaces. Anodization is an electrochemical oxidation technique in which the surface of the anode is oxidized inside an electrolyte arrangement.

Nanotubular morphologies (with measurements of less than 100 nm) can be orchestrated on regular Ti surfaces, and nanotube size can be controlled by modifying response parameters, including electrolyte type and focus, voltage, span, and temperature.

The experimental titanium sample was etched with strong acids, e.g., H_2SO_4 and H_2O_2, at a predictable temperature and for a specific time. Etching is then stopped by added distilled water. The recovered plates are washed further with ethanol in an ultrasonic bath for 20 min and then dried.

Nanostructured Ti could offer a solution towards microbe-related contamination, which is still a genuine problem for orthopedic implants. An implant surface that reduces initial bacterial adherence and remains antibacterial for long periods of time is profoundly attractive for diminishing contamination and promoting better osseointegration.

When the adhesion of *Staphylococcus aureus*, *Staphylococcus epidermidis* and *Pseudomonas aeruginosa* to traditional Ti, anodized Ti and nanorough Ti was compared, nanorough Ti was shown to reduce bacterial adherence the most by e-pillar dissipation.

In conclusion, biomaterial properties impact bacterial adherence and biofilm formation, and more effective biomaterials can be produced.

REFERENCES

[1]. Worthington P., 2003, Introduction: history of implants. Osseointegration in dentistry: an overview. *Quintessence Publishing;* Illinois. p. 2.

[2]. Deepak K, Ahila SC, Muthukumar B, Vasanthkumar M., 2013, Comparative evaluation of effect of laser on shear bond strength of ceramic bonded with two base metal alloys: an in-vitro study. *Indian J Dent Res.;* 24:610–5.

[3]. An YH, Friedman RJ., 1998, Concise review of mechanisms of bacterial adhesion to biomaterial surfaces. *J Biomed Mater Res (Appl Biomater)* 43: 338-348.

[4]. Pye, A.D.; Lockhart, D.E.; Dawson, M.P.; Murray, C.A.; Smith, A.J., 2009, A review of dental implants and infection. *J. Hosp. Infect,* 72, 104–110.

[5]. Jayaraman M, Meyer U, Buhner M, Joos U, Wiesmann HP., 2004, Influence of titanium surfaces on attachment of osteoblast-like cells in vitro. *Biomaterials.* 25(4):625–631.

[6]. Kunzler TP, Drobek T, Schuler M, Spencer ND., 2007, Systematic study of osteoblast and fibroblast response to roughness by means of surface-morphology gradients. *Biomaterials.* 28(13):2175–2182.

[7]. Simmons CA, Valiquette N, Pilliar RM., 1999, Osseointegration of sintered porous-surfaced and plasma spray-coated implants: An animal model study of early postimplantation healing response and mechanical stability. *Journal of Biomedical Materials Research.* 47(2):127–138.

[8]. Buser D, Schenk RK, Steinemann S, Fiorellini JP, Fox CH, Stich H., 1991, Influence of surface characteristics on bone integration of titanium implants. A histomorphometric study in miniature pigs. *Journal of Biomedical Materials Research.* ; 25(7):889–902.

[9]. Filiaggi M, Pilliar R, Coombs N., 1993, Post-plasma spraying heat treatment of the HA coating/Ti-6Al-4V implant system. *J Biomed Mater Res.;* 27:191–198.

[10]. Beutner R, Michael J, Schwenzer B, Scharnweber D., 2010, Biological nano-functionalization of titanium-based biomaterial surfaces: a flexible toolbox. *Journal of the Royal Society Interface.* 7: S93–S105.

[11]. Schliephake H, Scharnweber D., 2008, Chemical and biological functionalization of titanium for dental implants. *Journal of Materials Chemistry.*18 (21):2404–2414.

[12]. Schliephake H, Scharnweber D, Dard M, Sewing A, Aref A, Roessler S., 2005, Functionalization of dental implant surfaces using adhesion molecules. *Journal of Biomedical Materials Research Part B-Applied Biomaterials.*73B (1):88–96.

[13]. Jose B, Antoci V, Zeiger AR, Wickstrom E, Hickok NJ., 2005, Vancomycin covalently bonded to titanium beads kills Staphylococcus aureus. *Chemistry &Biology.* 12(9):1041–1048.

[14]. Lange K, Herold M, Scheideler L, Geis-Gerstorfer J, Wendel HP, Gauglitz G., 2004, Investigation of initial pellicle formation on modified titanium dioxide (TiO2) surfaces by reflectometric interference spectroscopy (RIfS) in a model system. *Dental Materials*. 20(9):814–822.

[15]. Becker J, Kirsch A, Schwarz F, Chatzinikolaidou M, Rothamel D, Lekovic V, Laub M, Jennissen HP., 2006, Bone apposition to titanium implants biocoated with recombinant human bone morphogenetic protein 2 (rhBMP-2). A pilot study in dogs (vol 10, pg 217,) *Clinical Oral Investigations*, 10(3):225–225.

[16]. Marsh P, 2005, Dental plaque: biological significance of a biofilm and community life style *J. Clin. Periodontol*.32 7–15.

[17]. Davies D, 2003, Understanding biofilm resistance to antibacterial agents Nature Rev. *Drug Discov*.; 2 114–22.

[18]. Palmquist, A.; Lindberg, F.; Emanuelsson, L.; Branemark, R.; Engqvist, H.; Thomsen, P., 2009, Morphological studies on machined implants of commercially pure titanium and titanium alloy (Ti6Al4V) in the rabbit. *J. Biomed. Mater. Res*. B, 91B, 309–319. 55.

[19]. Brunette D M, Tengvall P, Textor M, Thompson P, 2001, *Applications, Springer-Verlag*, Berlin and Heidelberg; 231–266.

[20]. Liu X, Chu P, Ding C., 2004, Surface modification of titanium, titanium alloys, and related materials for biomedical applications. *Mater. Sci. Eng*. R; 47: 49–121.

[21]. Bagno A, Bello C., 2004, Surface treatments and roughness properties of Ti-based biomaterials. *J.Mater. Sci. Mater. Med*.; 15: 935-949.

[22]. Kim K H, Ramaswani N., 2009, Electrochemical surface modification of titanium in dentistry. *Dent. Mater. J*. 22; 28(1): 20–36.

[23]. Xiao S J, Textor M, Spencer N D, Sigrist H, Langmuir, 1998, 14: 5507–5516.

[24]. Li P, Ohtsuki C, Kokubo T, Nakanishi K, Soga N. J., 1992, *Am. Ceram. Soc*.75 (8): 2094 2097.

[25]. Brinker C, Scherer G., 1990, Sol–Gel Science: The Physics and Chemistry of Sol–Gel Processing. *American Press*, San Diego.

[26]. Advincula M, Fan X, Lemons J, Advincula R., 2005, Surface modification of surface sol-gel derived titanium oxide films by self-assembled monolayers (SAMs) and non-specific protein adsorption studies. *Colloids Surf. B Biointerfaces*; 42(1): 29–43.

[27]. Li P, Kangasniemi I, de Groot K, Kokubo T., 1994, Bone like Hydroxyapatite Induction by a Gel-Derived Titania on a Titanium Substrate. *J. Am. Ceram. Soc*. 77: 1307–1312.

[28]. Ohring M., 1992, Materials Sciences of Thin Film: Deposition and Structure, *Academic Press Ltd*, Boston, 277.

[29]. Hampden-Smith M J, Kodas T T., 1995, Chemical Vapor Deposition of Metals: Part 2. *Overview of Selective CVD of Metals*. *Chem*. *Vap*. *Deposition*; 1: 39-48.

[30]. Mas-Moruna C, Espanol M, Montufar E, Mestres G, Aparicio C, Javier F, Ginebra M., 2013, Biomaterials Surface Science (eds. Taubert A, Mano J F, Rodríguez-Cabello J C), Wiley-VCH Verlag GmbH & Co. KGaA, *Weinheim;* 337–374.

[31]. Xiao S-J, Kenausis G, Textor M., 2001, Titanium in Medicine: Material Science, Surface Science, Engineering, Biological Responses and Medical Applications (eds. eds. Brunette D M, Tengvall P, Textor M, Thompson P), *Springer-Verlag*, Berlin and Heidelberg 417–455.

[32]. Gusev A. I., Rempel A. A., 2004, Nanocrystalline Materials. — Cambridge: Cambridge *International Science Publishing*, — 351 p.

[33]. Morosanu C. E.; 1990, Thin Films by CVD, *Elsevier*, Amsterdam.

[34]. Kodas,T. M. Hampden-Smith; 1997, The Chemistry of Metal CVD, *VCH Publisher*, New York.

[35]. Wagner, R. S.; Ellis, W. C. 1964, Applied Physics Letters, 4, (5), 89-90.

[36]. Lee J. 2013, Synthesis of biphasic Al/Al_2O_3 nanostructures under microgravity and laser structuring on Al/Al_2O_3 surfaces for selective cell guidance. Germany.

[37]. Zhao, Q.; Xu, X.; Zhang, H.; Chen, Y.; Xu, J.; Yu, D., 2004, *Applied Physics* A, 79, (7), 1721-1724.

[38]. Lee, S. T.; Zhang, Y. F.; Wang, N.; Tang, Y. H.; Bello, I.; Lee, C. S.; Chung, Y. W. 1999, *Journal of Materials Research*, 14, (12), 4503-4507

[39]. Sow, E. A. 2008, Importance of CVD-process parameters for the synthesis of novel $Al/Al2O3$ and $Ga/Ga2O3$ composite nanostructures. *Saarländische Universitäts- und Landesbibliothek, Saarbrücken*,

[40]. Shamala, K. S. L. Murthy, C. S. Narasimha; K. R., 2004, *Mater*. *Sci*. *Eng*. B 106, 3, 269.

[41]. Bartzsch H., Glosz D., Bocher B., Frach P., Goedicke K.; 2003, *Surf*. *Coat*. *Technol*. 174 774.

[42]. Exner H., Reinecke A.-M., Nieher M.; J., 2002, *Ceram*. *Process*. Res. 3, 2, 66.

[43]. Godlinski, D. Kuntz, M. Grathwohl G.; J. Am., 2002, *Ceram*. *Soc*. 85, 10 2449.

[44]. Harimkara,S. P. N. B. Dahotre;2008, Materials Characterization 5, 9 700.

[45]. Davist, M. P. Kapadiat, J. Dowden,W. M. Steen, C. H. G. Courtney; J. Phys. D: 1986, *Appl*. *Phys*. 19 1981.

[46]. Heinrich J. G., Gahler A., Günster J., Schmücker M., Zhang J., Jiang D., Ruan M.; 2007, *Mater J. Sci.* 42 5307.

[47]. Jasim, M. R. D. Rawlings, D. R. F. West; J. 1992 *Mater. Sci.* 27, 3903.

[48]. Sul Y, Johansson C B, Jeong Y, Albrektsson T., 2001, *Med. Eng. Phys.* 23: 329–346.

[49]. Triantafyllidis, D. Li, L. Stott F.,2005, *Mater. H. Sci. Eng.*, A 390, 1, 271.

[50]. Jervis, T. R. M. Nastasi, A. J. J. Griffin, T. G. Zocco, T. N. Taylor, S. R. Foltyn; 1997, Surf. Coat. Technol. 89, 1,158.

[51]. Hao, L. J. Lawrence; J. 2007, *Mater. Sci. - Mater. Med.* 18, 5, 807.

[52]. Qi, J. Wang, K. L. Zhu; Y. Mater M. J., 2003, *Process. Technol.* 139, 1, 273.

[53]. Rizvi, N. H. P. Apte; J., 2002, *Mater. Process. Technol.* 127, 2, 206.

[54]. Gregson;V. G., 1984, Laser Heta Treatment Procesing, North-Holland.

[55]. Mazumder J.; 1983, Laser Heat Treatment: The State of the Art, J. Met. 35, 5.

[56]. Zum Gahr, K.-H Schneider; J., 2000, Ceram. Int. 26, 363.

[57]. Bradley, L. L. Li, F. H. Stott; (1999), Appl. Surf. Sci. 138, 233.

[58]. Lausmaa J. 2001, Mechanical, Thermal, Chemical and Electrochemical Surface Treatment of Titanium. In: Brunette DM, editor. Titanium in medicine: material science, surface science, engineering, biological responses and medical applications. Berlin: *Springer*, 1019.

[59]. Tibbitt, M.W. & Anseth, K.S., 2009, Hydrogels as extracellular matrix mimics for 3D cell culture. *Biotechnol. Bioeng.* 103, 655–663.

[60]. Van Brakel, R.; Cune, M.S.; van Winkelhoff, A.J.; de Putter, C.; Verhoeven, J.W.; van der Reijden, W., 2000, Early bacterial colonization and soft tissue health around zirconia and titanium abutments: An in vivo study in man. *Clin. Oral Implant. Res.*, 22, 571–577.

[61]. Marshall, K. C., 1973, Mechanisms of adhesion of marine bacteria to surfaces. Proceedings of the Third International Congress on Marine Corrosion and Fouling. *United States National Bureau of Standards Special Publication*.

[62]. An YH, Friedman RJ, 1998, Concise review of mechanisms of bacterial adhesion to biomaterial surfaces. *J Biomed Mater Res (Appl Biomater)* 43: 338-348.

[63]. Singh, A.V.; Vyas, V.; Salve, T.S.; Cortelli, D.; Dellasega, D.; Podesta, A.; Milani, P.; Gade, W.N. , 2012, Biofilm formation on nanostructured titanium oxide surfaces and

micro/nanofabrication-based preventive strategy using colloidal lithography. *Biofabrication* 4, 025001:1–025001:2.

[64]. Flemming, H. C. & Wingender, J., 2010, The biofilm matrix. *Nat Rev Microbiol* 8, 623–633.

[65]. Wolfe HF, 2005, Biofilm plaque formation on tooth and root surfaces. In: Wolfe, H.F. Rateitschak, K.H. (eds*). Periodontology*, ed 3. Stuttgart: Thieme; 24.

[66]. Kolenbrander PE, Anderson RN, Blehart DS., 2002, Communications among oral bacteria. Microbiol Mol Bio Rev; 66:486-05.

[67]. Kalykakis GK, Nissengard R., 1998, Clinical and microbial findings on osseointegrated implants, comparison between partially dentate and edentulous subjects. *European J Prosthod Rest Dent*; 6:155-9.

[68]. Li J, Helmerhorst EJ, Socransky SS., 2004, Identification of early microbial colonizers in human dental biofilm. *J Appl Microbiol;* 97:1311-88.

[69]. Furst MM, Salvi GE, Lang NP., 2007, Bacterial colonization immediately after installation of oral titanium implants. *Clin Oral Implants Res*; 18:501-8.

[70]. Hannig M, Khanafer AK, Hoth-Hannig W, Al-Marrawi F, Açil Y: 2005, Transmission electron microscopy comparison of methods for collecting in situ formed enamel pellicle. *Clin Oral Investig* 9.30-37.

[71]. Diebold U. 2003, The surface science of titanium dioxide. 48: 53–229.

[72]. Puckett S D, Taylor E, Raimondo T, Webster T J. 2010, The relationship between the nanostructure of titanium surfaces and bacterial attachment. *Biomaterials;* 31: 706–713.

[73]. Dale G R, Hamilton J W, Dunlop P S, Lemoine P, Byrne J A. 2009, Electrochemical growth of titanium oxide nanotubes: the effect of surface roughness and applied potential. J Nanosci. *Nanotechnol;* 9(7): 4215–4219.

[74]. Hannig C; Hannig M, 2009, The oral cavity --a key system to understand substratum-dependent bioadhesion on solid surfaces in man. *Clinical Oral Investigations* 13:123-139.

[75]. Shani S., Friedman M., Steinberg D. 2000 The anticariogenic effect of amine fluorides on Streptococcus sobrinus and glucosyltransferase in biofilms. *Caries Res.* 34, 260–267 10.

[76]. Auschill, T.M., Arweiler, N.B., Netuschil, L., Brecx, M., Reich, E., Sculean, A., Artweiler, N.B., 2001. Spatial distribution of vital and dead microorganisms in dental biofilms. Arch. *Oral Biol.* 46, 471-476.

[77]. Netuschil, L., Reich, E., Unteregger, G., Sculean, A., Brecx, M., 1998. A pilot study of confocal laser scanning microscopy for the assessment of undisturbed 10 dental plaque vitality and topography. Arch. *Oral Biol.* 43, 277-285.

[78]. Boulos, L., M. Prevost, B. Barbeau, J. Coallier, and R. Desjardins. 1999. LIVE/DEAD BacLight: application of a new rapid staining method for direct enumeration of viable and total bacteria in drinking water. *J. Microbiol. Methods* 37:77–86.

[79]. Al-Ahmad A, Follo M, Selzer AC, Hellwig E, Hannig M, Hannig C. 2009 Bacterial colonization of enamel in situ investigated using fluorescence in situ hybridization. *J Med Microbiol* 58:1359-66.

[80]. Quirynen, M.; Bollen, C.M. 1995, The influence of surface roughness and surface-free energy on supra- and subgingival plaque formation in man. A review of the literature. *J. Clin. Periodontol*. 22, 1–14. 28.

[81]. Bell D C, Mankin M, Day R W and Erdman N 2014 Successful application of Low Voltage Electron Microscopy to practical materials problems *Ultramicroscopy* 145 56-65.

[82]. Joy D C and Joy C S 1996 Low Voltage Scanning Electron Microscopy *Micron* 27 247-263.

[83]. Drummy L F, Yang J and Martin D C 2004 Low voltage electron microscopy of polymer and organic molecular thin films *Ultramicroscopy* 99 247-256

[84]. Liu J 2000 High-Resolution and Low Voltage FE-SEM Imaging and Microanalysis in Materials Characterization *Mater. Character*. 44 353-363.

[85]. Hannig C, Hannig M: 2009 The oral cavity-a key system to understand substratum-dependent bioadhesion on solid surfaces in man. *Clin Oral Investig*;13.123-139.

[86]. Bollen, C.M.; Lambrechts, P.; Quirynen, M. 1997, Comparison of surface roughness of oral hard materials to the threshold surface roughness for bacterial plaque retention: A review of the literature. *Dent. Mater*., 13, 258–269. 29.

[87]. Jung DJ, Al-Ahmad A, Follo M, Spitzmüller B, Hoth-Hannig W, Hannig M, Hannig C: 2010, Visualization of initial bacterial colonization on dentine and enamel in situ. *J Microbiol Methods*;81.166-174.

[88]. Hannig M, Joiner A. 2006 The structure, function and properties of the acquired pellicle. *Monogr Oral Sci*;19:29-64.

[89]. Marsh PD: 2005 Dental palque: Biological significance of a biofilm and community lifestyle. *J Clin Periodontol*;32 Suppl 6:7-15.

[90]. Teughels W, Van Assche N, Sliepen I, Quirynen M 2006 .[91]. Duarte AR, Neto JP, Souza JC, Bonachela WC 2013 Detorque evaluation of dental abutment screws after immersion in a fluoridated artificial saliva solution. *J Prosthodont* 22: 275-281.

[92]. Li Y, Burne RA, 2001 Regulation of the gtfBC and ftf genes of Streptococcus mutans in biofilms in response to pH and carbohydrate. *Microbiology* 147: 2841-2848.

[93]. Rupp, F.; Scheideler, L.; Olshanska, N.; de Wild, M.; Wieland, M.; Geis-Gerstorfer, J. 2006 Enhancing surface free energy and hydrophilicity through chemical modification of microstructured titanium implant surfaces. *J. Biomed. Mater. Res.* Part A, 76, 323-334.

[94]. Rupp, F.; Scheideler, L.; Rehbein, D.; Axmann, D.; Geis-Gerstorfer, J. 2004 Roughness induced dynamic changes of wettability of acid etched titanium implant modifications. *Biomaterials*, 25, 1429-1438.

[95]. Rosenberg, E.S.; Torosian, J.P.; Slots, J. 1991 Microbial differences in 2 clinically distinct types of failures of osseointegrated implants. *Clin. Oral Implant.* Res, 2, 135–144.

[96]. Leonhardt, A.; Berglundh, T.; Ericsson, I.; Dahlen, G. 1992 Putative periodontal pathogens on titanium implants and teeth in experimental gingivitis and periodontitis in beagle dogs. *Clin. Oral Implant.* Res., 3, 112–119.

[97]. Pye, A.D.; Lockhart, D.E.; Dawson, M.P.; Murray, C.A.; Smith, A.J. 2009 A review of dental implants and infection. J. *Hosp. Infect*, 72, 104–110.

[98]. De Freitas, M.M.; da Silva, C.H.; Groisman, M.; Vidigal, G.M., Jr. 2011 Comparative analysis of microorganism species succession on three implant surfaces with different roughness: An in vivo study. *Implant. Dent.*, 20, e14–e23.

[99]. Ercan, B. Taylor, E. Alpaslan, E. Webster T.J. 2011, Diameter of titanium nanotubes influences anti-bacterial efficacy. *Nanotechnology*, 22 p. 295102.

[100]. Gongadze E, Kabaso D, Bauer S, Slivnik T, Schmuki P, van Rienen U, Iglič A. 2011 Adhesion of osteoblasts to a nanorough titanium implant surface. *Int. J. Nanomed.*; 6: 1801–1816.

[101]. Bauer, S. Pittrof, ATsuchiya, H. Schmuki. P 2011, Size-effects in TiO_2 nanotubes: diameter dependent anatase/rutile stabilization. *Electrochemistry Communications*, 13 pp. 538–541.

[102]. Neoh, K.G. Wang, R Kan, E.T 2015 Surface nanoengineering for combating biomaterials infections L. Barnes, I. Cooper (Eds.), Biomaterials and medical device – associated infections, *Woodhead Publishing* pp. 133–161.

[103]. Kim, K. Paranthaman M., Norton D.P., Aytug T., Cantoni, C. Gapud A.A., Goyal, A. Christen, D.K. 2006 Supercond. *Sci. Technol.* 19, R23

[104]. Zhang, F.; Zhang, Z.; Zhu, X.; Kang, E. T.; Neoh, K. G. 2008 Silk-Functionalized Titanium Surfaces for Enhancing Osteoblast Functions and Reducing Bacterial Adhesion *Biomaterials*, 29, 4751– 4759.

[105]. Zinger, O. Zhao, G. Schwartz, Z. Simpson, J. Wieland, M. Landolt, D. Boyan, B. 2005 *Biomaterials* 26, 1837.

[106]. Anand S, Paxson A.T, Dhiman R, Smith JD, Varanasi KK. 2012 Enhanced condensation on lubricant-impregnated nanotextured surfaces. *ACS Nano. Artilce* ASAP.

CURRICULUM VITAE

Personal Information	
Name Surname	Arzu EROL
Place of Birth	Karabük
Date of Birth	1983
Nationality	☑ T.C. ☐ Other:
Phone Number	
Email	erol.arzu@yahoo.com
Web Page	

Educational Information	
B. Sc.	
University	Haliç University
Faculty	Faculty of Science and Arts
Department	Molecular Biology and Genetics
Graduation Year	2007

M. Sc.	
University	Fatih University
Institute	Institute of Graduate Studies in Science and Engineering
Department	Biology
Programme	Molecular Biology and Genetics
Graduation Year	2009

Ph. D.	
University	İstanbul University
Institute	Institute of Graduate Studies in Science and Engineering
Department	Department of Biotechnology
Programme	Biotechnology Programme
Graduation Year	2017

Publications

Arzu Erol (2017) Behaviour of Streptococcus Mutants on Enamel Surface Coated with Initial Bio lm, In Vivo. Int J Dentistry Oral Sci. S7:002, 8-14.

Arzu Erol (2017) Micrograph – Examination of the Artistic Value of Microscope Photographs, Medeniyet Art, IMU Art, Design and Architecture Faculty Journal, Volume: 3, Number:1, 2017, p. 66-78 ISSN 2587-1684.